

Increasing Task-Sharing Performance by Haptically Assisting a Tunnel-in-the-Sky Approach

D.G. Beeftink

April 19, 2017



Increasing Task-Sharing Performance by Haptically Assisting a Tunnel-in-the-Sky Approach

MASTER OF SCIENCE THESIS

For obtaining the degree of Master of Science in Aerospace Engineering
at Delft University of Technology

D.G. Beeftink

April 19, 2017



Delft University of Technology

Copyright © D.G. Beeftink
All rights reserved.

DELFT UNIVERSITY OF TECHNOLOGY
DEPARTMENT OF
CONTROL AND SIMULATION

The undersigned hereby certify that they have read and recommend to the Faculty of Aerospace Engineering for acceptance a thesis entitled “**Increasing Task-Sharing Performance by Haptically Assisting a Tunnel-in-the-Sky Approach**” by **D.G. Beeftink** in partial fulfillment of the requirements for the degree of **Master of Science**.

Dated: April 19, 2017

Readers:

dr.ir. C. Borst

dr.ir. M. M. van Paassen

prof.dr.ir. M. Mulder

dr.ir. J. C. F. de Winter

Acknowledgments

Being able to write my master thesis at the coolest department of the Faculty of Aerospace Engineering has been a privilege. At C&S, knowledge on a wide variety of subjects and a willingness to help is always - quite literally - just around the corner. Clark, I would like to thank you for your moral and academic support; not only would we crush DUECA code together, we had a lot of fun doing it as well. In 2017 I think we had only one planned meeting, but I had the opportunity to pick your brain almost daily, either at the coffee machine or in your office. This way of supervising really helped to get going again the moment before I got stuck. Dirk, your knowledge in haptics and your skills in programming have saved me more than once. I don't know how many times I left your office with an exchange of a 'thanks a lot' and 'you're welcome', but for sure there were a lot. René, your deep knowledge on DUECA resolved some of the toughest issues in a heartbeat, thanks for being the ultimate last resort. And Max, thanks for your insightful feedback and helping me keep the bigger picture in mind.

The first part of my thesis I have been working in 2.44, a so-called flex room, which, with the help of the great people at the service desk, we made our own. This group has been the reason that graduating during the summer holidays was still somewhat fun. Although the focus was always on the vrimibo, this was a great place for meaningful and sometimes less meaningful discussions during the rest of the week. When I had to commit myself to the world of DUECA, I moved to the graduation room under SIMONA: SIM 008. The experience and knowledge inside and around this room has greatly benefitted the quality of my work. 2.44 and SIM 008, thanks for being so nerdy!

I also would like to thank my parents, brother and sisters for their support throughout my thesis. Thanks for the visits all the way in Delft, when I failed to visit you all the time. I promise I will come to Hengelo soon enough!

Last but surely not least: Zita. Our morning coffees and chilled weekends were highlights of my week, giving me the energy to work and shine during the weekdays. Thank you for being so awesome and supportive!

Derek

Contents

Acknowledgments	vii
Nomenclature	xvii
I IEEE Paper	1
II Preliminary Thesis	19
1 Introduction	21
1-1 Background	21
1-1-1 Tunnel-in-the-Sky Display	21
1-1-2 Haptic feedback	22
1-2 Description of the problem	22
1-2-1 Problem statement	24
1-3 Research direction	24
1-4 Research approach	25
1-5 Preliminary structure	26
2 Literature review	27
2-1 Tunnel-in-the-Sky	27
2-1-1 Tunnel design	28
2-1-2 Scaling of the tunnel	30
2-2 Haptic feedback	31
2-2-1 Haptic models	32
2-2-2 Haptic feedback tuning	34
2-2-3 Haptic authority	36

3	Preliminary analysis	39
3-1	Trajectory	39
3-2	Reference frames	39
3-3	Controllers	41
3-3-1	Predictive control strategies	41
3-3-2	Control inputs and outputs	44
3-4	Implementation of haptics	45
3-4-1	Dynamics of the model	46
3-4-2	Results of haptic feedback	47
III	Appendices	49
A	Simulink Architecture	51
B	Experiment Briefing	57
B-1	Goal of the experiment	58
B-2	Experiment Task	58
B-3	Apparatus	59
B-4	Experiment Procedures	59
B-5	Your Rights	60
C	Experiment Conditions	61
C-1	Conditions	62
C-2	Latin square design	63
D	Rating Scale Mental Effort	65
D-1	Rating Scale Mental Effort	66
D-2	Mental effort ratings	67
E	Approval of Ethics Committee	69
F	Rejection of Participants	71
G	Additional Data	73
G-1	Time series	74
H	Processing of Eye-Tracker Data	83
H-1	Filtering raw data	84
H-2	Determine the split value	85
I	Statistical Analysis	87
I-1	Syntax SPSS	88
I-2	Results	89

List of Figures

1-1	Qualitative relation between tunnel size and tracing performance according to Wilckens (Wilckens, 1973) (figure extracted from Mulder and Mulder (Mulder & Mulder, 2005))	23
2-1	3 displays depicting the different independent variables, splay-only, compression-only and a combination of both, respectively (Mulder, 2003a)	28
2-2	The geometry of the tunnel displays applied in the experiment (Mulder, 2003b) . . .	29
2-3	Tunnel display without and with superimposed predictor and director (Grunwald, Robertson, & Hatfield, 1980)	29
2-4	Qualitative diagram of average tracking errors versus tunnel size (Wilckens, 1973) . .	30
2-5	Closed-loop, linear pilot/aircraft model describing lateral control (Mulder & Mulder, 2005)	31
2-6	Visual flight director (top) and haptic flight director (bottom) (de Stigter, Mulder, & van Paassen, 2007)	34
2-7	Closed-loop NMS model as used by Smisek et al. (Smisek, Van Paassen, Mulder, & Abbink, 2013)	35
2-8	Stick position based guidance force according to tuned stiffness (Smisek et al., 2013)	35
2-9	Block diagram of a situation of shared haptic control (Sunil, Smisek, Van Paassen, & Mulder, 2014)	37
3-1	3D plot of generated trajectory	40
3-2	Definition of GRF and TCTF coordinate system as seen in Z direction	40
3-3	Sideview of the longitudinal flight path predictor	42
3-4	Control loop used for longitudinal control.	42
3-5	Sideview of the lateral flight path predictor	43
3-6	Control loop used for lateral control	44

3-7	Results of longitudinal, predictive control for multiple prediction times	45
3-8	Results of lateral, predictive control for multiple prediction times	46
3-9	Haptics implemented in the control loop	46
3-10	Haptic and human control inputs according to the Simulink model ($HA = 0.5$) . . .	48
A-1	Complete architecture of the controller in used for offline simulations in Simulink . .	53
A-2	Architecture of the longitudinal predictor in Simulink	54
A-3	Architecture of the lateral predictor in Simulink	55
A-4	Architecture of the longitudinal, lateral and throttle controller in Simulink	56
B-2	The SIMONA (Simulation, MOtion and NAVigation) Research Simulator (SRS) at Delft University of Technology	59
D-1	Rating Scale Mental Effort	66
F-1	Boxplot of all the participants and the rejected data	72
G-1	Time series of the horizontal error of all the runs with a visual tunnel size of 60 <i>m</i> .	75
G-2	Time series of the vertical error of all the runs with a visual tunnel size of 60 <i>m</i> . . .	75
G-3	Time series of the roll rates of all the runs with a visual tunnel size of 60 <i>m</i>	76
G-4	Time series of the pitch rates of all the runs with a visual tunnel size of 60 <i>m</i>	76
G-5	Time series of the human roll forces of all the runs with a visual tunnel size of 60 <i>m</i>	77
G-6	Time series of the human pitch forces of all the runs with a visual tunnel size of 60 <i>m</i>	77
G-7	Time series of the haptic roll forces of all the runs with a visual tunnel size of 60 <i>m</i> .	78
G-8	Time series of the haptic pitch forces of all the runs with a visual tunnel size of 60 <i>m</i>	78
G-9	Time series of the horizontal error of all the runs with a visual tunnel size of 20 <i>m</i> .	79
G-10	Time series of the vertical error of all the runs with a visual tunnel size of 20 <i>m</i> . . .	79
G-11	Time series of the roll rates of all the runs with a visual tunnel size of 20 <i>m</i>	80
G-12	Time series of the pitch rates of all the runs with a visual tunnel size of 20 <i>m</i>	80
G-13	Time series of the human roll forces of all the runs with a visual tunnel size of 20 <i>m</i>	81
G-14	Time series of the human pitch forces of all the runs with a visual tunnel size of 20 <i>m</i>	81
G-15	Time series of the haptic roll forces of all the runs with a visual tunnel size of 20 <i>m</i> .	82
G-16	Time series of the haptic pitch forces of all the runs with a visual tunnel size of 20 <i>m</i>	82
H-1	Filtered eye-tracker data	84
H-2	Filtered eye-tracker data	85
I-1	SPSS syntax for all variables except the subjective rating data	88

I-2	SPSS syntax for the subjective rating data	88
I-3	Test of normality of the secondary task success statistical analysis	89
I-4	Results of Mauchly's test of sphericity	90
I-5	Within-subjects effects effects as obtained by the repeated measures ANOVA	91
I-6	Rating Scale Mental Effort	92

List of Tables

C-1	Evaluation conditions	62
C-2	Training conditions	62
C-3	Tuning conditions	62
C-4	Latin square design of the experiment	63
D-1	Mental effort rating of each participant for each run	67

Nomenclature

Roman symbols

b	Damping coefficient	Nms/rad
e	Error	m
g	Gravitational acceleration	m/s^2
F	Force	N
H	Transfer function	$[-]$
I	Mass moment of inertia	kgm^2
k	Spring coefficient	Nm/rad
K	Gain	$[-]$
p	Roll rate	$^\circ/s$
q	Pitch rate	$^\circ/s$
R	Radius	m
t	Time	s
T	Period of time	s
V	Velocity	m/s
x	Direction in a reference frame	m
y	Direction in a reference frame	m
z	Direction in a reference frame	m

Greek symbols

γ	Flight path angle	$^\circ$
δ	Deflection	$^\circ$
Δ	Absolute change	
ϕ	Roll angle	$^\circ$
χ	Track angle	$^\circ$
$\dot{\chi}$	Rate of track change	$^\circ/s$
ψ	Heading angle	$^\circ$
ω_c	Cross-over frequency	rad/s

Subscripts

AC	Aircraft
c	Commanded
dir	Directed
e	Error
GRF	In the geodetic reference frame
H	Haptic
Meas	Measured
p	Pilot
pred	Predicted
r	Roll-subsidence
Ref	Reference
s	Stick
TCTF	In the trajectory-centered trajectory-fixed reference frame
tr	Track
x	In the direction of x
y	In the direction of y
z	In the direction of z

Abbreviations

ANOVA	Analysis of variance
DOF	Degree-of-freedom
DUECA	Delft University Environment for Communication and Acti- vation
GRF	Geodetic reference frame
HA	Haptic authority
HF	Haptic feedback
HMI	Human-machine interaction
HTS	Haptic tunnel size
NASA	National Aeronautics and Space Administration
NMS	Neuromuscular system
RMS	Root-mean-square
RSME	Rating Scale Mental Effort
ST	Segment type
SIMONA	Simulation, Motion and Navigation
SRS	SIMONA Reasearch Simulator
TCTF	Trajectory-centered trajectory-fixed
TIS	Tunnel-in-the-Sky
TLX	Task load index
VTS	Visual tunnel size

Part I

IEEE Paper

Increasing Task-Sharing Performance by Haptically Assisting a Tunnel-in-the-Sky Approach

D.G. Beefink, C. Borst, D. Van Baelen, M.M. van Paassen, and M. Mulder

Control & Simulation, Department Control & Operations

Delft University of Technology, Delft, The Netherlands

Email: derekbeefink@gmail.com, {c.borst, d.vanbaelen, m.m.vanpaassen, m.mulder}@tudelft.nl

Abstract—To investigate the effects of haptic feedback on the task-sharing performance during approach when using a Tunnel-in-the-Sky display, a within-subject simulated experiment with 12 participants was conducted in the SIMONA Research Simulator at Delft University of Technology. The experiment consisted of a primary Tunnel-in-the-Sky tracking task, where the pilots had to fly with one non-haptic and two haptic settings. Primary task performance was measured by means of position errors and roll and pitch rates. A secondary task was presented to the pilots as bucket shaped figures superimposed on the outside visuals, where the participants had to indicate the direction of the divergent figure. Secondary task performance was measured by success rate, average time to answer correctly and - by means of eye-tracker measurements - head-up time and number of gaze switches. Next to these objective measures pilots provided a subjective measure of their mental effort after each run. Lastly, the haptic and human induced forces were recorded, to be able to measure whether the pilot was fighting or cooperating with the haptic feedback provided. Results of the experiment show that haptic feedback can significantly increase task-sharing performance of the pilot, especially for a challenging primary task, but that too dominant haptic feedback can introduce a risk of over-reliance.

I. INTRODUCTION

Since the advancement of computer technology in the cockpit, physical design constraints of instruments have been taken away, allowing designers to apply new control formats and ways of information presentation. Using new displays, cockpits have become more intuitive and easy to understand by pilots [1]. Lintern et al. suggest however, that these features should be implemented with care, making sure that their design does not add to the cockpit complexity [2].

An example of one of these displays is the Tunnel-in-the-Sky (TIS) display that shows the trajectory to be flown in perspective fashion. This makes flying a trajectory more intuitive to pilots, compared to the bars indicating desired pitch and roll angles as indicated by a primary flight display (PFD). Integrating multiple instrument readings allows the TIS display to provide the operator with a preview of the trajectory ahead, supporting pilots to get a quick grasp of the situation at hand. Having a preview of the trajectory available helps better understand actions to be taken in the future, as it is already clear what is expected of the pilot further along the tunnel. However, making all relevant information available on one display can potentially absorb a disproportionate

amount of the pilot's attention. In a two-person cockpit the focus of one pilot will be outside, where the other checks the instruments inside the cockpit. In a one-person cockpit however, the pilot has to divide his focus between the flight instruments and what happens outside, between looking head-down and head-up. A TIS display tends to draw attention inside, shifting the pilot's focus head-down, thereby decreasing task-sharing performance [3].

Mulder and Mulder [4] indicate that this phenomenon is more apparent for smaller tunnels, as workload increases further as the tracking task is considered more challenging; this shows that integrated flight instruments designed for workload reduction can actually increase the workload, a pitfall also mentioned by Anderson [5]. The research described in this paper investigates whether smart use of haptics could mitigate this problem.

In several studies the benefits of haptic feedback in terms of primary task performance have been shown [6]–[9]. Wickens [10], [11] shows multiple examples of advantages of cross-modal, in these cases *visual* and *auditive* communications over intra-modal displays when performing a dual task. In this research it is hypothesized that the same holds for a cross-modal system using vision and haptics. Where a display shows the pilot the correct course of action through the visual modality, a haptic guidance system relays this information through the haptic modality. The continuous haptic guidance will not only work as a means of communicating the right course of action, it will also guide the pilot towards the right direction by means of shared control.

Whether the same holds for the task-sharing performance during a TIS assisted approach will be the focus of the study described in this paper. It is expected that the task-sharing performance measured by means of tracking performance and secondary task success will go up when haptic feedback, in combination with a superimposed flight path predictor and predictor window, is applied. When these symbols visualise the underlying haptic cueing system, they will help the operator understand the haptic feedback when looking at the TIS display, increasing the acceptance of the haptics, further improving task-sharing performance [12].

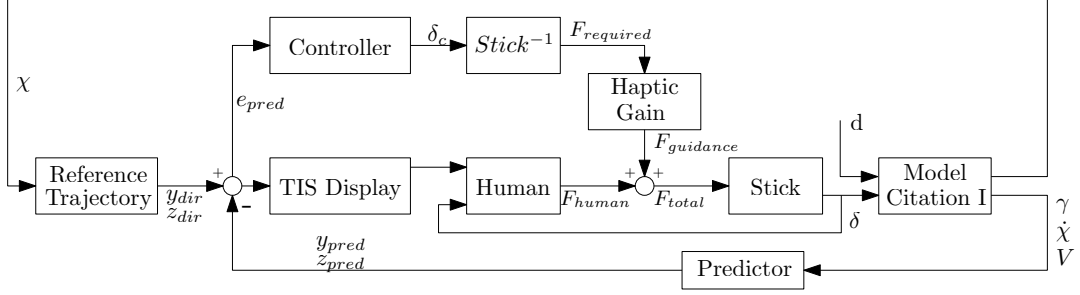


Fig. 1: The implementation of shared control between human and haptic controller

In previous studies it has been found that stronger feedback can cause over-reliance, decreased acceptance, and confusion to the pilot [7], [9], [13], [14]. Therefore the research presented will not only investigate the increase in task-sharing performance, but will also consider the possible pitfalls by gaining empirical insight in the relation between human behaviour and the level of haptic assistance during the haptically assisted TIS approach.

II. BACKGROUND

In Figure 1 shows that the human receives information through two channels; one is the haptic feedback through the stick position, the other is the TIS display. The TIS display uses the reference trajectory and the predicted aircraft states to indicate the predicted error. The pilot uses this information to determine the required steering input. Without haptic feedback this would be the only way for the pilot to determine the error. The haptic feedback aids the pilot in two ways: by means of guidance and by means of communication. Guidance is provided by the haptic controller shown in the upper inner loop; this controller converts the predicted error in a required force, of which a portion is let through by the haptic gain resulting in a guidance force. The stick position after haptic and human forces are applied to it provides communication to the pilot, allowing the pilot to perceive the predicted error not only by looking at the TIS display, but also by feeling the position of the stick.

A. Tunnel-in-the-Sky Display

The first research on TIS displays took place in the 1970s, where Wilckens [15] proposed a qualitative relation between tunnel size and tracking performance. In 1980, Grunwald et al. [16] performed an experiment demonstrating the feasibility of a tunnel display during an actual flight. Since then much research has been performed on the effect of the tunnel's geometry and size, among others by Mulder and Mulder [4] in 2005, who quantified Wilckens' theory on tunnel size and flight performance and reproduced these theoretical results during an experiment.

This TIS display with superimposed predictor window and symbol were used in the experiment; a schematic image of

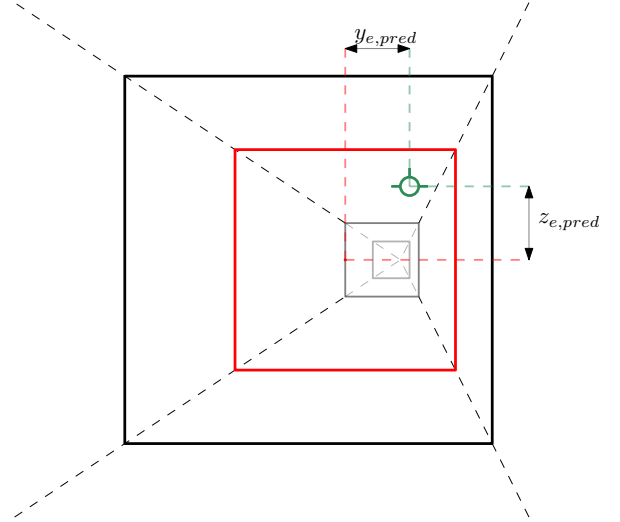


Fig. 2: Schematic Tunnel-in-the-Sky display with a superimposed predictor window and predictor symbol, indicating the predicted errors

this tunnel can be found in Figure 2. Here the red square indicates the outer boundary of the tunnel at the aircraft location after the pre-set prediction time (T_{pred}), and the green flight path predictor shows the indicated aircraft position based on the predictor laws explained in Section II-A1. These symbols are implemented to give to pilots an insight in the behaviour of the haptic controller, which will be discussed in more detail in Section II-B.

1) *Predictor Laws*: Measured aircraft states are used by the predictor to obtain the predicted aircraft states and a predicted error after T_{pred} seconds. This error is then used as input for the haptic controller. Small angles were assumed when designing the predictor laws, meaning that $\sin(x) = x$, $\cos(x) = 1$ and $\tan(x) = x$. Moreover, all distances and angles were calculated in the trajectory-centered, trajectory-fixed (TCTF) reference frame. The origin of this frame is

located at the point on the trajectory closest to the aircraft. Its x -axis points towards the direction of the trajectory, the z -axis points down and the y -axis is orthogonal to the other axis and pointing to the right compared to the direction of the trajectory.

A different predictor law was used for longitudinal and lateral control, as the aircraft dynamics are different in these directions. The longitudinal predictor law determines the vertical position of the flight path predictor, which is based on the current vertical error with respect to the trajectory and the flightpath angle multiplied by the prediction time and the aircraft velocity. When assuming small angles for γ , this results in Equation 1.

The schematics of this predictor law are displayed in Figure 3. $z_{ac,T_{pred}}$ - the position of the center of the predictor frame relative to the origin of the TCTF reference frame - can be determined directly, as the trajectory to be flown is known and can be determined T_{pred} seconds in the future. It was found that no second order dynamics ($\dot{\gamma}$) were required for haptic control in the vertical direction and would only make the predictor symbol very sensitive to steering and disturbance inputs.

$$z_{ac,T_{pred}} = z_e + \gamma T_{pred} V \quad (1)$$

The difference between the predicted aircraft position, $z_{ac,T_{pred}}$ and the predicted location of the trajectory, $z_{ref,T_{pred}}$ is the predicted vertical error; this was used as input for the haptic controller.

$$z_{e,pred} = z_{ref,T_{pred}} - z_{ac,T_{pred}} \quad (2)$$

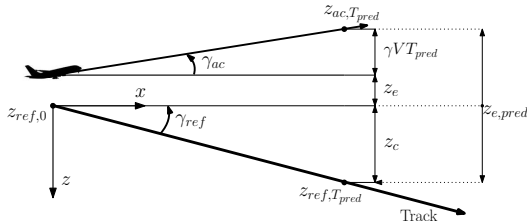


Fig. 3: Side view of the longitudinal flightpath predictor

The horizontal position of the predictor is determined by the circular path prediction law as presented by Grunwald [17] and shown in Equation 3. A schematic overview of the circular path predictor law is shown in Figure 4. Similar to the vertical case, $y_{ac,T_{pred}}$ can be determined in the TCTF reference frame which is indicated by the y and x -axis. The first two terms of $y_{ac,T_{pred}}$ consist of the current error and the track angle error (or heading angle in the TCTF reference frame) multiplied by the velocity and prediction time. The third term is the second-order Taylor expansion of the second term, accounting for the track angle rate of change. The last term based on the roll rate and a gain is called the roll-rate extension [17] and

accounts for high frequency behaviour of the aircraft. The roll-rate extension is very sensitive to turbulence, making it hard to use for the pilots. As it adds only a small part to the dynamics, it was chosen to omit this term resulting in Equation 4.

$$y_{ac,T_{pred}} = y_e + \chi_e V T_{pred} + \dot{\chi} \frac{1}{2} V T_{pred}^2 + p \cdot K_p \quad (3)$$

$$y_{ac,T_{pred}} = y_e + \chi_e V T_{pred} + \dot{\chi} \frac{1}{2} V T_{pred}^2 \quad (4)$$

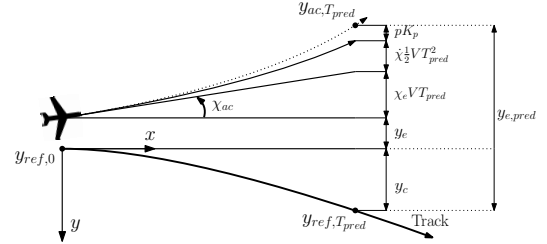


Fig. 4: Top view of the lateral flightpath predictor

The trajectory position after T_{pred} seconds, $y_{ref,T_{pred}}$ - describing the lateral position of the center of the predictor frame - can be determined directly. When both $y_{ac,T_{pred}}$ and $y_{ref,T_{pred}}$ are known, the predicted error can be calculated as shown in Equation 5 and used as input for the haptic controller. In this case $y_{ac,T_{pred}}$ has a negative value due to the orientation of the TCTF reference frame.

$$y_{e,pred} = y_{ref,T_{pred}} - y_{ac,T_{pred}} \quad (5)$$

B. Haptic feedback

There are many ways of communicating information through haptic cues. A distinction can be made between *proactive* [9] or *reactive* [18] feedback models and *guidance* [19] or *warning* [20] systems. Where *proactive* feedback exerts forces on the stick indicating the desired control input to the pilot, *reactive* feedback would, for example, increase stiffness of the stick, making it harder to give a non-desired control input.

A haptic feedback model using vibrotactile *warnings* that alert the aircraft operator when undesirable events happen can be either *proactive* (when alerting for exceeded position or velocity bounds) or *reactive* (when alerting for exceeded control input bounds). It does not help the pilot to get to the correct state, it only warns the pilot that she has moved away from a acceptable state [18]. An example is Boeing's stick shaker, which indicates a near stall situation [21].

A haptic *guidance* model uses haptic cues in a *proactive* way to urge pilot in the right direction. In this case the desired direction is the direction for which certain errors decrease. It can communicate a required change in velocity, pitch or roll rates for example [18]. Not only does this type

of haptic feedback communicate, it can also guide the pilot in certain tasks. However, if the haptic feedback does not correspond with the pilot's assessment of the situation, it can be easily misunderstood and confuse the pilot [14]. Design of the feedback is therefore paramount to its added value.

1) *Haptic Design*: Controlling the lateral position by deflecting the aileron goes through three integrative steps: from aileron deflection (δ_a) to a change in roll angle (ϕ), which results in a change in heading (ψ) which in turn results in a change in lateral position, resulting in a task hard to control by a human operator. Sachs [22] showed that using the predictor laws designed by Grunwald [17], which contain these higher-order dynamics as well, can reduce the task to a much simpler one. By including the predictor law into the control loop, part of the triple integrator introduced by the higher-order dynamics of the control task is canceled out by the double differentiator (due to the second and third term in Equation 4) of the predictor law. This results in equivalent dynamics similar to that of a single integrator, creating a situation where only proportional control is required when steering the predictor symbol.

The longitudinal control task is easier to control, as there are only two integrative steps from the elevator deflection (δ_e) to a change in flightpath angle (γ) to a change in altitude. This double integrator only requires a single differentiator in the predictor law to create equivalent dynamics similar to that of a single integrator. This single differentiator is provided by the last term in Equation 1.

By containing the higher-order dynamics to the predictor, the operator only has to provide proportional control to steer the aircraft. To make the haptic feedback as clear as possible, it is designed with the same control strategy in mind. The translation between predicted error and haptic forces is done through a haptic gain only, so that a pilot can more easily link the error shown on the TIS display and the haptic forces that he feels. Moreover, keeping the predictor symbol in the middle of the red predictor window (see Figure 2), could be considered a pursuit tracking task with preview. McRuer's cross-over model shows that for such a task the human prefers to steer through proportional control [23]. The complete block diagram of the shared control design is shown in Figure 1.

2) *Haptic Controller*: Using the prediction laws described in Section II-A1, a controller was designed using a linearized version of the Citation I model used in the experiment. This controller uses the predicted error and commands a stick deflection such that the aircraft follows the reference trajectory. The stick deflection is then converted through the inverted stick stiffness ($\frac{1}{K_s}$) to a required force ($F_{required}$). The required force is then multiplied by a haptic gain and divided by the haptic tunnel size ($\frac{K_H}{HTS}$), represented by the haptic authority block in Figure 1, and results in a guidance force ($F_{guidance}$). The resulting control laws are shown in

Equations 6 and 7.

$$F_{y, guidance} = y_{e, pred} \cdot K_{roll} \cdot \frac{1}{K_s} \cdot \frac{K_H}{HTS} \quad (6)$$

$$F_{z, guidance} = z_{e, pred} \cdot K_{pitch} \cdot \frac{1}{K_s} \cdot \frac{K_H}{HTS} \quad (7)$$

3) *Tuning of the Controller*: For each control law, two parameters were tuned to obtain a controller with an acceptable settling time. For longitudinal control these were T_{pred} and K_{pitch} and for lateral control these were T_{pred} and K_{roll} . Multiple offline simulations have been run to determine the settling time in a situation of an initial offset of 40 m and a settling threshold of 5% for different gains and prediction times. The results of which are shown in Figure 5. For lateral control stable prediction times are between 3 and 6 s, which corresponds to De Stigter [9], who found that when using the predictor laws described in Section II-A1, a prediction time for lateral control T_{pred} should be between 3 and 8 s. For longitudinal control the optimal prediction time lies around 2 s. It was decided to keep T_{pred} the same for both cases. A prediction time of 3 s was chosen as it is still fast enough for longitudinal control, but not so fast for the lateral controller to become unstable. Based on a prediction time of 3 s, the optimal values for K_{pitch} and K_{roll} could be determined at 10 and 14 respectively, the design points are indicated by the black dots in Figure 5.

4) *Haptic Profile*: The haptic tunnel size (HTS) is inserted in the last term of Equation 6 and 7 and determines the limits of the haptic profile. Once the predicted error exceeds the border of the haptic tunnel, the haptic feedback no longer increases. This is displayed in Figure 6, where the haptic force will increase up until the predicted error reaches the tunnel border, located at $-\frac{HTS}{2}$ and $\frac{HTS}{2}$. If the predicted error would increase and move closer to the tunnel border, the force displayed in the top view of the side stick would increase as well. The gradient ($\frac{\Delta F}{\Delta e_{pred}}$) of the haptic profile determines how fast and how much the haptic force will increase, describing a proportional relationship between the error on the display and the feedback through the side stick.

III. EXPERIMENT DESIGN

To investigate the effects of haptic feedback on the task-sharing performance of pilots, a within-subject simulated experiment was designed and performed. Twelve pilots with different flight experience had to perform a Tunnel-in-the-Sky (TIS) flight exercise, twice aided by haptic feedback of different levels of force and once not aided by any haptic feedback. To investigate the change in effect of the haptic feedback for different levels of difficulty, the experiment was performed for two tunnel sizes and contained lateral and longitudinal flight segments.

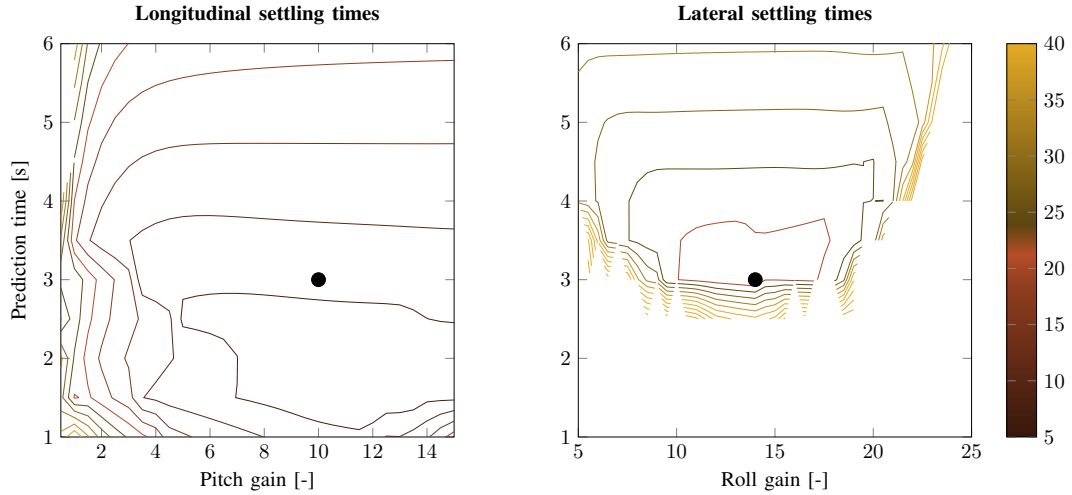


Fig. 5: Obtained settling times during offline simulations with initial offsets of 40 m and a settling threshold of 5%, with the black dots indicating the chosen design points

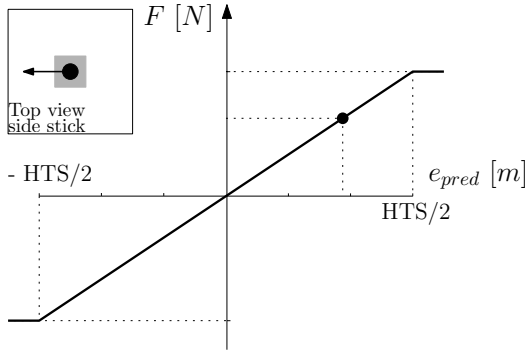


Fig. 6: Top view and haptic profile showing the relation between error, position and haptic feedback

A. Participants and Instructions

A group of commercial and private pilots was selected for the experiment. By using participants comfortable with flying, most of the learning effect of handling the plane was eliminated, so focus of the training could be on understanding the experiment-specific tasks. The experience of the pilots ranged from 37 hours to more than 3000 hours of motorised flight experience as can be seen in Table I.

Each participant received the same briefing and training before the experiment. Each pilot was instructed to first focus on flying as close to the center of the tunnel as possible (primary task) and use their remaining mental capacity to solve the secondary task superimposed on the outside visuals. To make sure the tasks get the right priority from the pilots, an answer to the secondary task only counts when the aircraft is in the tunnel. Each pilot was introduced to all the different conditions during the training phase, where pilots were encouraged to move through the tunnel and feel the increase

TABLE I: List of pilots participating in the experiment

#	Age	Flight hours
1	23	75
2	22	100
3	46	1800
4	37	205
5	23	105
6	27	270
7	26	105
8	46	100
9	23	143
10	23	37
11	41	3365
12	28	175

and decrease in haptic feedback based on the position of the predictor symbol. The length of the training phase was determined by looking at the performance in both tasks; once the performance leveled off, the training was complete. This means that not every participant got the same amount of training runs, but removing the learning effects before the evaluation phase was considered a priority.

1) *Primary Task Description:* The primary task during each run was to stay in the middle of the tunnel. The participants were assisted by a Tunnel-in-the-Sky and a superimposed predictor frame and symbol on a head-down display. The display layout can be found in Figure 7, participants had to fly either through a 20 m or 60 m tunnel, the 60 m tunnel is shown in the figure.

The trajectories flown consisted of four straight descending and four curved level segments, which were separated by short straight and level parts. Both the curved and straight segments are of the same length and duration and result in 20 s of measurements after a run-in time of 3 s (used to

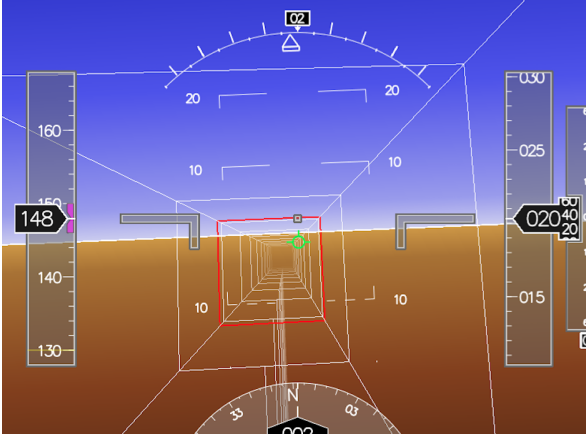


Fig. 7: Primary task, as it is shown on a head-down TIS display

get rid of transient effects). The top and side view of both trajectories can be found in Figure 8, which shows that both trajectories are mirror images of each other. This is done so that the participants are less likely to remember the trajectory by heart. Moreover, possible asymmetric effects due to the trajectory lay-out will be canceled out this way. Both trajectories had four longitudinal (A, B, C, D) and lateral (1, 2, 3, 4) segments resulting in the same height profile. Only the labeled segments were used for measurements, so the last sloping part was excluded from the data analysis as pilots can behave differently when they see the end of the tunnel.

2) *Secondary Task Description:* The participants were given a secondary task displayed in the outside visuals. This is done because of two reasons. One, theory suggests that haptic feedback will free up the visual modality, so a pilot should be able to perform better in visual tasks when assisted by haptic feedback. Two, a visual task superimposed on the outside visuals would represent an approach situation where a pilot needs to look outside regularly. How well the participant executes the secondary task indicates her task-sharing performance. Borst et al. [12] have performed a similar experiment on designing a safety augmentation system for aircraft. The secondary task used in that research was used in this experiment as well and was superimposed on the outside visuals. One of the 25 displayed shapes has a different orientation compared to the others. All participants had to indicate through the trim button on top of the side stick where the opening of this odd shape was located. Every four seconds the secondary task reset the orientation of the common and unique shape, so the participants had to answer the secondary task within four seconds to get a correct answer. After each reset the shapes change color from magenta to red and back, which helps the pilot distinguish between two successive tasks. The pilot could correct her answer within these 4 seconds, but would not get an indication whether the answer was correct or not during the runs. A picture of this visual-detection task is shown in Figure 9.

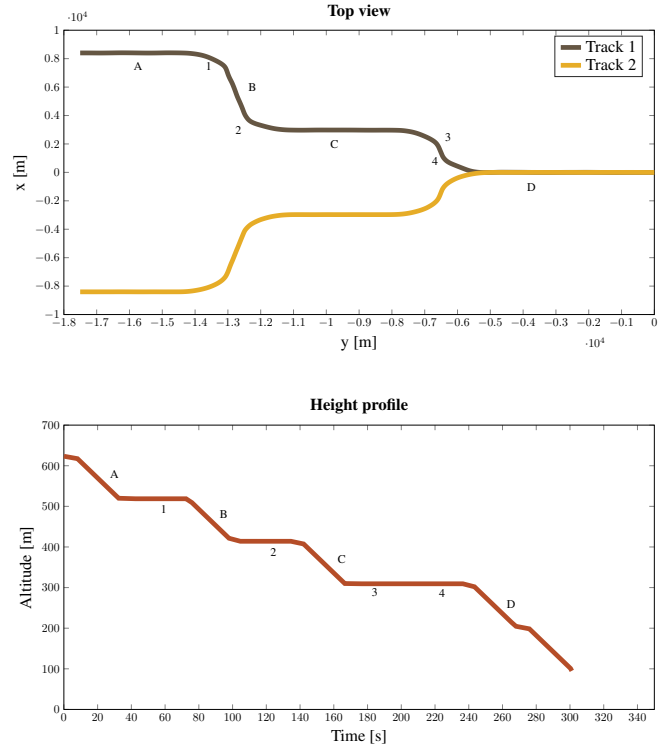


Fig. 8: Top and side view of the two trajectories flown



Fig. 9: Outside visuals, with the superimposed secondary task showing the odd figure with the opening to the left

B. Independent Variables

The experiment was set up to measure the effects of haptic feedback on the task-sharing performance during primary tasks of changing difficulty. At any one point in time, each participant was dealing with a certain combination of the following three independent variables:

1) *Visual tunnel size:* Two visual tunnel sizes (VTS) were used to increase or decrease the task difficulty. It was hypothesized that a smaller tunnel will require more focus to

fly through than a larger tunnel. In their cybernetic analysis of a TIS flight exercise Mulder and Mulder [4] tested tunnels with widths of between 10 and 80 m. And found that smaller tunnels yield better performance in terms of tracking, but require a higher control activity to do so, increasing the perceived difficulty. This increase in performance happens up to a limit as suggested by Wilckens [15] and confirmed by Mulder and Mulder [4]. They found that a 10 m tunnel is near and for some pilots over the stability boundary, while an 80 m tunnel is contributes little in terms of increase in tracking performance as it is close to the sensitivity boundary for aircraft similar to that used in the experiment. For this experiment, tunnel sizes of 20 and 60 meters have been used to create primary tasks of different difficulty, as these can be flown by all pilots and still show improvement in the tracking task.

2) *Haptic tunnel size*: The haptic tunnel size (HTS) is a measure of how fast the haptic force increases in case of a predicted error, as explained in Section II-B1. Next to a non-haptic setting, two haptic tunnel sizes were used in the experiment: 60, and 20 m, matching the visual tunnel sizes used. The first one reaches its maximum force at a predicted error of 60 m and the second, most severe one, reaches its maximum haptic force at 20 m. Table II shows which condition corresponds to which visual and haptic tunnel size and indicates where the haptic setting matches the visual setting. In Figures 10, 11 and 12 a schematic overview and haptic profile of the first three conditions from Table II are given. It can be seen that the same error results in different feedback for different haptic settings. In the 20 m case, shown in Figure 12, the maximum feedback force has been reached already, where in the 60 m feedback case, shown in Figure 12, the border of the tunnel is not yet reached, corresponding to the position of the predictor symbol compared to the edge of the visual tunnel. In Figure 10 no haptic feedback is provided at all. Note that the predictor symbol is shown as it is seen by the pilot, not as it is seen from the top, so in this view it is flipped 90°. For a 20 m visual tunnel size and for longitudinal segments, the layout of the haptics is the same.

TABLE II: The visual and haptic tunnel size of each condition

#	VTS	HTS	VTS vs. HTS
1	60	0	No haptics
2	60	60	Match
3	60	20	Mismatch
4	20	0	No haptics
5	20	60	Mismatch
6	20	20	Match

The side stick has the same dynamics in every direction, but the aircraft does not. As control in the vertical direction is much faster, less forces are required to steer the aircraft. The maximum haptic force in vertical direction is 2.9 N, where it is 8.6 N for the horizontal channel. As these forces are

equivalent to less than 1 kg of force, it can be seen that both haptic channels can easily be overruled by the human operator.

3) *Segment type*: During each run the pilots will fly through two segment types (ST): lateral and longitudinal. The longitudinal segments had a flight path angle of -3° which is comparable to what aircraft fly during normal operation. The lateral segments were similar to rate 1 turns, where the aircraft had to maintain a bank angle of 30° and resulted in a heading change of 40° . Both segments took around 27 s to fly through, with a run-in and run-out time between 3 and 4 s. This provided 20 s of measurements during each segment. All measured segments were separated by a straight segment of 10 s, removing most of the transient effects. It is hypothesized that flying through the lateral segments is more challenging than through the longitudinal segments. This variable therefore, just as the varying visual tunnel size, will help indicate the effect of haptic feedback during tasks of changing difficulty.

C. Dependent Measures

To measure the effects of varying independent variables, measures in four categories were defined and recorded. The following four areas of interest can be distinguished for testing the hypotheses: primary task performance, task-sharing performance, haptic performance and subjective measures.

1) *Primary task performance*: The general performance of the pilot during each run and for each condition. By measuring the *root-mean-square values* (RMS) of the *horizontal* and *vertical position errors*, conclusions can be drawn on the primary task performance for each condition. Moreover the *roll* and *pitch rates* of the aircraft are measured to get insights in what kind of steering inputs were required to reach the measured performance.

2) *Task-sharing performance*: To determine the mental capacity the pilot has to spare when performing the primary task, the *success rate* and *average time to answer* the secondary task were measured. By means of an eye-tracker, the *head-up time* of each pilot were measured, indicating how much time he could allocate to the secondary task.

3) *Haptic performance*: To investigate how the haptic feedback is used by the pilots, *control activity* of both *human* and *machine* was measured. This helps to explain the effect of adding haptic feedback to the human control effort and gives insights in how compliant the human is to the haptic forces. Using the *haptic* and *human forces*, the haptic contribution was determined according to:

$$Haptic\ contribution = \frac{|F_{haptic}|}{|F_{human}| + |F_{haptic}|} \quad (8)$$

4) *Mental effort rating*: As a measure of effort needed during the complete run, each pilot was asked to indicate his *mental effort* on a Rating Scale Mental Effort [24] after

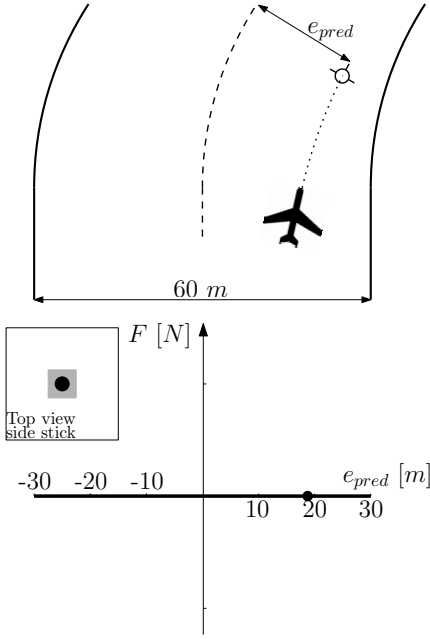


Fig. 10: Haptic profile of the non haptic setting and a VTS of 60 m

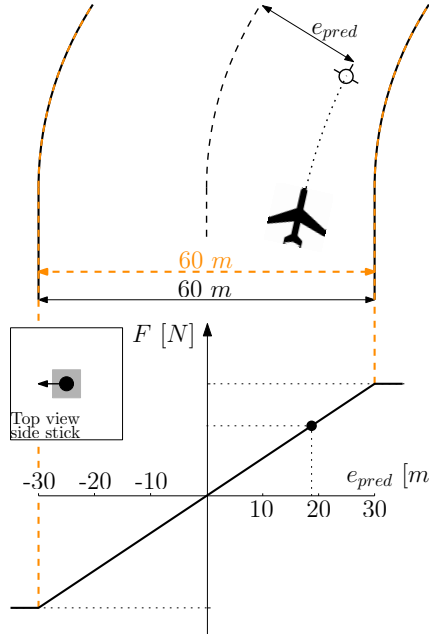


Fig. 11: Haptic profile of a HTS of 60 m and a VTS of 60 m

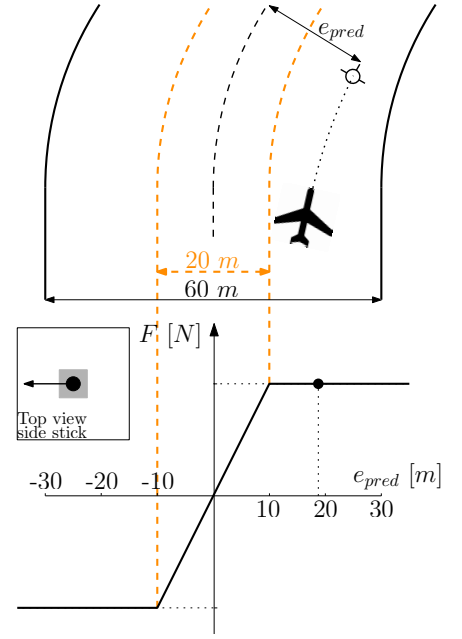


Fig. 12: Haptic profile of a HTS of 60 m and a VTS of 20 m

each run. This measure can be used to get a sense of mental workload experienced during each condition.

D. Apparatus

1) *Flight simulator*: The experiment was performed in the SIMONA (SIMulation, MOTion and NAVigation) Research Simulator (SRS) at Delft University of Technology, which can be seen in Figure 13. This SRS is a 6 degree-of-freedom (DOF), motion-based research flight simulator with a configurable flight deck. It has a wide-view ($180^\circ \times 40^\circ$) collimated outside visual display with a refresh rate of 120 Hz. It uses electric control loading so that stick dynamic properties are configurable.

2) *Setup*: The aircraft model used by the simulator is the DASMAT nonlinear Cessna Citation I model [26] developed at the Aerospace Engineering Faculty at Delft University of Technology. The aircraft was controlled only through elevator and aileron deflection as commanded by the right-handed side stick. The auto throttle was engaged, which kept the aircraft at 148 ± 4 kts at all times and the landing gear was retracted during the complete experiment.

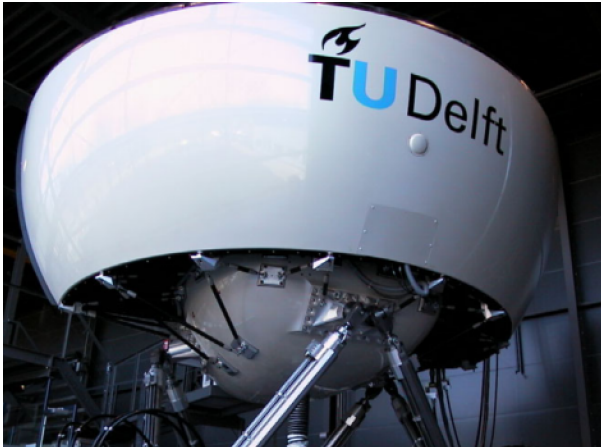
3) *Side stick*: The participants will control the aircraft using a 2 DOF side stick, with which they control roll and pitch of the aircraft. As the stick is control-loaded, haptic feedback can be provided through it. The motion range was $\pm 18^\circ$ for pitch and $\pm 10^\circ$ for roll. Second order (mass, spring and damper) dynamics were simulated on the side stick. The following transfer function describes the relationship between forces exerted on the stick and its rotation:

$$H_s(s) = \frac{1}{I_s s^2 + b_s s + K_s} \quad (9)$$

For both the pitch and roll direction an inertia of $I_s = 0.03 \text{ N s}^2/\text{°}$, $b_s = 0.22 \text{ N s}/\text{°}$ and $k_s = 1 \text{ N}/\text{°}$ was used.

4) *Eye-tracker*: To get a clearer understanding of the reaction of the participants to haptic or visual cues an eye-tracker from faceLAB [27] was installed for the experiment. A head model of each pilot was made at the start of each session, so that the direction of his gaze could be determined. The device can track eye rotations up to $\pm 45^\circ$ along the y -axis (up and down) and $\pm 22^\circ$ along the x -axis (left and right), and head rotations up to $\pm 90^\circ$ in y -direction and $\pm 45^\circ$ in x -direction [27]. As the eye-tracker data was synchronized and contains a time-stamp, together these measurements can determine whether the pilot is looking up or down and at what moment.

In the post-experiment processing, the eye-tracker data was filtered using a median filter, which removes all points more than 3σ away from the median value of six of its neighbours left and right. Data analysis shows that only peaks shorter than 100 ms are removed this way, which is lower than the minimum time a human needs to switch and adjust his gaze according to Majaranta et al. (min = 180 ms) [28] and Mollenbach et al. (min = 124 ms) [29]. Therefore it can be considered a correct way of filtering. After this the most head-up and head-down position is determined by taking the median of the top and bottom 20% of the eye-tracker data. The value



(a) Outside view



(b) Inside view

Fig. 13: The SIMONA (SIMulation, MOTion and NAVigation) Research Simulator (SRS) at Delft University of Technology [25]

in the middle of these medians is considered the split value, all data above this point is considered head-up, while all data below this point is considered head-down. In Figure 14 the filtered eye-tracker data for one segment is shown. The lines indicate the top, bottom and split values, while the marker indicates whether a new secondary task appeared or a task got answered. It can be seen that this candidate looks up when a new task appears and looks down once he has found the answer. In this segment the candidate only gave correct answers.

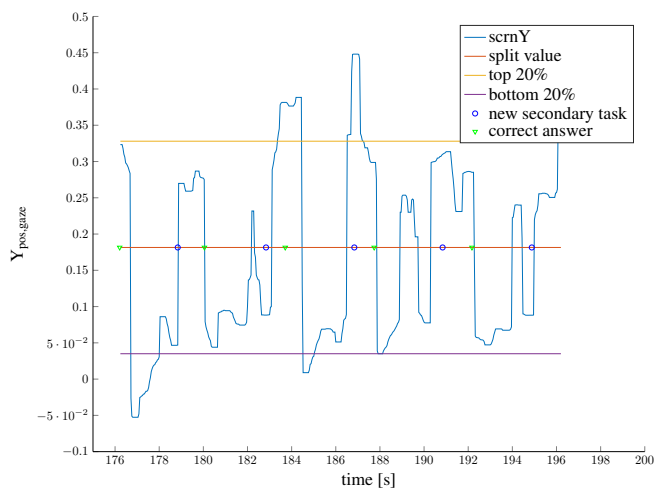


Fig. 14: Filtered eye-tracker data including secondary task appearance and time of answers

E. Experiment Procedures

1) *Training*: In the first two training runs the pilots could familiarize themselves with the dynamics of the modeled aircraft and the workings of the flight path predictor and the predictor window without haptics. In the runs thereafter the

haptic feedback was introduced, during which the pilots were encouraged to move through the tunnel to explore the effects of the haptic feedback. During the last part of the training the secondary task was introduced as well. This task was then practiced for different visual and haptic tunnel sizes. Pilots were considered well-trained once the RMS errors and secondary task performance leveled off. This was done to remove the learning effect from the evaluation phase. The training run trajectory is similar to the one in the evaluation phase, only the segments are of half length.

2) *Evaluation*: The evaluation phase of the experiment consisted of twelve runs, with six different combinations of visual and haptic tunnel size on two different trajectories, which are mirror images of each other. The order of runs was randomised and each participant started with a different condition in a balanced Latin-square design. During each run of around five minutes, the participants would fly through four straight sloped (longitudinal) and four level curved (lateral) segments. A break was planned after run six, in order to keep the pilot fit and focused for the last runs.

After each run, the pilots were asked to rate their mental effort on the Rating Scale Mental Effort and to comment on the haptic they thought they felt. As feedback and encouragement to the pilots, the RMS errors in horizontal and vertical direction and the percentage of correct answers to the secondary task were shared.

3) *Haptic only run*: For a haptic tunnel size of 20 m, the aircraft is able to follow the trajectory by means of haptic inputs only. The scores of this run in terms of primary task performance and haptic inputs were recorded as well; these scores serve as a baseline performance for the 20 m haptic setting. For a haptic tunnel size of 60 m the aircraft could not follow the trajectory and would eventually crash, so no scores

could be recorded for a complete run, making comparison to the shared control situation impossible.

F. Hypotheses

Using the defined experiment setup the following hypotheses were researched:

1) *Haptic feedback will increase the task-sharing performance of the pilot:* The continuous haptic guidance will not only work as a means of communicating the right course of action, it will also guide the pilot towards the right direction by means of shared control. These two advantages should leave the pilot with more mental capacity to perform the secondary task. It is therefore expected that the secondary task performance will increase when haptic feedback is applied. Additionally, the head-up time is expected to increase as it is hypothesized that the haptic feedback will free up the visual modality. In order to accept the hypothesis it will be checked that the primary task performance will not deteriorate when haptic feedback is applied.

2) *The added benefit of haptic feedback on the task-sharing performance of the pilot will be more distinct for a more challenging primary task:* As mental workload will increase when the difficulty of the primary task increases, the effect of the haptic aid is hypothesized to become larger. It is expected that the secondary task performance will increase more, compared to the non-haptic case, for a condition with a smaller tunnel size or a curved (instead of straight) segment as those tasks require more mental effort from the pilot.

3) *After a certain threshold, increase in haptic forces will result in less acceptance and less clear communication to the pilot:* Haptic feedback helps the operator in two ways: guidance and communication. The guidance will help by providing steering inputs in the right direction and therefore changing the course of the aircraft. These steering inputs can be felt by the operator and allow her to determine the errors not only by looking to the TIS display, but also by feeling the haptic forces on the stick. In previous studies it has been found that stronger feedback can cause decreased acceptance and less clear communication to the pilot [7], [9], [13], [14]. By using two haptic settings and an eye-tracker, the experiment conducted aimed at getting insights in the communication part of the haptic feedback. It is expected that a strong - to the pilot unexpected - haptic input will cause to pilot to check the TIS display to help her understand the situation and thus cause her to look down more often. When the haptic tunnel has stricter boundaries than the visual tunnel, a lower acceptance and therefore more gaze switches to the TIS display are expected.

IV. RESULTS

A. Primary task performance

For the primary task performance the horizontal and vertical error with respect to the middle of the tunnel have been used as dependent measures. The roll and pitch rates

have been recorded and examined to provide insight in the comfort of the flight. Figures 15 and 16 show the 95% confidence intervals of the horizontal and vertical errors during longitudinal and lateral flight segments for the 60 m and 20 m tunnel, respectively.

The confidence bands of the horizontal error during the horizontal segments contain a bias towards a positive error. This means that the aircraft position is on average a little to the left of the trajectory during these segments. This may be caused by the fact that the pilot is seated on the right side during the experiment, meaning that his reference frame is not perfectly aligned with that of the aircraft. It can also be seen that the vertical error increases during the longitudinal segments, meaning that the pilot is drifting away from the center of the tunnel, as he compensates too little for the descending trajectory. During the lateral segments, the vertical error increases at first and decreases again after a while, meaning that the pilot gives a too severe pitch up input during in the beginning of the lateral segment.

The 95% confidence bands are more narrow in the case of the 20 m tunnel, indicating that it is easier for the pilots to determine and stay close to the center of the tunnel. Moreover, it can be seen that the bandwidth of errors in both directions decreases when more haptic feedback is applied, this holds for both segment types and tunnel sizes.

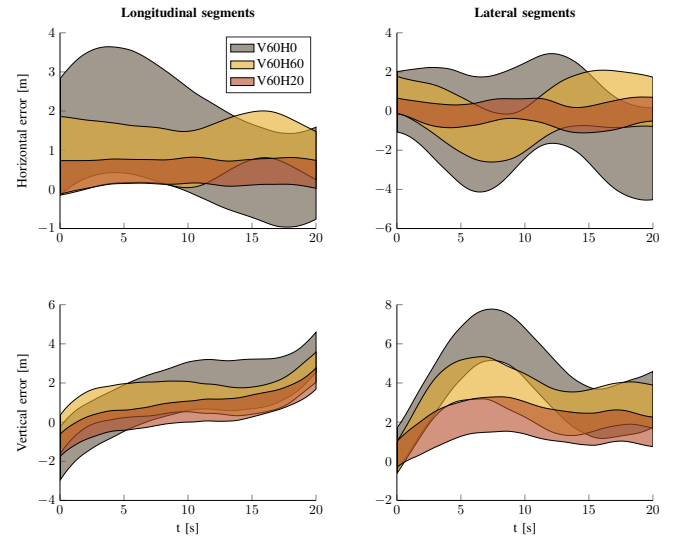


Fig. 15: 95% confidence interval of the position errors for all haptic settings and a visual tunnel size of 60 m

Figure 17 shows a box plot of the RMS values of the errors of all participants for all conditions. As in Figures 15 and 16 a clear improvement in primary task performance can be seen when the level of haptic feedback increases. This performance increase is larger in the 60 m tunnel case, as the baseline (no haptics) performance is worse for this tunnel size. The

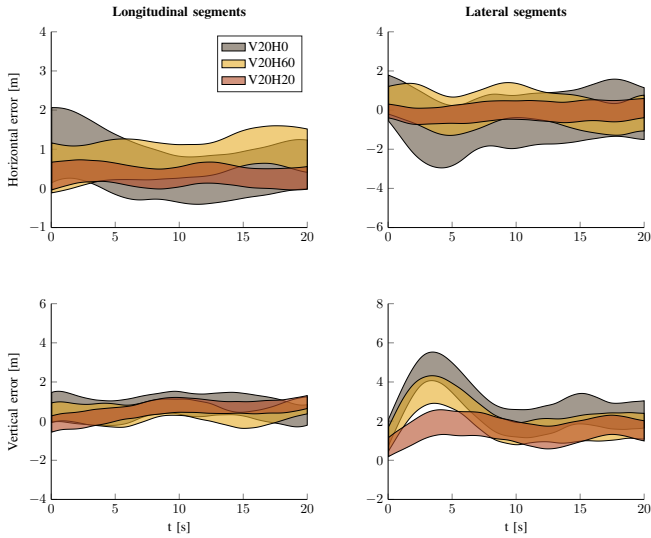


Fig. 16: 95% confidence interval of the position errors for all haptic settings and a visual tunnel size of 20 m

errors in both directions are higher for the lateral segments, showing that this segment type is indeed more difficult. For the conditions with a haptic tunnel size of 20 m, the aircraft was able to follow the trajectory by haptic inputs alone. The results of this haptic-only run are displayed by the dot in the third and sixth column. It can be seen that the haptic-only case is on par with the best shared control case in terms of horizontal error. For the vertical error, shared control generates smaller errors, except for the lateral parts with a visual tunnel size of 60 m, where the haptic performance is within the box, close to the median score of the shared control cases. This means that human and machine together perform better than the machine alone.

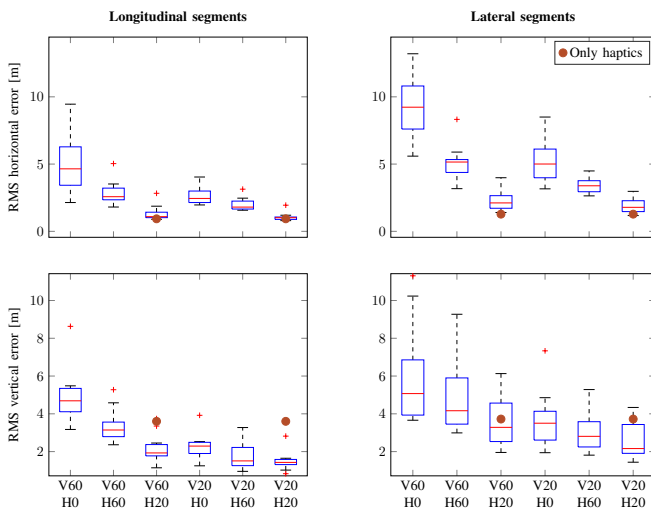


Fig. 17: RMS values of the position errors for all conditions

From a repeated measures analysis of variance (ANOVA)

significant differences ($p < 0.01$) in horizontal and vertical error were found for all three independent variables: segment type (ST), visual tunnel size (VTS) and haptic tunnel size (HTS). A post-hoc analysis was performed to do a pairwise comparison (one haptic setting compared to another). It was found that the differences between all three haptic settings were highly significant ($p < 0.01$) as well after a Bonferroni correction to adjust for multiple comparisons. The repeated measure also indicates significant interaction for $VTS \times HTS$ and $ST \times HTS$, confirming that the primary task performance increases more in a 60 m tunnel and a lateral segment for increasing haptic aid.

Figure 18 shows the RMS values of roll and pitch rates of all participants for all conditions. It can be seen that pitch and roll rates are higher for lateral segments. Both rates decrease when more haptic feedback is applied, resulting in a more comfortable flight. This indicates that the haptic feedback not only improves the precision of the flight, but does this in a comfortable manner. Just as for the RMS values of the error in Figure 17, the effect of the haptic aid is more pronounced in the horizontal direction. The haptic-only run shows lower pitch and roll rates for all segments.

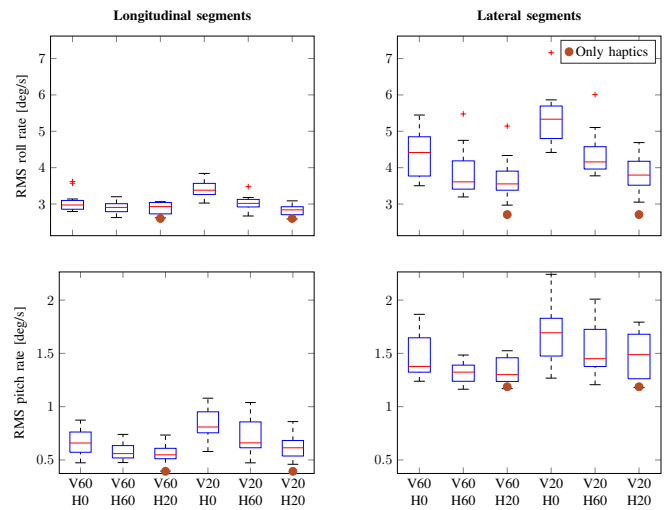


Fig. 18: RMS values of the roll and pitch rates for all conditions

From a repeated measures ANOVA significant differences ($p < 0.01$) in pitch and roll rates were found for all three independent variables: segment type (ST), visual tunnel size (VTS) and haptic tunnel size (HTS). From a post-hoc analysis with Bonferroni correction it was found that the differences in roll rates were significant ($p = 0.035$) for all HTS. For roll rates all difference between haptic settings were found to be highly significant ($p < 0.01$). For pitch rates, no significant difference was found for the difference between HTS 20 and 60.

B. Task-sharing performance

The effect of haptics on the primary task performance was shown to be positive as it reduces the RMS errors and pitch and roll rates. But in order to evaluate the task-sharing performance, the secondary task performance should be considered as well. In Figure 19 the box plots of two indicators for the secondary task performance are shown: the percentage of *correctly answered secondary tasks* and the *average time to answer*.

The secondary task performance is hypothesized to go up when haptic feedback increases and is expected to be most distinct for the most challenging task (i.e. a lateral segment in a 20 m tunnel) as the baseline performance is expected to be lowest here. The top two plots show the secondary task performance in terms of *percentage of correct answers* and it can be seen that except for the lateral 60 m tunnel segments, the performance increases with the level of haptic feedback. The bottom two plots show that the *average time to answer* decreases with increasing haptic feedback for all conditions, except for the easiest task, the longitudinal 60 m tunnel segments.

Two other metrics measured to determine the level of task-sharing performance are the *head-up time* and *gaze switches*; box plots of these metrics can be found in Figure 20. These metrics give an insight into how clear the haptics are to the operator. When the haptic cues are hard to understand it is expected that the pilot looks down to the TIS display longer and more often.

The *head-up time* was also expected to increase when more haptic aid was applied, but although some trends can be seen indicating this to be true in the top row of Figure 20, the data is not really conclusive. A possible explanation is that a decrease in *time to answer* will allow a larger portion of the time to be spent head-down on the primary task, counteracting the expected effect of the freed up visual modality on head-up time. This behaviour can be seen in Figure 14 as well, where a participant looks down again right after answering the secondary task and only looks up again after seeing the new secondary task appear in his peripheral vision, effectively decreasing the head-up time for decreasing answering time. A positive relation between level of haptic feedback and number of *gaze switches* can be found in the bottom two plots in Figure 20.

For the objective measures used to determine the task-sharing performance a repeated measures ANOVA was performed to determine the significance of the results. These are presented in Tables III and IV. It is found that the haptic and visual tunnel size have a significant effect on the *percentage of correct answers* to the secondary task. Where it has to be noted that a post-hoc analysis using a Bonferroni correction points out this is not the case for the difference

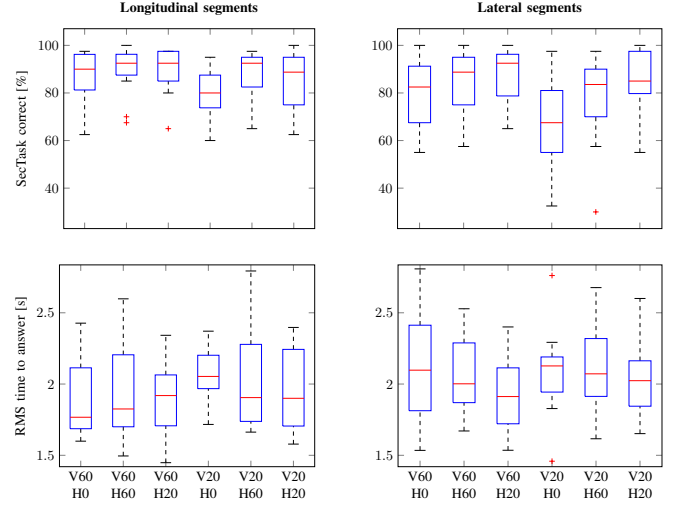


Fig. 19: Percentage of correct answers and average time to give a correct answer

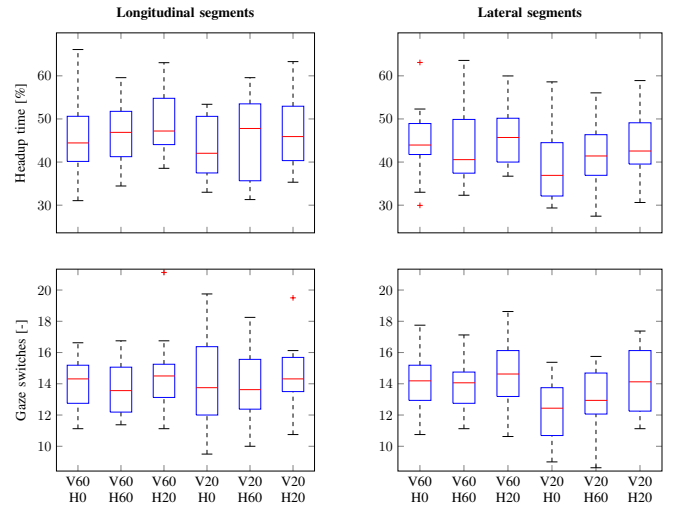


Fig. 20: Head-up time and gaze switches

between a haptic tunnel size of 60 m and 20 m, but still true when comparing the haptic and non-haptic case. The effect of tunnel segment type on the secondary task success is only just significant ($p = 0.05$). When looking at the interactions found by the ANOVA, it can be seen that both visual tunnel size ($VTS \times HTS$, $p = 0.047$) and segment type ($ST \times HTS$, $p < 0.01$) have a significant influence on the increase of *percentage of correct answers* due to the increase in haptic feedback. When considering Figure 19, it can be seen that for a smaller visual tunnels and lateral segments, haptic feedback is more effective in increasing secondary task performance.

The trends in *average time to answer correctly* are less clear. Statistical analysis shows that there is a significant difference in measured data for different segment types and haptic settings. A post-hoc analysis showed that this does not

hold for the difference between a haptic tunnel size of 60 m and 20 m ($p = 0.125$). No significant interactions were found.

A significant change in *head-up time* has been observed between segment types and - by means of a post-hoc Bonferroni analysis - between the no-haptic and 20 m haptic case. Other pairwise comparisons of haptic tunnel sizes do not show significant effects. Here too, no significant interactions were found.

There is an increase to be seen in the number of *gaze changes* when haptic feedback is increased, this increase is only significant between a haptic tunnel size of 60 m and 20 m however. The other differences are not significant as can be seen in Table IV and there were no significant interactions.

TABLE III: Main effects from the analysis of variance secondary task success rate and the average time needed to give a correct answer

<i>SecTask success</i>	<i>ST</i>	$F_{1,11} = 4.823$	$p = 0.05$
	<i>VTS</i>	$F_{1,11} = 13.22$	$p < 0.01$
	<i>HTS</i>	$F_{2,22} = 12.083$	$p < 0.01$
<i>RMS tanswer,correct</i>	<i>ST</i>	$F_{1,11} = 26.873$	$p < 0.01$
	<i>VTS</i>	$F_{1,11} = 4.283$	$p = 0.06$
	<i>HTS</i>	$F_{2,22} = 3.787$	$p = 0.04$

TABLE IV: Analysis of variance for the headup time and gaze switches

<i>Headup time</i>	<i>ST</i>	$F_{1,11} = 9.599$	$p = 0.01$
	<i>VTS</i>	$F_{1,11} = 2.466$	$p = 0.145$
	<i>HTS</i>	$F_{2,22} = 4.312$	$p = 0.03$
<i>Gaze switches</i>	<i>ST</i>	$F_{1,11} = 4.648$	$p = 0.054$
	<i>VTS</i>	$F_{1,11} = 8.206$	$p = 0.153$
	<i>HTS</i>	$F_{2,22} = 3.228$	$p = 0.059$

C. Haptic performance

To see if the haptic feedback is working as intended, the human and haptic control forces have been measured throughout each run. In Figure 21 the box plot of the RMS values of the haptic inputs is shown. For the conditions without feedback, the RMS of the haptic feedback force is exactly zero. When the feedback increases, the haptic forces do as well. The highest forces are found during runs with a haptic tunnel size of 20 m in the lateral segments and are around 2.5 N on average. For the run with haptic inputs, only the haptic roll forces in longitudinal segments are comparable to those for runs *with* human inputs as well. In lateral segments the haptic forces of runs *without* human interaction are lower than for the runs *with* human interaction. The pitch inputs of the haptic controller in the longitudinal segments are higher *without* than *with* human interaction, for the lateral segments the pitch inputs are comparable for runs *with* and *without* human involvement.

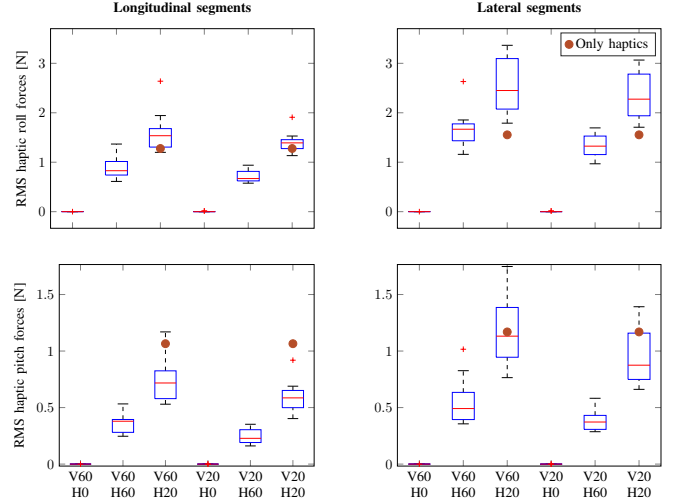


Fig. 21: RMS values of the haptic forces for roll and pitch

Any change in an independent variable results in a significant change in the RMS of the haptic control forces ($p > 0.01$); this holds for changes between all haptic settings. The changes seen in Figure 21 are dominated by changing haptic feedback, which is expected, as the independent variable HTS is closely linked to the dependent measure haptic force. Moreover, significant interaction was found $VTS \times HTS$, indicating that the effect of an increase in haptic feedback does depend on tunnel size. For this statistical analysis, the non-haptic conditions were not taken into account.

Properly applied feedback should decrease the level of human control activity. Figure 22 shows the box plot of the RMS values of the human control forces in roll and pitch direction. The trend here moves against that of the haptic forces; when haptic feedback increases, human control activity decreases, indicating that the human operator is letting the haptic controller take over part of the control.

A repeated measure ANOVA shows that human roll forces change significantly when changing the independent variables as shown in Table V. Unexpectedly, for the human induced pitch force this is not true for a change in haptic settings. Only between no haptics and a haptic tunnel size of 60 m does the human induced pitch force change significantly ($p < 0.01$), a possible explanation is the large spread in human pitch inputs for the 20 m haptic setting, shown in Figure 22. Significant interactions were found for $VTS \times HTS$ ($p = 0.02$) and $ST \times HTS$ ($p = 0.023$).

The haptic contribution is a measure of the amount of haptic forces compared to the total force on the stick. A haptic contribution of zero means that the human operator does all the steering, whereas a haptic contribution of one indicates that the haptic controller is doing all the steering. A time signal

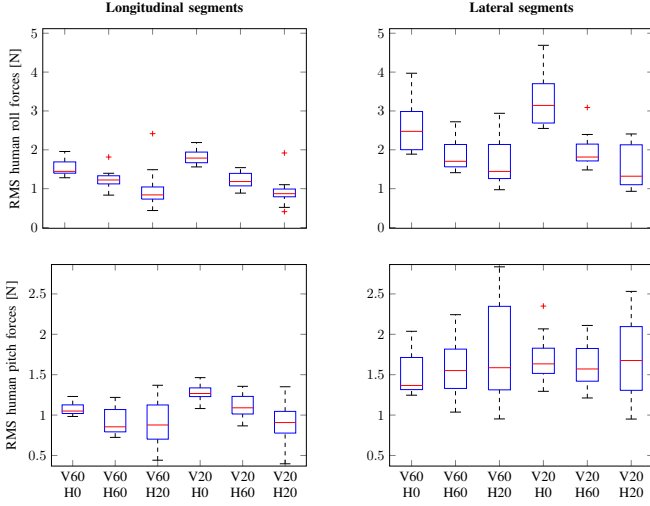


Fig. 22: RMS values of the human forces for roll and pitch

TABLE V: Main effects from the analysis of variance of the RMS human forces

$RMS F_{human,roll}$	ST	$F_{1,11} = 55.252$	$p < 0.01$
	VTS	$F_{1,11} = 39.857$	$p = 0.046$
	HTS	$F_{2,22} = 59.002$	$p < 0.01$
$RMS F_{human,pitch}$	ST	$F_{1,11} = 31.967$	$p < 0.01$
	VTS	$F_{1,11} = 39.857$	$p < 0.01$
	HTS	$F_{1,082,11.904} = 0.975$	$p = 0.35$

of the haptic contribution was generated and in Figure 23 the RMS values of these time signals for each condition are given.

The haptic contribution changes significantly for changing visual and haptic tunnel size, as shown in Table VI. The segment type has no significant effect on the proportion of haptic forces in both pitch and roll direction. For the haptic contribution in pitch direction the only interaction found was between VTS and HTS, in roll direction there was not only interaction between VTS and HTS; but also between ST and HTS. All these interaction were highly significant ($p < 0.01$). Only the haptic conditions have been used for the statistical analysis.

TABLE VI: Main effects from the analysis of variance of the haptic contribution (only for haptic conditions)

$Haptic\ contribution\ roll$	ST	$F_{1,11} = 2.050$	$p = 0.18$
	VTS	$F_{1,11} = 25.009$	$p < 0.01$
	HTS	$F_{2,22} = 100.628$	$p < 0.01$
$Haptic\ contribution\ pitch$	ST	$F_{1,11} = 0.242$	$p = 0.632$
	VTS	$F_{1,11} = 25.941$	$p < 0.01$
	HTS	$F_{2,22} = 79.735$	$p < 0.01$

D. Mental effort rating

In addition to the objective measures, a subjective measure was recorded as well. After each run the participant was asked to rate their mental effort required for executing

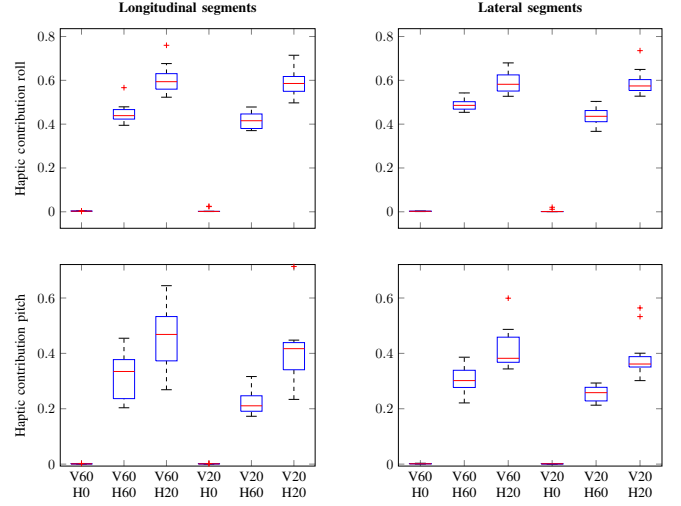


Fig. 23: RMS values of the actual haptic contribution in horizontal and vertical direction

both the primary and secondary task on a rating scale from 0 (no mental effort) to 150 (extreme mental effort). These results were normalized for each participant; the normalized z-scores can be found in Figure 24. As a run consists of both longitudinal and lateral segments, the mental effort ratings are those for a combination of segment types. A well-designed haptic feedback controller should decrease the mental effort needed by the pilot. This trend is indeed visible and again more distinct for the 20 m tunnel size.

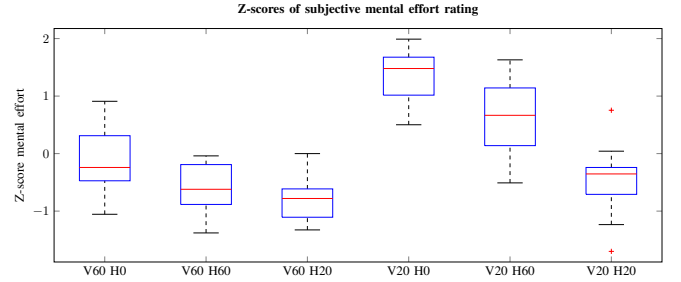


Fig. 24: Z-scores of subjective rating of the mental effort of the participants for each condition

The subjective effort rating shows significant differences for both the haptic ($F_{1,11} = 47.715$; $p < 0.01$) and visual tunnel size ($F_{2,22} = 42.263$; $p < 0.01$). A pairwise comparison using Bonferroni also shows significant differences between all haptic settings ($p < 0.01$). The difference in mental effort due to tunnel segment was not recorded, as all runs contained both segments. Moreover, significant interaction between visual and haptic tunnel size was found, indicating that the effect of haptic feedback on the mental effort rating is greater for the 20 m tunnel, which can be seen in Figure 24 as well.

V. DISCUSSION

When considering Figures 15 and 16 a few phenomena stand out. As mentioned in Section IV-A, the aircraft flies on average a little to the left of the trajectory during longitudinal segments. An explanation for this is that the pilot aligns the aircraft with the runway that is visible in the outside visuals during the last two horizontal segments, while seated on the right side in the cockpit. As an operator will use his eyes' position as reference, aligning these with the runway ahead will cause a slight bias in aircraft position to the left.

Secondly, for all haptic settings the vertical error during the longitudinal segments increases, which is especially apparent in the 60 m tunnel. This indicates that the pilots do not account for the descending trajectory enough to stay in the middle of the tunnel. More haptic feedback does little to improve this error, which could be because a prediction time of 3 s is too large for tight longitudinal control. Because of this, the current error (z_e) term within the predicted error ($z_{e,pred}$) is too small. This corresponds to the findings of Grunwald [17], which indicate that a prediction time of 3 s is quite large for longitudinal control, resulting in a worse tracking performance. This is confirmed by the roll and pitch rates of the haptic-only runs, which are lower than those of the shared control runs for all segments, indicating that the haptic controller has a more conservative approach in correcting errors. This holds true especially in the vertical direction, where the haptic controller prefers to use slow pitch rates over removing the error as soon as possible.

Lastly, the most clear and surprising phenomenon can be seen for the vertical error bands during the lateral segments; the vertical error increases during the first part of the turn and decreases again after around 4 s and 7 s for the 60 m and 20 m tunnel, respectively. A possible explanation for this behaviour is that the pilots were not used to the dynamics of the aircraft. This may have caused the pilots to over-compensate to keep the turn level when commencing a turn, causing the aircraft to climb in the beginning of the lateral segments, only later steering to correct this mistake. It can also be seen that the 20 m haptic setting greatly reduces this phenomenon, as the pilots can not only see, but also feel they are making a mistake.

The results of the haptic-only run (HTS20) show that for the best performance in terms of horizontal error, the human should have been completely compliant to the haptic inputs, as the haptic controller by itself matches the best performance of the shared control runs. It can be seen that the human pilot adds an inefficiency here, resulting in a less optimal result. A haptic design like this might be good for performance, but over-reliance and degradation of human awareness are serious risks. For the vertical errors in the longitudinal segments, shared control clearly outperforms the haptic-only case, thus putting a larger emphasis on human involvement, decreasing the risks of over-reliance and degradation of human

awareness. Whether or not a haptic controller that could steer the aircraft completely by itself is a good thing, should be investigated, especially in relation to the aforementioned risks.

This means that, when designing a system like this, the level of haptic feedback provided to the operator should be determined carefully. If - like for the 20 m haptics case - the automation is able to fly the aircraft by itself, the risk of over-reliance presents itself. As the human operator could just sit back and let the aircraft fly, which is not desirable, especially in more intensive parts of the flight envelope, like the approach phase. Over-reliance on automation is a real problem in aviation. The National Transportation Safety Board found this to be the cause of the first fatal accident in 5 years in commercial aviation in the United States in 2014 [30]. In 2016, the first hull loss of Emirates in 31 years also happened because of over-reliance and a poor understanding of automation by the human pilots [31]. Opting for the less present haptic feedback setting results in a human control input between 50% and 80% during the complete flight, while still improving the task-sharing performance significantly.

When increasing the level of haptic feedback from 60 m to 20 m, two things happen: the secondary task success rate and average time to answer do not increase, but the number of gaze changes increases significantly. This indicates that the pilots have trouble understanding - or maybe getting confused by - the more present haptic feedback. In order to understand what is going on they have to look at the TIS display. This means that the measured increase in tracking performance between the haptic tunnel sizes of 60 m and 20 m should be attributed mostly to an increase in guidance and less to multi-modal communication. This confirms that after a certain threshold, an increase in haptic forces can force the pilot to look down for a visual explanation of the forces that are felt as stated in the third hypothesis.

Looking at the decreasing subjective effort rating during an increase in haptic forces, it seems as if the pilots accept even the 20 m haptic forces, as their perceived mental effort decreases. The decrease in performance compared to the haptic-only case however, indicate that the pilots are not completely accepting the haptic inputs. Therefore this part of the third hypothesis cannot be confirmed nor rejected.

Considering that when the 60 m haptic feedback is applied the human still contributes significantly to the control of the aircraft, while the task-sharing performance increases and the pilots do not need to check the TIS display more often, the first hypothesis can be confirmed for this haptic feedback setting. Moreover, considering the fact that the improvement is more distinct for a more challenging primary task, the second hypotheses stated in Section III-F can be accepted as well.

VI. CONCLUSION

Adding haptic feedback to a Tunnel-in-the-Sky approach does increase tracking performance. Moreover, it increases task-sharing performance in terms of secondary task success, average time to answer and head-up time. These effects are more distinct for a more challenging primary task like a smaller tunnel and a curved trajectory. These effects were already observed for the least present haptic case. Adding more haptic feedback can make communications less clear for the pilot, causing him to look at the Tunnel-in-the-Sky more often in order to understand the haptic cues given by the controller. Stronger haptic feedback can also decrease the level of acceptance of the haptic inputs by the operator, even though the mental effort of the operator does decrease when haptic feedback is increased. Next to this, a risk of over-reliance is introduced when the haptic controller can follow the trajectory by itself and the human does not necessarily need to provide control inputs.

REFERENCES

- [1] J. Gibson, *The Ecological Approach to Visual Perception*. Boston: Houghton Mifflin, 1979.
- [2] G. Lintern, T. Waite, and P. Talleur, "Functional Interface Design for the Modern Aircraft Cockpit," *International Journal of Aviation Psychology*, vol. 9, no. 3, pp. 203–223, 1999.
- [3] C. Borst, M. Mulder, M. M. Van Paassen, and J. A. Mulder, "Path-Oriented Control/Display Augmentation for Perspective Flight-Path Displays," *Journal of Guidance, Control, and Dynamics*, vol. 29, no. 4, pp. 780–791, 2006. [Online]. Available: <http://arc.aiaa.org/doi/10.2514/1.16469>
- [4] M. Mulder and J. A. Mulder, "Cybernetic Analysis of Perspective Flight-Path Display Dimensions," *Journal of Guidance, Control, and Dynamics*, vol. 28, no. 3, pp. 398–411, 2005.
- [5] M. W. Anderson, "Flight Test Certification of Multipurpose Head-Up Display for General Aviation Aircraft," *Journal of Aircraft*, vol. 33, no. 3, pp. 532–538, 1996.
- [6] T. Lombaerts, G. Looye, J. Ellerbroek, and M. Rodriguez, "Design and Piloted Simulator Evaluation of Adaptive Safe Flight Envelope Protection Algorithm," no. January, pp. 1–25, 2016.
- [7] M. Mulder, D. Abbink, and E. Boer, "Sharing Control With Haptics Seamless Driver Support From Manual to Automatic Control," *Human Factors: The Journal of the Human Factors and Ergonomics Society*, vol. 54, no. 5, pp. 786–798, 2012.
- [8] S. de Stigter, M. Mulder, and M. M. van Paassen, "On the Equivalence Between Flight Directors and Flight Path Predictors in Aircraft Guidance," *Proc. of the AIAA Modeling and Simulation Technologies Conference, San Francisco (CA)*, no. AIAA-2005-5962, pp. 1–20, 2005.
- [9] —, "Design and Evaluation of a Haptic Flight Director," *Journal of Guidance, Control, and Dynamics*, vol. 30, no. 1, pp. 35–46, 2007. [Online]. Available: <http://arc.aiaa.org/doi/abs/10.2514/1.20593>
- [10] C. D. Wickens, "The Structure of Attentional Resources," in *Attention and Performance VIII*, R. Nickerson, Ed. New York: Routledge Taylor & Francis Group, 1980, ch. 12, pp. 239–255.
- [11] —, "Multiple resources and performance prediction," *Theoretical Issues in Ergonomics Science*, vol. 3, no. 2, pp. 159–177, 2002.
- [12] C. Borst, F. Grootendorst, D. Brouwer, C. Bedoya, M. Mulder, and M. van Paassen, "Design and Evaluation of a Safety Augmentation System for Aircraft," *Journal of Aircraft*, vol. 51, no. 1, pp. 12–22, 2014.
- [13] E. Sunil, J. Smisek, M. M. Van Paassen, and M. Mulder, "Validation of a tuning method for haptic shared control using neuromuscular system analysis," *Conference Proceedings - IEEE International Conference on Systems, Man and Cybernetics*, vol. 2014-Janua, no. January, pp. 1499–1504, 2014.
- [14] S. M. C. Alaimo, L. Pollini, M. Innocenti, and J. P. Bresciani, "Experimental Comparison of Direct and Indirect Haptic Aids in Support of Obstacle Avoidance for Remotely Piloted Vehicles," vol. 2, pp. 628–637, 2012.
- [15] V. Wilckens, "Improvements in Pilot/Aircraft-Integration by Advanced Contact Analog Displays," *NASA Technical Documents*, 1973.
- [16] A. Grunwald, J. Robertson, and J. Hatfield, "Evaluation of a computer-generated perspective tunnel display for flight-path following," *NASA Technical Documents*, no. March, 1980.
- [17] A. J. Grunwald, "Predictor Laws for Pictorial Flight Displays," *Journal of Guidance and Control*, vol. 8, no. 5, pp. 545–552, 1985.
- [18] S. Petermeijer, D. Abbink, M. Mulder, and J. de Winter, "The Effect of Haptic Support Systems on Driver Performance and Behavior : A Literature Review," *IEEE Transaction on Haptics*, vol. 8, no. April 2013, pp. 1–13, 2013.
- [19] D. Abbink and M. Mulder, "Neuromuscular Analysis as a Guideline in designing Shared Control," *Advances in Haptics*, pp. 499–517, 2010.
- [20] F. O. Flemisch, J. Kelsch, C. Loper, A. Schieben, J. Schindler, and H. Matthias, "Cooperative Control and Active Interfaces for Vehicle Assistance and Automation," *FISITA World Automotive Congress*, no. 2, pp. 301–310, 2008.
- [21] Boeing, "Statistical summary of commercial jet airplane accidents - Worldwide operations 1959 2011," 2011.
- [22] G. Sachs, "Perspective Predictor / Flight-Path Display with Minimum Pilot Compensation Introduction," vol. 23, no. 3, 2000.
- [23] D. T. McRuer and H. R. Jex, "A Review of Quasi-Linear Pilot Models," *Human Factors in Electronics, IEEE Transactions on*, vol. HFE-8, no. 3, pp. 231–249, 1967.
- [24] F. Zijlstra, "Efficiency in work behaviour: A design approach for modern tools," *Delft University press*, no. January 1993, pp. 1–186, 1993. [Online]. Available: <http://www.csa.com/partners/viewrecord.php?requester=gs{&}collection=TRD{&}recid=N9516953AH>
- [25] O. Stroosma, M. van Paassen, and M. Mulder, "Using the SIMONA Research Simulator for Human-Machine Interaction Research," in *AIAA Modeling and Simulation Technologies Conference and Exhibit*, no. August. Austin, Texas: AIAA, 2003, pp. 1–8.
- [26] C. Van der Linden, "DASMAT-Delft University Aircraft Simulation Model and Analysis Tool: A Matlab/Simulink Environment for Flight Dynamics and Control Analysis," Delft, 1996.
- [27] SeeingMachines, "faceLAB 5 - Eyetracking for Research," 2009.
- [28] P. Majaranta, U.-K. Ahola, and O. Špakov, "Fast gaze typing with an adjustable dwell time," *Proceedings of the 27th international conference on Human factors in computing systems - CHI 09*, p. 357, 2009. [Online]. Available: <http://dl.acm.org/citation.cfm?id=1518701.1518758>
- [29] E. Mollenbach, J. P. Hansen, M. Lillholm, and A. G. Gale, "Single stroke gaze gestures," *Proceedings of the 27th international conference extended abstracts on Human factors in computing systems - CHI EA '09*, p. 4555, 2009. [Online]. Available: <http://portal.acm.org/citation.cfm?doi=1520340.1520699>
- [30] National Transport Safety Board, "Descent Below Visual Glidepath and Impact with Seawall, Asiana Airlines Flight 214, Boeing 777-200ER, HL7742, San Francisco, California July 6, 2013," p. 142, 2014.
- [31] J. Flottau and J. C. Frankfurt, "Systems Awareness , Complexity Focus Of Emirates Accident Investigation," *Aviation Week & Space Technology*, pp. 28–29, 2016.

Part II

Preliminary Thesis

Chapter 1

Introduction

1-1 Background

In the early years of aviation there were only few instruments around, but during the advancement of aviation more and more information became available to the pilot. Until the point instruments were competing for space on the flight deck and attention of the pilot. "The average transport aircraft in the mid-1970s had more than 100 cockpit instruments and controls, and the primary flight instruments were already crowded with indicators, crossbars, and symbols" (Wallace, 1994). To deal with increasing complexity of the airspace and aircraft, the glass cockpit was developed, incorporating electronic flight displays increased safety and efficiency of flights by increasing pilot's situation awareness (Wallace, 1994).

The advancement of electronic flight displays and instruments allows for display design not possible before, being able to depict information in a way more similar to reality (e.g. artificial horizon) than just a dial moving up or down. Cockpits have become more intuitive and easy to understand by pilots, as adult humans are typically very good at recognizing the functional implications of natural information (Gibson, 1979). There are concerns however, that the modern cockpit can overload the pilot with information. Since the advancement of computer technology in the cockpit, physical design constraints of instruments have been taken away, allowing designers the apply new control formats and ways of information presentation (Lintern, Waite, & Talleur, 1999). With the arrival of the computer-era a whole new set of possibilities opened up, Lintern et al. suggest that these features should be implemented with care, making sure that there design does not add to the cockpit complexity. This thesis work considers the benefits and limitations of a Tunnel-in-the-Sky display and haptic feedback design and researches possible synergies between these technologies and will focus on the change in task-sharing performance of the pilot.

1-1-1 Tunnel-in-the-Sky Display

The starting point for this research is the Tunnel-in-the-Sky display, which shows the trajectory to be flown in 3D fashion, making it more intuitive to pilots compared to the bars indicating desired pitch and roll angles. The first research on Tunnel-in-the-Sky displays took place in

the 1970s, where Wilckens (Wilckens, 1973) proposed a qualitative relation between tunnel size and tracking performance which can be. In 1980, Grunwald et al. (Grunwald et al., 1980) performed an experiment demonstrating the feasibility of a tunnel display during an actual flight. Since then a lot of research has been performed on the effect of the tunnel's geometry and size, among others by Mulder and Mulder (Mulder & Mulder, 2005) in 2005, who quantified Wilckens' theory on tunnel size and flight performance and reproduced these theoretical results during an experiment.

Integrating multiple functions into one display like the Tunnel-in-the-Sky display will help operators to get a quick grasp of the situation at hand, as pilots can see the required trajectory, instead of just a heading and flightpath angle. Having a tunnel in front of you also helps better understand actions to be taken in the future, as it is already clear what is expected of the pilot further down the tunnel. Having all these features in one display however can potentially absorb a disproportionate amount of the pilot's attention resulting in a worse task-sharing performance of the pilot, this is one of the pitfalls associated with workload reduction through integrated flight instruments (Anderson, 1996).

1-1-2 Haptic feedback

A way suggested to increase task-sharing performance is haptic feedback (Lombaerts, Looye, Ellerbroek, & Rodriguez, 2016). Currently, haptic feedback can mainly be found as coupling between the steering columns of both pilots, where one pilot will feel the force exerted on the control stick by the other pilot. Another type of haptic feedback present in aircraft is a vibrotactile warning through the stick in case stall nearly occurs, this stick shaker concept was patented by Boeing in 1998 (Gast, 1998).

These types of haptic feedback are quite simple and applicable only in a limited number of situations (e.g. near stall). Haptic feedback offers more possibilities though. As haptic feedback adds an extra modality through which a pilot get information, other sensory modalities like vision could free up for other tasks, which means the task-sharing performance would increase (Wickens, 2002). If the haptic feedback does not correspond with the pilot's assessment of the situation however, they can be easily misunderstood and confuse the pilot (Alaimo, Pollini, Innocenti, & Bresciani, 2012). Design of the feedback is therefore paramount to its added value.

1-2 Description of the problem

Due to increasing air traffic and stricter regulations around airports, pilots are required to fly approach trajectories with high precision. Flying these relatively complex trajectories will increase the mental workload of a pilot during arguably the most critical phase of flight. During the final approach and landing a pilot is busy setting its flap and landing gear, tracking its trajectory and flight path and looking out for abnormalities, while flying at low speed and altitude (Lee, 2010).

Tunnel-in-the-Sky (TIS) displays are considered as a solution to this issue, as they can support pilots to fly these complex curved trajectories, since properly designed TIS increases tracking performance of a pilot (Grunwald et al., 1980). Performance can be further increased when

decreasing the tunnel size, as indicated by Wilckens (Wilckens, 1973), proven by Mulder and Mulder (Mulder & Mulder, 2005) and illustrated in Figure 1-1.

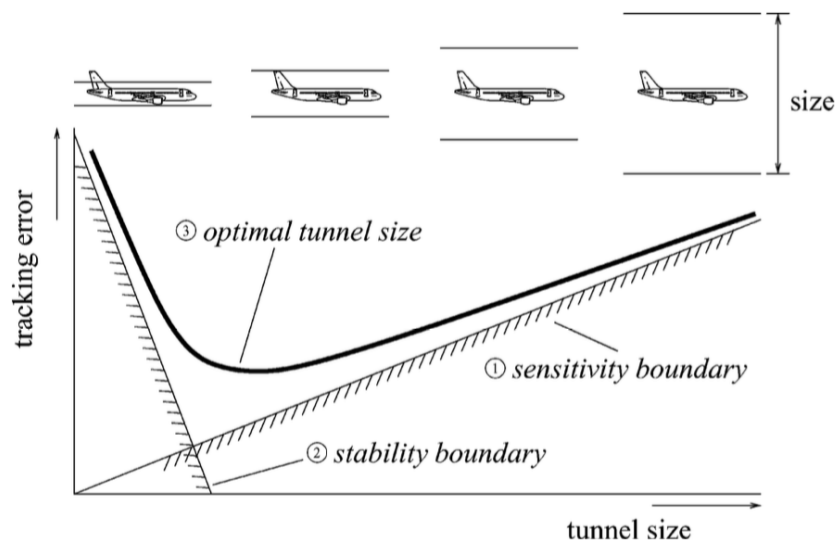


Figure 1-1

This increase in tracking performance comes at a cost, Mulder and Mulder found, when performing a dual experiment in a simulator and an actual aircraft. For the simulated case the performance increased as tunnel size decreased from 80 to 20 meters width for each participant, but at the same time the control activity did. During the real flight experiment, the participants showed more difficulties staying inside the smaller tunnels, indicating that they were flying on their limits and the extra tasks associated with real flight made the task at hand too difficult.

Modern displays and in particular TIS displays integrate multiple flight instruments into one intuitive display for the pilot to use. However, displaying the most relevant information on one display only can cause the pilot's focus to shift too far towards this one display reducing his task-sharing performance (Gursky, Olsman, & Peinecke, 2014).

An approach to increase task-sharing performance of a pilot is using haptic feedback. Haptic feedback allows the pilot to use multiple sensory modalities - in this case tactile and visual. Wickens suggests that performance degradation is reduced when complementary sensory modalities are used to provide control information, but that insufficient research exists to fully understand how using multiple resources work together in real world tasks (Wickens, 2002). Combining the TIS display with haptic feedback is an unexplored area of research, but has the potential of decreasing workload and improving task-sharing performance.

There is a number of limitations associated with haptic feedback. Operators tend to find forced feedback an annoyance if its presence is too strong and unclear haptic cues could confuse the pilot instead of helping him (Abbink, Mulder, & Boer, 2012). Communicating guidance information through haptic feedback has been done in the design of driver support systems for a while now, and with success; reducing control activity with no reduction or even small improvements of task performance (Petermeijer, Abbink, Mulder, & de Winter, 2013). For

aviation this is more difficult to implement, as an extra dimension is present and more diverse control strategies can be applied. However, also in aviation experiments it has been shown that an increase in performance is possible without annoying the operators (de Stigter, Mulder, & van Paassen, 2005), this suggests that more high level guidance information can be communicated through haptic feedback, which could be used to increase task-sharing performance as well.

1-2-1 Problem statement

Head-down displays in general and integrated flight displays like TIS especially will direct a pilot's focus downward, reducing his awareness of the environment and other states of the aircraft and thus his task-sharing performance. Haptic feedback could reduce the need to look down by communicated the information on the display through haptic forces on the stick held by the pilot.

1-3 Research direction

As explained in Section 1-2, the main topic of this research is if and how novel aviation technology can assist a pilot during flight, making the flight safer, more efficient and more comfortable. More specifically, to see if haptic feedback can mitigate the decrease of task-sharing performance when flying complex trajectories with the Tunnel-in-the-Sky display. This research will consider the most demanding and critical part of the flight envelope; the approach. Will the look-up time of the pilot increase when information is not only displayed by means of visual cues on head-down displays but also communicated as haptic cues on the control stick?

The most important feature of the haptic feedback will be its intuitiveness, the haptic feedback needs to act as a pilot acts. This means that the haptic will have to look ahead down the trajectory and anticipate heading changes - as a pilot would. The haptic feedback controller will also be different for longitudinal control than for lateral control, as pilots use different control strategies as well. The feedback should give proper guidance to the pilot, but should not be considered a nuisance. The pilots should feel the forced feedback, but should always be able to overrule it. This will require careful design using literature and test runs.

If this is done properly it is hypothesized that a pilot will show improved task-sharing performance. This can be translated in the following research question:

1. What will happen to the task-sharing performance of a pilot when applying haptic feedback during Tunnel-in-the-Sky assisted approach?

In order to answer this question we must be able to measure task-sharing performance. This can be done by providing the pilots a secondary task to be performed. This task needs to motivate the participants to look up from the TIS display. When the pilots do indeed move their eyes away from the display and primary task performance does not decrease it can be concluded that haptic feedback improves task-sharing performance.

The next consideration addressed during this research is whether haptic feedback has an increased effect on more demanding tasks, in this case; a smaller tunnel. This is something that

is expected, as an easy task can be easily performed with mental capacity to spare, but a task requiring the full mental capacity of a pilot can force the pilot to skip subtasks. As it is hypothesized that multi-modal feedback will help the pilot to free up mental capacity, the pilot should be able to successfully perform tasks not possible without haptic feedback. The research question for this part of the research is:

2. What is the difference in effect of haptic feedback on task-sharing performance of the pilot for more challenging primary tasks?

As indicated in Section 1-2, the difficulty of a task can be increased by decreasing tunnel size. By changing the tunnel size and measuring the difference in task-sharing performance with and without haptic feedback, this research question can be answered.

1-4 Research approach

In order to investigate the research questions posed in Section 1-3, an experiment need to be set up. In this case this will be done in a simulator as an experiment in and aircraft will be hard to reproduce, expensive and very time-consuming. Depending on availability the experiment will be conducted in the SIMONA or the HMI lab at the faculty of Aerospace Engineering of Delft University of Technology.

The participants will be experienced pilots who will fly several trajectories with and without haptic feedback and through tunnels of varying size. During the experiment the force excited on the stick by the controller will be dictated by its haptic authority. Where a haptic authority of 100% will provide full control without the operator touching the control stick - still allowing the operator to overrule the stick - and setting the haptic authority to 0% will be equivalent to full manual control.

In the outside visuals a secondary, visual task will be displayed. With an eye-tracker the look-up time of each participant during each condition will be measured. Standard performance and workload indicators will be used to assess the primary task. Where for the secondary task performance will be measured through look up time and actual score. The eye-tracker will also provide information about where the pilot looks directly after a haptic cue.

Performing the experiment like this, will allow for the research questions to be split in subquestions. When all the subquestions of a research question can be answered, the research question itself can be answered as well. Research Question 1 can be split up as follows:

1. What will happen to the task-sharing performance of a pilot when applying haptic feedback during Tunnel-in-the-Sky assisted approach?
 - 1.1. What happens to the head-up time of a pilot when applying haptic feedback in addition to a head-down display?
 - 1.2. What happens to the primary task performance when applying haptic feedback?
 - 1.3. What happens to the secondary task performance when increasing haptic authority?
 - 1.4. Where does the participant look directly after a haptic cue is given?

When the Question 1.1. to Question 1.4. can be answered, Question 1 will be answered as well. An increase in head-up time will indicate that mental capacity was freed up by the haptic feedback. Question 1.2. considers the possibility that the performance of the primary task decreases because of the secondary task, in a well designed experiment this should not be the case. The answer to Question 1.3. will be a little harder to predict, as it is hypothesized that haptic feedback will help the operator, but too much haptic feedback might be confusing or annoying, resulting in a reduction of secondary task performance. Finally, Question 1.4. will give an insight in the fact if the haptic feedback confuses the subjects or not.

Question 2 can be split up as well:

2. Will the effect of haptic feedback on task-sharing performance of the pilot be larger for a more challenging primary task?
 - 2.1. Does the look-up time of the pilots increase more when haptic feedback is applied in a smaller tunnel compared to a larger tunnel?
 - 2.2. Is there a threshold for the tunnel size above which haptic feedback will have no notable effect?
 - 2.3. Will there be a difference in effect of haptic feedback on task-sharing performance during lateral and longitudinal approach segments?

Again, when all subquestions can be answered, the second research question can be answered as well. By means of using smaller tunnel size, the difficulty of the primary task can be increased. Question 2.2. considers the fact that haptic feedback will only have a visible effect on task-sharing performance when the primary task is forcing the pilot to use most of his mental capacities. If haptic feedback has indeed more effect on difficult tasks and the assumption that longitudinal and lateral control are not equally difficult, Question 2.3. will be confirmed.

1-5 Preliminary structure

In this preliminary thesis, the groundworks have been laid for the design and implementation of a piloted experiment in a flight simulator. In Chapter 2 a literature review is performed, looking at several possibilities for Tunnel-in-the-Sky design choices, at haptic feedback research performed so far and at several experiment design options. Lastly, in Chapter 3 the Simulink model of the controller and haptic interface will be explained.

Chapter 2

Literature review

Developments in computer hardware and software have opened up countless possibilities in cockpit and instrument design. This new way of processing data using computers is called high technology, in contrast to low technology it does not force the use of functional properties at the interface since many physical constraints will be taken away. Lintern et al. (Lintern et al., 1999) explain the concept of functional interface design and outline how it might enable the use of high technology and automation in the service of robust and cognitively economical action in an aircraft cockpit. They argue that using direct design, computer-supported interfaces allow functional properties to be displayed to the operator in an intuitive way. The goal of direct design is to present functional properties in such a way, extra computations by the operator are not necessary to understand the situation. The tunnel-in-the-sky interface is an example of direct design and has been researched and tested by many scientists, their work is discussed in this literature review and can be found in Section 2-1.

2-1 Tunnel-in-the-Sky

The Tunnel-in-the-Sky (TIS) display shows the route to be flown by the pilot in a way easy to perceive by the operator. Groundwork for the tunnel-in-the-sky design known today was done by Gibson, a perceptual psychologist investigating human information processing and their visual perception of three-dimensional scenes in motion (Gibson, 1950). Gibson et al. (Gibson, Olum, & Rosenblatt, 1955) hypothesize that in order to get a realistic visual perception, the idea of locomotion of an observer should be created by an optical flow pattern in which texture gradients are of paramount importance.

Several studies have been performed and confirmed that a TIS display is able to increase path-following performance of the operator. Grunwald showed the effectiveness of this display for both fixed-wing aircraft (Grunwald, Robertson, & Hatfield, 1981) and helicopters (Grunwald, 1984). It is found that a properly designed tunnel integrates information in such a way that it is intuitive for pilots and compatible with tasks imposed by the air navigation system. A tunnel design clearly leads to a better performance than just a electronic attitude director indicator (Grunwald et al., 1980).

2-1-1 Tunnel design

Over the years, several designs of pathway-in-the-sky interfaces have been created with a general trend from trajectories shown using pathways displays to trajectories shown using tunnels. Comparing the research of Way (Way, 1987) and Regal and Whittington (Regal & Whittington, 1995) indeed shows that a tunnel-in-the-sky scores better than a pathway-in-the-sky design in terms of performance, situation awareness and pilot acceptance. Moreover, Newman and Mulder in their literature on pathway displays (Newman & Mulder, 2003) state: "Adding "walls" appears to drive the lateral tracking tolerances tighter than the simple highway. Adding a top to form a tunnel-in-the-sky tightens the vertical tracking. This tightening is desirable for penetrations and approaches, but may increase workload unnecessarily during en-route and other operations."

Considering the primary task in mind will be an approach, it seems relevant to further look into the tunnel design. Mulder has written three companion papers about an information-centered analysis of the tunnel-in-the-sky display. (Mulder, 2003a, 2003b; Mulder & van der Vaart, 2006). To investigate which features provide which information to the pilot, Mulder (Mulder, 2003a) considers two fundamental questions: 'How do pilots know where they are relative to the tunnel trajectory?' and 'How do they know where they are going?'

In the case of a straight tunnel, there is two types of lines that can be considered. Mulder (Mulder, 2003a) distinguishes two types of geometric features, lines parallel to the direction of motion, which give information about the optical splay angle (gradient of perspective), and lines perpendicular to the direction of motion, which give information about the optical density (compression). In Figure 2-1 these geometrical features are shown.

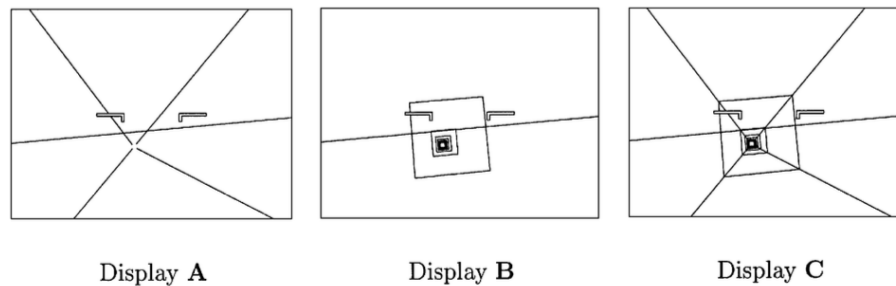


Figure 2-1: 3 displays depicting the different independent variables, splay-only, compression-only and a combination of both, respectively (Mulder, 2003a)

Mulder finds that the path-following performance is highest for display C. In a follow-up paper (Mulder, 2003b) Mulder discusses the effect of geometrical features of curved trajectories. Where similar features also convey information about splay and density. The displays tested during this research are shown in Figure 2-2. Here the best scoring display regarding path-tracking performance at a speed of 110 m/s is display A, having regularly placed, connected frames on poles. Considering the nature of the primary task (approach) and the availability of the tunnel-in-the-sky module (developed at the aerospace engineering faculty), display A seems the most likely candidate to be used during the experiment to be performed.

Superimposing a predictor/director

Grunwald (Grunwald et al., 1980) performed an experiment in a fixed-base simulator with the vehicle dynamics of a CH-47 tandem-rotor helicopter, linearized about a 33.5 m/s (110 ft/s)

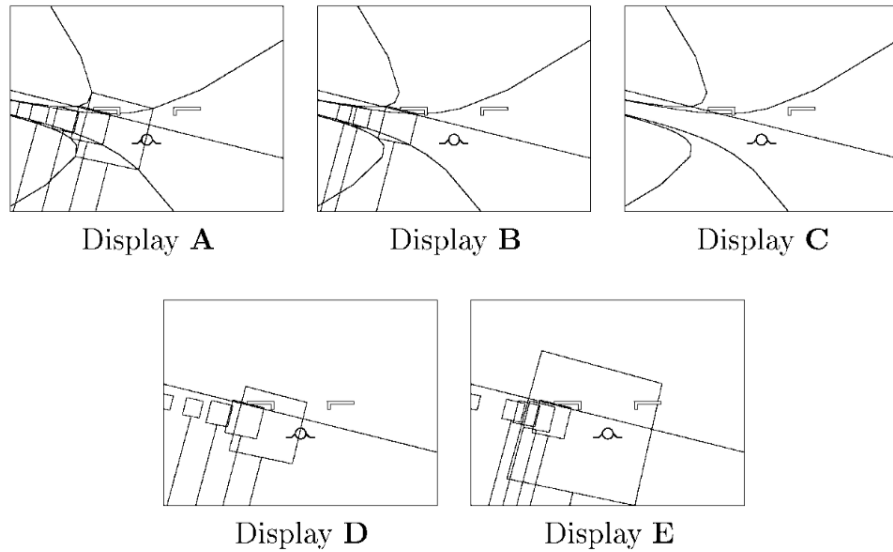


Figure 2-2: The geometry of the tunnel displays applied in the experiment (Mulder, 2003b)

forward velocity and a level flight trim condition. Using three types of displays: an electronic attitude director indicator, a tunnel-in-the-sky, and a tunnel-in-the-sky with a predictor and director superimposed on the display. For all three displays he ran three scenarios: following a desired trajectory in the presence of disturbances; entering the trajectory from a random position, outside the trajectory; and detecting and correcting failures in automatic flight. For all scenarios, the tunnel with superimposed director/predictor (with an optimized prediction time of 4 to 7 seconds) scored best in terms of performance. Pilot acceptance of the tunnel plus director/predictor was found to be favorable and the time needed for familiarization with the display was found to be relatively short. The two displays, without and with predictor/director can be seen in Figure 2-3.

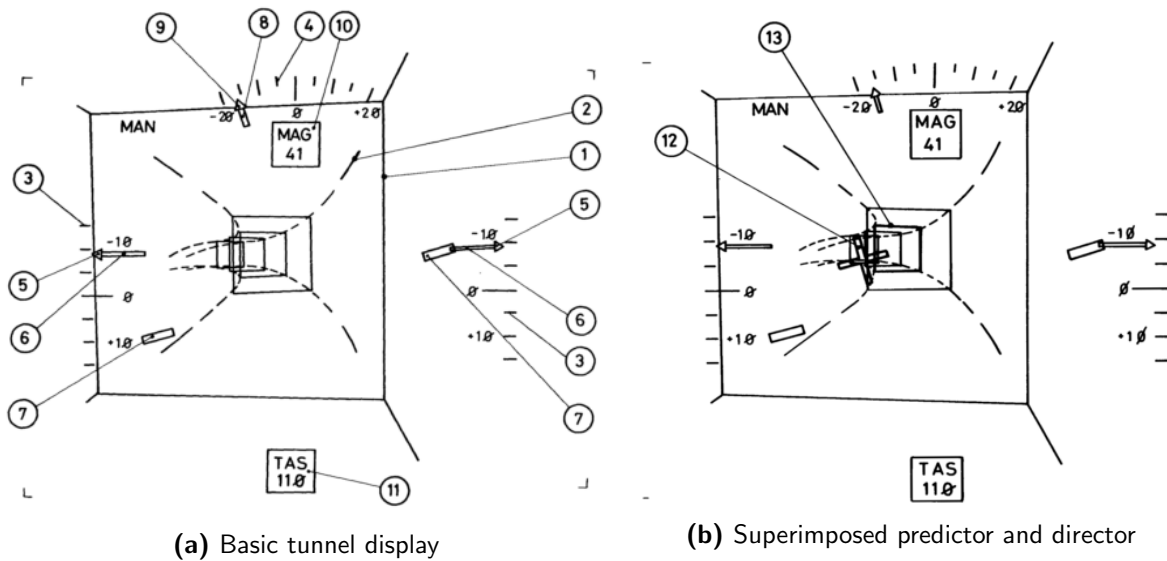


Figure 2-3: Tunnel display without and with superimposed predictor and director (Grunwald et al., 1980)

Grunwald also found significant decrease in roll and pitch activity in the trajectory-entry and trajectory-following experiment when superimposing a director/predictor on the tunnel display. When researching the increase in task-sharing performance and thus indirectly the decrease in control activity. When superimposing a director and predictor symbol, the task at hand reduces to a simple tracking task, pilot behaviour for these kind of tasks can be modelled quite accurately and could be preferable during this experiment.

2-1-2 Scaling of the tunnel

The size and scaling of the tunnel is relevant for the perception and performance of the operator. As one can imagine, a very large tunnel will not force a pilot to very accurately follow a certain trajectory. A very small tunnel however, will introduce a high sensitivity on the path-tracking performance. Ideal scaling depends also on the operator itself however, a better adapted pilot will be able to use a smaller tunnel. Wilckens summarizes these findings in a qualitative way in Figure 2-4.

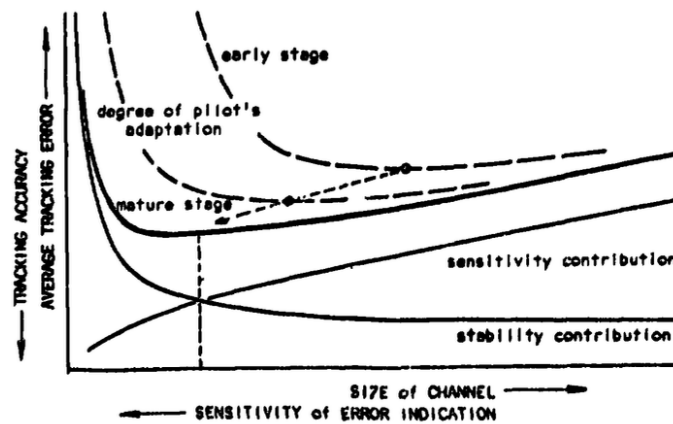


Figure 2-4: Qualitative diagram of average tracking errors versus tunnel size (Wilckens, 1973)

Wilckens argues that a too small tunnel will induce oscillatory overshoots, indicated by the part of the sensitivity contribution left to the vertical line. Whether a tunnel is too small depends on the skills of the pilot, as is indicated by the top three lines in Figure 2-4. Too the right side of the vertical is the part where the tunnel is too large and too 'easy' to follow. Because of the ease of following, the pilot workload is lower for a larger tunnel size. Next to Wilckens (Wilckens, 1973), other studies (Grunwald, 1984; Mulder, 1999) indicate that a decrease in tunnel size will increase pilot workload as well.

Mulder and Mulder (Mulder & Mulder, 2005) indeed prove that the second (stability) boundary suggested by Wilckens exists, both theoretically and experimentally. In a cybernetic analysis they find that outer-loop phase margin and thus stability of a hierarchical pilot model will decrease when the difference in bandwidths in the control loops gets to small, this will be induced by a too small tunnel. The hierarchical pilot model used can be found in Figure 2-5, the inner loop describes attitude control, the middle loop flightpath control and the outer loop describes position control.

In their analysis Mulder and Mulder consider the cross-over frequencies, ω_c^{in} , ω_c^{mid} , ω_c^{out} of each loop. In the executed experiments they see that when the tunnel becomes smaller, the bandwidths of the hierarchical pilot control system must increase to be able to deal with the

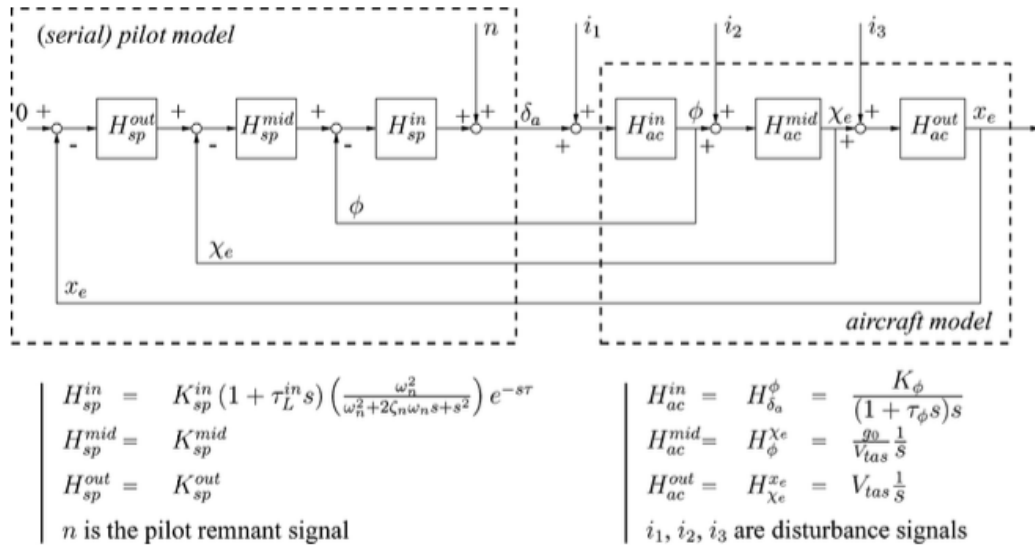


Figure 2-5: Closed-loop, linear pilot/aircraft model describing lateral control (Mulder & Mulder, 2005)

more demanding tracking task. The conclusion from their theoretical analysis is that increasing the bandwidth of the outer-loop feedback increases tracking performance. However, when the bandwidth of the outer-loop approaches that of the combined pilot feedback of the attitude and flight path, performance deteriorates because of a rapid decrease in the stability margin.

Considering the goal of this research: determining if there is an increase in task-sharing performance when haptic feedback is introduced, a default task with a relative high workload might be preferable. This would mean that for the experiment a smaller tunnel inducing a higher workload might be most suitable to find improvements in task-sharing performance when introducing haptic feedback.

The tunnel size should not exceed the limits of the pilots however. A relatively easy tracking task (using only the aileron deflection as control channel), enables pilots to perform using a tunnel with a width of 10 meters. But in a real flight experiment 20 meters was too tight for one (of the two) participants (Mulder & Mulder, 2005). The task in the proposed experiment (two control channels), will be in between these two experiments regarding difficulty level. So the ideal tunnel width is expected to be between 20 and 40 meters, more accurate sizing can be done by trial and error tuning. In the experiment, multiple tunnel sizes could be used to find out the relation between the effects of haptic feedback and tunnel size on task-sharing performance.

2-2 Haptic feedback

Haptic feedback is a means of communicating information to an operator by sending force signals that can be felt by the operator. These cues can be perceived faster than visual cues, but usually contain less information. Where visual cues can communicate relatively abstract things, force feedback can basically *warn* or *guide* an operator in one direction or another. In the automotive industry, haptic *guidance* is already present in some modern cars. In aviation, the most common type of haptic feedback is the stick shaker, which *warns* the the pilot he is

nearing a stall situation for example.

In this section, several haptic models and their advantages and disadvantages will be explained. The tuning of haptic feedback and the term haptic authority (de Stigter et al., 2007) will be explained as well.

2-2-1 Haptic models

There are many ways of communicating information through haptic cues, some or more clear to the operator than others. These models can be categorized in several ways. One could choose to distinguish *proactive* or *reactive* feedback models, *guidance* or *warning* systems, or, having a *compliant* or *uncompliant* control stick. These models all have their own advantages and disadvantages.

A *proactive*, *guiding* and *uncompliant* stick can guarantee an increase in performance, but requires very compliant behavior from the operator. De Stigter et al. (de Stigter et al., 2007) describe such a model, where the operator gets information through the position of the stick. This model does not allow the pilot to move the stick, but he can control the aircraft by exerting forces on the stick.

In the same paper (de Stigter et al., 2007) a haptic feedback system using a *proactive*, *guiding* and *compliant* stick is described. This model requires the pilot to keep the stick in its centered position to maintain its optimal flightpath. Information about changes in the aircraft's attitude is communicated through forces exerted by the stick on the pilot's hand.

The models described above are less conventional, but show the broad range of options for haptic feedback design. However interesting, these models are less relevant to the experiment to be designed, as they require quite an extreme change in control behavior from pilots, where the focus of this research is on haptic feedback as *aid* to the pilot. More relevant feedback models will be discussed in more detail in the remainder of this section.

Vibrotactile warning model

A haptic feedback model using vibrotactile *warnings* that alert the aircraft operator when undesirable events happens can be either *proactive* (when alerting for exceeded position or velocity bounds) or *reactive* (when alerting for exceeded control input bounds), by definition it requires a *compliant* stick. It does not help the pilot to get to the correct state, it only warns the pilot that he has moved away from a acceptable state. Petermeijer et al. (Petermeijer et al., 2013) describe warning systems as follows:

- A system that is activated after a threshold is exceeded.
- A system that informs the operator about an inadvertent situation but does not guide the pilot to the correct state.
- Application of binary feedback, the system is either on or off, depending on the breach of threshold values.

An advantage of warning systems is that they generally have high pilot acceptance, since for the most part, the controls will be the same as without haptic feedback. Also the situation awareness of the pilot is the same as in a manual task, it won't degrade as all the steering needs to be done by the pilot still.

A disadvantage is that when an operator receives a binary signal, it is not always clear what she should do to resolve the issue at hand. Another difficulty with warning systems is that it needs to be tuned in such a way that it warns soon enough, but does not result in any false alarms. When false alarms do occur, it is likely that the operator will ignore the system in future occasions (Parasuraman & Riley, 1997), where too few warnings can leave the pilot with too little time to react.

If this haptic feedback model would be chosen for the experiment to be designed, a decrease in mental workload might be hard to measure. As for the largest part of the flight, the pilot will not get any haptic feedback at all. It could also cause the pilot to check his primary flight display more often if the haptic cues are unclear as standalone signals.

Guidance model

A haptic *guidance* model uses haptic cues in a *proactive* way to urge pilot in the 'right' direction, depending on the control law and the tuning the stick can be either *compliant* or *uncompliant*. In this case the 'right' direction is the direction for which certain errors decrease. It can communicate a required change in velocity, pitch or roll for example. Petermeijer et al. (Petermeijer et al., 2013) describe a haptic guidance system as:

- A system that continuously support the operator when it is activated.
- Provides feedback in such a way it assists the operator to take the right action.
- Scales the intensity of the feedback signal to the error between the current and desired state.

De Stigter et al. (de Stigter et al., 2007) illustrate the analogy between a visual flight director and a haptic flight director. Two different channels, relaying the same information. In Figure 2-6, the multi-modality of the haptic flight director is can be seen as the *additional* channel, relaying the haptics. It can be seen that in the haptic model, the forces of the haptic feedback are added to the forces exerted by the pilot.

Different types of haptic models can be used, some are already suggested in the introduction of the Section 2-2-1. A more widely used type of feedback is shared control, in this case there are two forces present on the stick, one from the operator and one from the haptic feedback system; the net force results then in the excitation of the stick.

How much of the force is provided by the operator and how much by the flight director is a matter of tuning. On the one extreme, the pilot has all control and the flight director does not exert any forces whatsoever, this situation is the same as manual control using a visual flight director displayed by the top diagram in Figure 2-6. The other extreme is a completely uncompliant stick which cannot be controlled by the operator, this situation can best be compared with

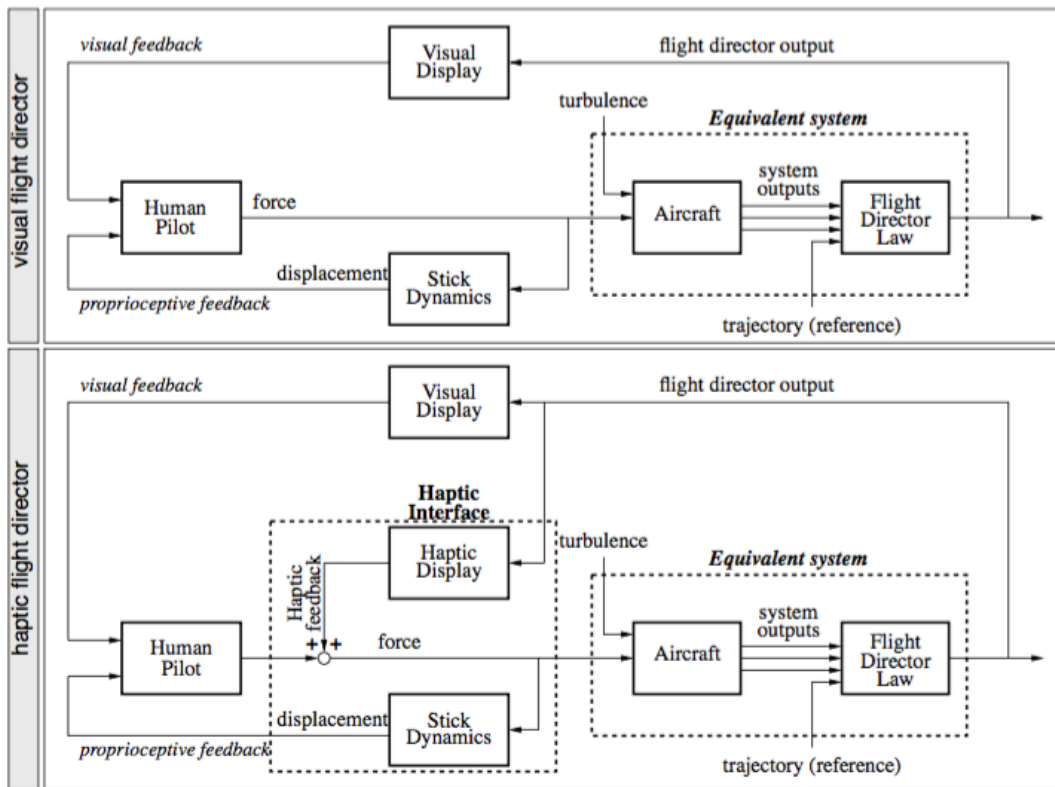


Figure 2-6: Visual flight director (top) and haptic flight director (bottom) (de Stigter et al., 2007)

completely autonomous flight. In the last example, the stick still conveys information on control inputs provided, but it does not allow for human intervention without shutting down the system. These are reasons why haptic feedback is usually tuned, tuning methods are described in Section 2-2-2.

2-2-2 Haptic feedback tuning

Both extremes are usually not desirable and also beside the point of shared haptic control. A haptic guidance model is ideally tuned in such a way it increases the performance and lowers the workload of the operator, without being an annoyance and maintaining situation awareness. In most studies tuning of the haptic model is based on empirical data or performed by trial and error (de Stigter et al., 2007; Flemisch et al., 2008; Lombaerts et al., 2016).

Smisek et al. (Smisek et al., 2013) however, propose an analytical method of tuning the haptic model. They start out by estimating the intrinsic properties of the neuromuscular system (NMS), the model of the NMS they use can be found in 2-7. Two feedback paths can be distinguished in the closed-loop NMS model. To estimate the intrinsic properties of the NMS, the method proposed by Smisek et al. mitigates the effects of the reflexive feedback as much as possible.

Humans can adapt their NMS in order change the admittance over a wide range of values. This is done through two mechanisms: fast subconscious spinal reflexes and muscle pair co-contraction (Abbink, 2006). A stronger reflex strength, generated by muscle spindle feedback will generate lower admittance and thus a stiffer NMS. Co-contraction of opposing muscles will cancel each other out partly or completely. In this case the resulting force will remain relatively

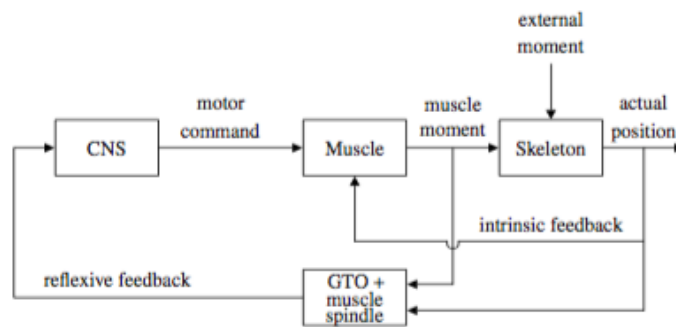


Figure 2-7: Closed-loop NMS model as used by Smisek et al. (Smisek et al., 2013)

constant, but the stiffness of the NMS will increase. Properties of the human NMS are typically determined in one of three tasks which can be distinguished by level of admittance, a force task, a relax task and a position task (De Vlugt, 2004).

As mentioned before, Figure 2-7 shows the NMS closed-loop system which has two feedback loops. One accounting for the reflexive feedback, the other accounting for intrinsic feedback. When determining the intrinsic properties of the NMS, it is useful to reduce the influence of the reflexive feedback. Of the available tasks for determining the intrinsic stiffness of the NMS, the relax task is most suitable as it requires the subject not to respond to haptic moments and so reducing the influence of the reflexive feedback loop (Smisek et al., 2013). Using a disturbance signal with a wide-band spectrum will lower the neural reflex gains which will increase phase margin and will limit the useful adaptation range of the reflexive feedback control loop (McRuer & Jex, 1967).

Once the intrinsic properties of the NMS are known, the side stick stiffness can be set in such a way that it bridges the gap between the ideal NMS stiffness and the ideal combined stiffness, this concept is illustrated in Figure 2-8.

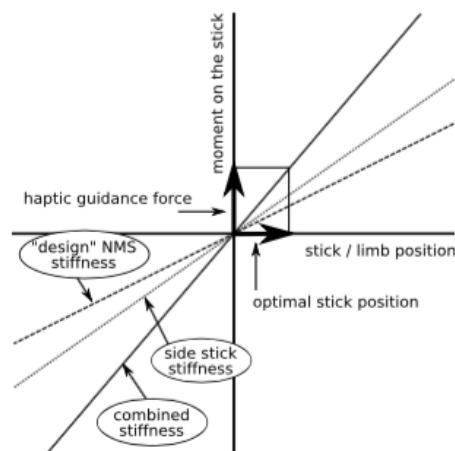


Figure 2-8: Stick position based guidance force according to tuned stiffness (Smisek et al., 2013)

The ideal combined stiffness is a matter of choice, it is a trade-off between sensitivity and stability. The possibilities for 'design' NMS stiffness can be divided in three categories (Smisek

et al., 2013):

1. **Intrinsic stiffness.** By tuning the haptic feedback in such a way it corresponds to the intrinsic NMS stiffness of the operator, the physical workload of the operator will be minimized. In this setting, the reflexive feedback loop in Figure 2-7 will not be used. Since the side stick stiffness will be significantly larger than the neuromuscular stiffness, an extra advantage is that the control system will have an acceptable response for hands-off control. The operator will be able to overrule the system when increasing his NMS stiffness however.
2. **Overspecified haptic feedback.** By tuning the haptic feedback in such a way it overcompensates for the intrinsic NMS stiffness, the operator will need to increase his own stiffness to get an appropriate system response. This can be tiring to the operator and might be hard to overrule, but can increase the maneuverability of the system.
3. **Underspecified haptic feedback.** By tuning the haptic in such a way it does not compensate for the intrinsic stiffness completely, the operator must provide an extra push in the right direction to get an appropriate response. If the operator would release the stick, the response caused by haptic guidance will be too small.

When an appropriate haptic guidance force is exerted on the stick while it is tuned to the intrinsic stiffness of the human NMS, the operator only has to stay relaxed to provide the desired output. It can be hypothesized that this relaxed state will decrease his mental workload and will increase his task-sharing performance.

2-2-3 Haptic authority

When modeling shared haptic control, the amount of force provided by the haptic controller is determined by the haptic authority. In Figure 2-9, the block diagram outlining this situation for a piloted aerial vehicle (PAV) is displayed. The controller gives a command it would give in case of full automation. This command is then converted to a force by the inverted stick dynamic model, which will be multiplied by a gain called the control authority, increasing this gain will increase the force of the haptic feedback. The forced feedback, together with the force put in by the human controller will determine the resulting force exerted on the stick which in turn will determine the stick deflection and command.

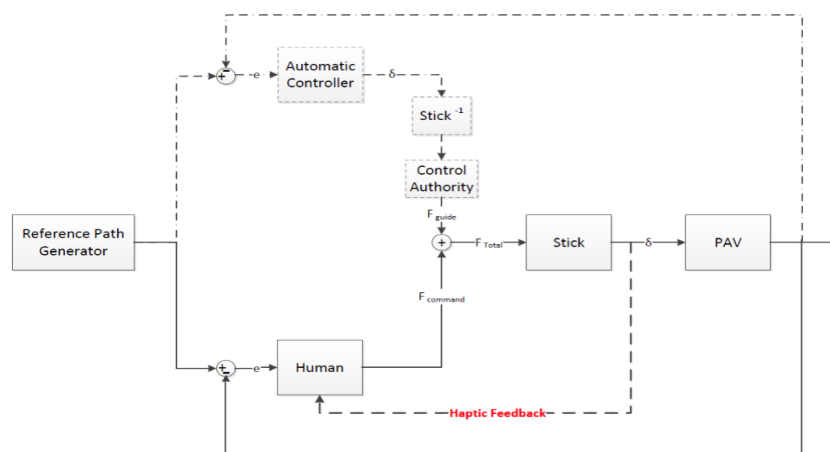


Figure 2-9: Block diagram of a situation of shared haptic control (Sunil et al., 2014)

Preliminary analysis

To get an understanding of the trajectory to fly and the haptic feedback to provide during the experiment that will be conducted, the flight test can be simulated and controlled in Simulink. Simulink can help tuning the controllers and simulate results of several control loops. Based on these results, decisions can be made for designing the haptic controller during the experiment. In this chapter it is discussed how trajectories will be generated, and how the controllers will work, what the control inputs are and what the final flight path will be using said controllers.

3-1 Trajectory

First of all an trajectory containing straight descending segments and level curved segments will be created, similar to an approach in reality. This trajectory will be displayed as a Tunnel-in-the-Sky on a head down display. Between segments there will be a few seconds of straight level flight, in order to analyze the effects of haptic feedback during the segments separately, this way longitudinal and lateral control can be split. The segments will be put together in such a way that the trajectory is different for each run, this way the pilot can not get familiar with the flight path. There will be a run-in and a run-out time between each measured segment to get rid of the transient phase between a turn and a straight part of flight.

Figure 3-1 shows a generated trajectory, where the dark blue parts are straight level segments with a duration of 15 s, where the cyan and yellow parts are sloped straight and level curved segments with a duration of 30 s, respectively.

3-2 Reference frames

Generating the trajectory is done in the Geodetic Reference Frame (GRF), where the x-axis points North, the y-axis points East and the z-axis points down. The x- and y-axis are shown in Figure 3-1 in the same way as defined in the GRF. The height is the same as the negative z values. For longitudinal control the z-position in the GRF can be used

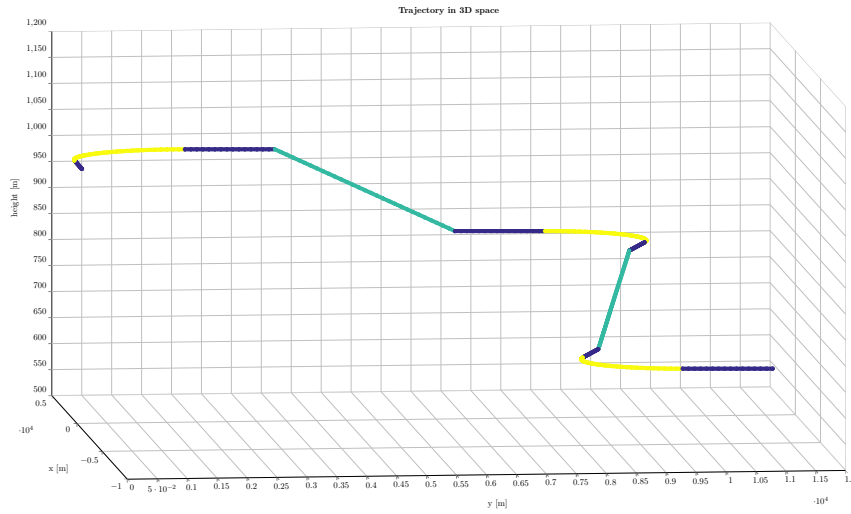


Figure 3-1: 3D plot of generated trajectory

and no transformation of the reference frame is required, as $z_{reference}$ and $z_{measured}$ can be used directly. For lateral control however, a reference frame based on the position of the aircraft or trajectory is needed. In this case the trajectory centered, trajectory fixed (TCTF) reference frame is used. In Figure 3-2 it is shown how both reference frames are defined.

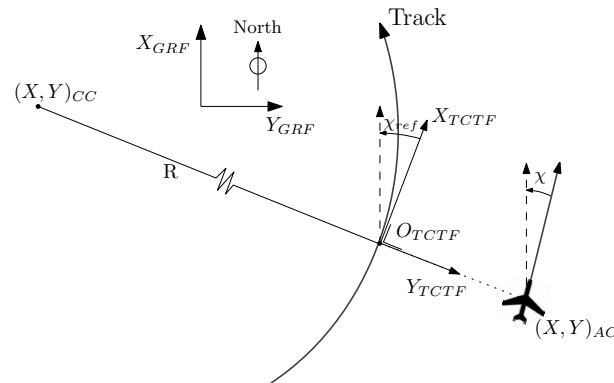


Figure 3-2: Definition of GRF and TCTF coordinate system as seen in Z direction

To get from GRF to TCTF, the coordinate system needs to be translated and rotated. The location of the origin of the TCTF reference frame in the geodetic reference frame, $(O_{TCTF})_{GRF}$, determines the translation. As every curves segment is described as part of a circle, the location of its circle center, $(X, Y)_{CC}$ is known. Using this location and the measured location of the aircraft, the origin of the TCTF reference frame can be determined according to Equation 3-1. Where the rightmost term effectively multiplies the unit vector between the aircraft and the circle center by the radius of that same circle.

$$(O_{TCTF})_{GRF} = \begin{pmatrix} X_{CC} \\ Y_{CC} \end{pmatrix} + R \begin{pmatrix} \frac{X_{AC} - X_{CC}}{\sqrt{\Delta X^2 + \Delta Y^2}} \\ \frac{Y_{AC} - Y_{CC}}{\sqrt{\Delta X^2 + \Delta Y^2}} \end{pmatrix} \quad (3-1)$$

To get to the TCTF reference frame, the GRF needs to be rotated as well. The difference in orientation between the two coordinate systems is the reference heading, χ_{ref} . By using this

variable and the fact that the z-coordinate stays the same, the total transformation equation can be given and is shown in Equation 3-2.

$$\begin{pmatrix} X \\ Y \\ Z \end{pmatrix}_{TCTF} = \left(\begin{pmatrix} X \\ Y \\ Z \end{pmatrix}_{GRF} - (O_{TCTF})_{GRF} \right) \begin{pmatrix} \cos\chi_{ref} & \sin\chi_{ref} & 0 \\ -\sin\chi_{ref} & \cos\chi_{ref} & 0 \\ 0 & 0 & 1 \end{pmatrix} \quad (3-2)$$

In the obtained TCTF reference frame, the error (difference between reference and measured position) in x-direction is per definition zero. If $Y_{AC,TCTF}$ is positive, the aircraft is outside the circular segment and has to steer towards the circle center, if $Y_{AC,TCTF}$ is negative it has to steer away from the circle center. Whether this is to the left or to the right depends on the direction of the turn.

3-3 Controllers

Now that the reference frame used for control of the aircraft, the controllers themselves can be designed. Using the linearized Cessna Citation I model made at the Faculty of Aerospace Engineering of the University of Technology Delft in Simulink will enable the modeling of the aircraft and designing and tuning of the controllers.

In the experiment the aircraft will be controlled by the human operator and the haptic controller together, it is therefore important that the controller uses a control strategy similar to the human. Humans will generally look ahead down the trajectory and anticipate turns to control the aircraft. Therefore the automatic controller will need to do the same; make use of a predictive control strategy.

The means of predicting the states of the aircraft after a certain prediction time and the control strategy for both longitudinal and lateral control will be explained in this section.

3-3-1 Predictive control strategies

As humans look ahead naturally in order to control a vehicle, a algorithm is needed for the controller to do the same. An input for this controller should be either a look-ahead distance or look-ahead time, in this case look-ahead time is used. Grunwald (Grunwald et al., 1980) researched the effect of a predictor symbol in combination with a TIS display and found that: "a predictor symbol predicting the vehicle position 4 to 7 s in advance yields the best compromise between positional accuracy and system damping."

Longitudinal control

Predicting the state of an aircraft in longitudinal direction is quite straightforward. First the current altitude is taken and the difference in height over T_{pred} s is added. The difference in height is the product of the tangent of the flight path angle (γ), the prediction time and the current speed of the aircraft. As $\tan\gamma = \gamma$ for small angle, the formula given in Equation 3-4 can be used.

Similarly the directed height can be calculated, but instead of the measured altitude and flight-path angle, z_{ref} and γ_{ref} from the trajectory data are used.

$$z_{pred}(t) = z_{meas}(t) + \gamma(t) \cdot T_{pred}V \quad (3-3)$$

$$z_{dir}(t) = z_c(t) = z_{ref}(t) + \gamma_{ref} \cdot T_{pred}V \quad (3-4)$$

These two formulas are visualized in Figure 3-3, this illustration shows what is predicted to happen in the future (z_{pred}) and what should happen in the future in case the control law works correctly.

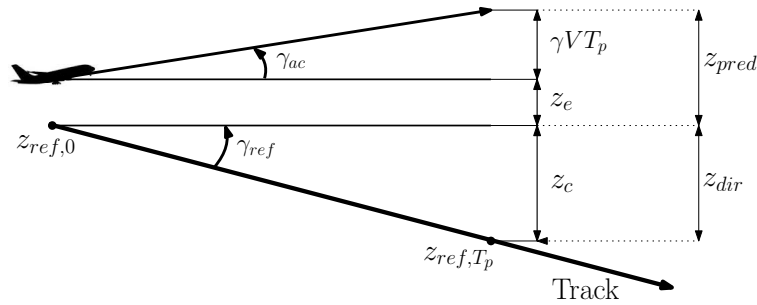


Figure 3-3: Sideview of the longitudinal flight path predictor

Translating Equations 3-9 and 3-10 into a block diagram allows it to be used in Simulink. Effectively the PID controller is translating the prediction position error, into a commanded elevator deflection. The position error is simply the difference between the predicted and directed state. The block diagram explaining this can be found in Figure 3-4.

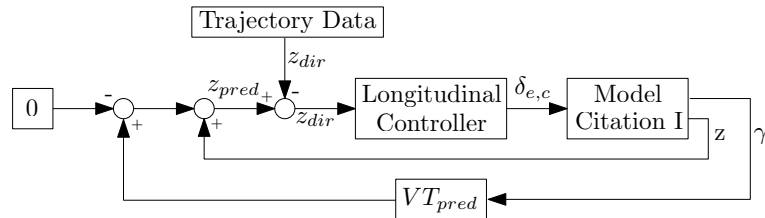


Figure 3-4: Control loop used for longitudinal control.

Lateral control

Predicting the lateral movement of an aircraft over time is a little less straightforward than the longitudinal case. There are more factors to take into account, using only the position error and heading will not give satisfactory results. In order to get a accurate enough controller, the circular flight path predictor is used (de Stigter et al., 2005).

As the TCTF reference frame is rotating from a lateral perspective, the predictor law needs to predict the future state of the aircraft with respect to the track, using relative position, relative lateral velocity, V_l and acceleration, a_l in the form of a second-order Taylor expansion shown in the following equation:

$$y_{pred}(t) = y_e(t) + \frac{\partial}{\partial t} y_e(t) \frac{T_{pred}}{1!} + \frac{\partial^2}{\partial t^2} y_e(t) \frac{T_{pred}^2}{2!} \quad (3-5)$$

Where the lateral velocity part can be expressed as:

$$\frac{\partial}{\partial t} y_e(t) \frac{T_{pred}}{1!} = \chi_e(t) \cdot T_{pred} V \quad (3-6)$$

and the lateral acceleration part as:

$$\frac{\partial^2}{\partial t^2} y_e(t) \frac{T_{pred}^2}{2!} = \dot{\chi}(t) \cdot \frac{1}{2} T_{pred}^2 V \quad (3-7)$$

Circular flight path predictor, can be extended with a so-called roll-rate extension, which takes into account - as the name suggests - the roll rate. Which is a gain (K_p) multiplied by the roll rate. De Stigter et al. (de Stigter et al., 2005) show that the gain required to cancel out the roll subsidence mode is:

$$K_p = \frac{g T_r T_{pred}^2}{2} \quad (3-8)$$

Where T_r is the characteristic roll subsidence time of the model which can be found by using the Matlab function damp.m and analyzing the Eigenmodes of the aircraft. Combining all these terms results in Equation 3-9.

$$y_{pred}(t) = y_e(t) + \chi_e(t) \cdot T_{pred} V + \dot{\chi}(t) \cdot \frac{1}{2} T_{pred}^2 V + p(t) \cdot K_p \quad (3-9)$$

Similarly to the longitudinal case, now too a definition of the directed state is needed as reference signal for the controller. This directed state will also be given with respect to the track and thus the TCTF reference frame and is calculated using the rotational speed of the aircraft along the track ($\Omega = \frac{V}{R}$) as shown in Equation 3-10.

$$y_{dir}(t) = y_c(t) = R \left(1 - \cos \left(T_{pred} \frac{V}{R} \right) \right) \quad (3-10)$$

The visualization of y_{pred} and Y_{dir} is shown in Figure 3-5. Where the effect of the roll-rate extension is indicated in by the dotted line at the top of the figure.

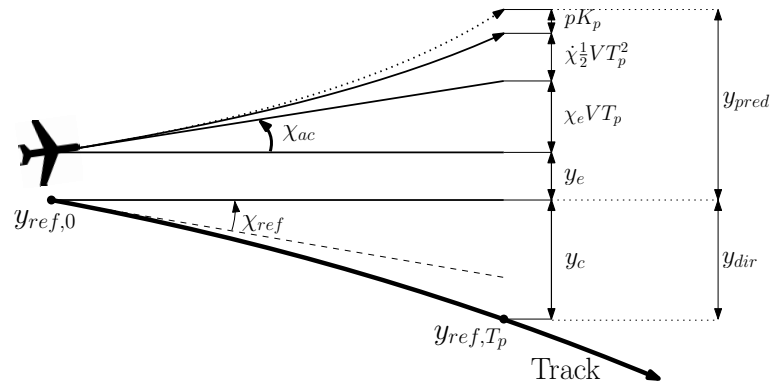


Figure 3-5: Sideview of the lateral flight path predictor

The block diagram outlining the controller based on the control laws stated above is illustrated in Figure 3-6. In this case 4 states are fed back after being multiplied with their relevant gains,

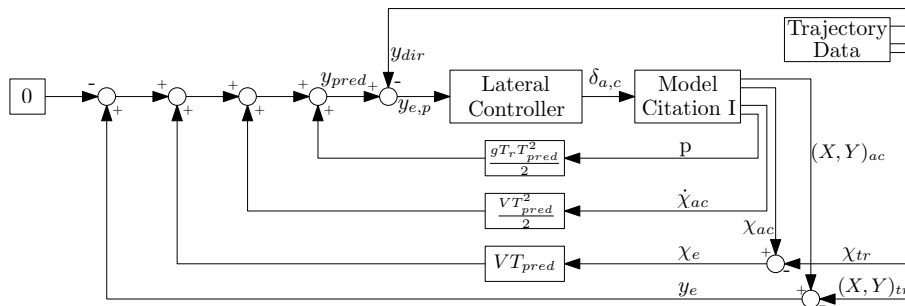


Figure 3-6: Control loop used for lateral control

so that they are expressed in the same dimension before added together and resulting in y_{pred} . From this value y_{dir} is subtracted and the resulting, predicted error, $y_{e,p}$, is used by the PID controller to generate an appropriate aileron command.

As y_e and χ_e are dependent on the track to be flown, trajectory data is subtracted from the output of the model to generate to correct values.

3-3-2 Control inputs and outputs

Longitudinal control

A trajectory was generated to see the effects of a change in slope in terms of control input and outputs. In the top graph of Figure 3-7 the trajectory side view can be seen. Next to the reference trajectory, the measured trajectories with a prediction time ranging from 3 to 6 seconds can be found. It can be seen that the aircraft follows the reference trajectory quite accurately.

In the middle graph of the Figure, it can be seen how accurately exactly, for all prediction times the error remain within 10 meters, which means it will stay even within the boundaries of the smallest tunnel (width is 20 meters). It can also be seen in this graph, that the predictive control strategy creates an error before the change in slope at 60 seconds, this is the part the aircraft is cutting the corner. This error reduces once the slope has changed.

The bottom graph of Figure 3-7 shows the elevator deflections, it can be seen that for longer prediction times, the control input is given sooner, as can be expected. The sooner the control input is given, the less deflection is needed to get the appropriate result. During the experiment, the most important part of the generated control inputs, is its intuitiveness to the pilot. The control inputs generated by the controller are relatively smooth, making it easier to understand as haptic feedback. They are also quite small (only 0.5 degrees out of a maximum deflection of 12.5 degrees), changing stick dynamics could help the pilot feel the feedback of these small control inputs.

Lateral control

The same set of graphs can be found in Figure 3-8, where the top graph shows the top view of the trajectory this time. So instead of time, the y-coordinates are on the x-axis, positive direction indicating East. In the lateral case the difference between the reference trajectory

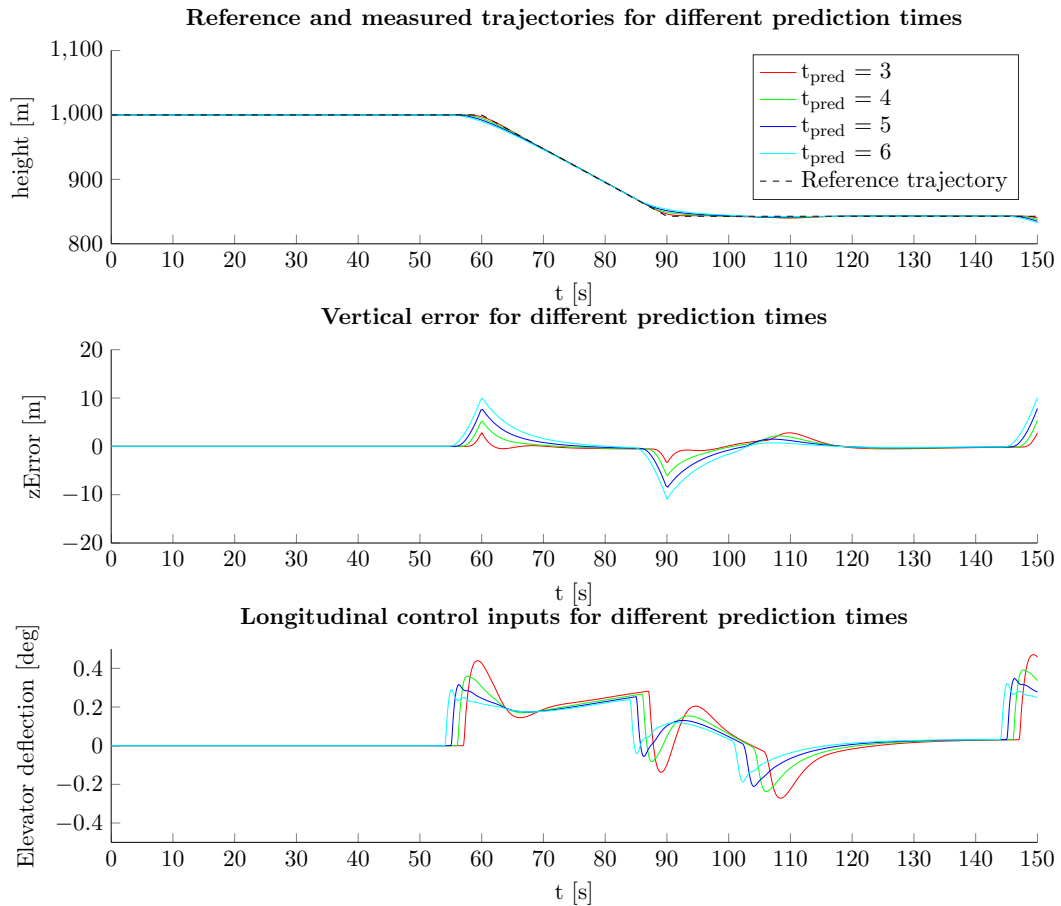


Figure 3-7: Results of longitudinal, predictive control for multiple prediction times

and measured trajectories is almost not visible.

The middle graph shows a clearer picture as it shows the error in the lateral direction, or the y-error in the TCTF reference frame. In this graph it can be seen that the performance of a 6 second prediction time is clearly worse than that of the others. This can have two reasons: the controller is tuned for a 5-second prediction time, or a 6-second prediction time is just not sensitive enough to high frequent behavior.

In the bottom graph of Figure 3-8 the control inputs given to the ailerons are shown. When looking closely a bump in the control at 15 seconds can be seen, this is where the heading error term kicks in, as this is the point where the circular segment starts. It will have to be seen if this is comparable to human control, otherwise the gain of this term or that of the others should be changed.

3-4 Implementation of haptics

Once the controllers work satisfactory, the haptics can be implemented. In Figure 3-9 the block diagram including haptic feedback can be found. It shows how moments and deflections are coupled through the stick dynamics. And how the level of guidance is indicated by the haptic

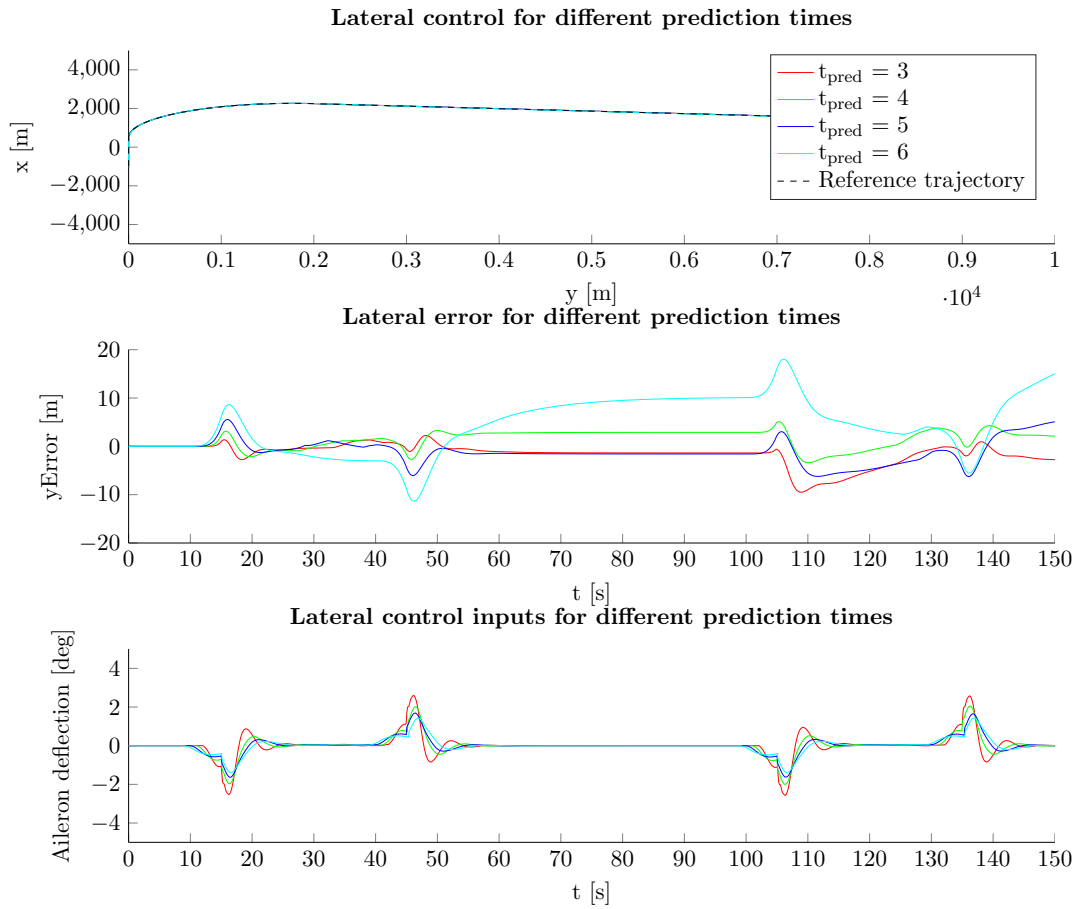


Figure 3-8: Results of lateral, predictive control for multiple prediction times

authority. It also shows a disturbance force that will be there when the experiment is executed, but is not used in the simulation, as the results are cleaner without this disturbance term.

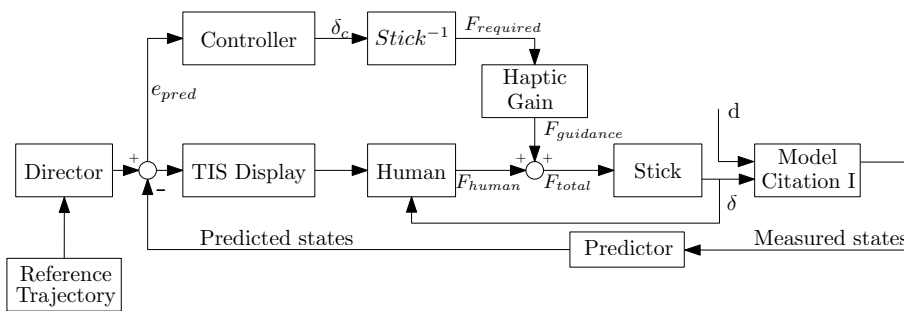


Figure 3-9: Haptics implemented in the control loop

3-4-1 Dynamics of the model

There is two blocks in the diagram that need a dynamic model in order for the simulation to be run. The stick and human dynamics.

The stick dynamics used in the model are mass-spring-damper dynamics, according to the

following transfer function:

$$H_s(s) = \frac{1}{I_s s^2 + b_s s + K_s} \quad (3-11)$$

For both the pitch and roll direction an inertia of $I_s = 0.02 [kg m^2]$, damping coefficient $b_s = 0.2 [Nms rad^{-1}]$ and spring coefficient $k_s = 2 [Nm rad^{-1}]$ will be used. This model translate moments to stick deflections, but can be inverted to translate the other way around.

Figure 3-9 contains a *human* block as well, getting both the stick position and displayed error as feedback. For the simulation a human model is therefore required. As the task at hand has a director and a predictor, the operator can control it as a tracking task. This can be modeled as a gain and delay terms (McRuer & Jex, 1967). An effective time delay is needed for information processing, $\tau_e = 0.3 s$ and a neuromuscular delay including reaction time and muscle activation, $\tau_N = 0.1 s$. Using a first order Pad approximation, results in the following pilot model (de Stigter et al., 2005):

$$H_{pilot} = H_{y_{pred}}^{\delta_{ac}} = K_p \frac{-0.15s + 1}{0.15s + 1} \frac{1}{0.1s + 1} \quad (3-12)$$

Where K_p is a pilot gain of 1, which is within the range suggested by De Stigter (de Stigter et al., 2005), the second term on the right-hand side is the information processing delay and the third term is the NMS delay.

This transfer function does not use the haptic feedback directly (only the reduced error because of the applied feedback is used), so the real control strategy of the pilot will not correspond exactly. The effect of the haptic feedback on the pilot is hard to predict, therefore tuning in the simulator will be required.

3-4-2 Results of haptic feedback

In Figure 3-10 the results of the control inputs when using haptic feedback with a haptic authority of 0.5 are shown for a prediction time of 3 s. It can be seen that the haptic forces and human forces move in the same direction, which should be the case. As said before, human feedback is not modeled using the stick deflection as a feedback, therefore this plot could look quite different in reality.

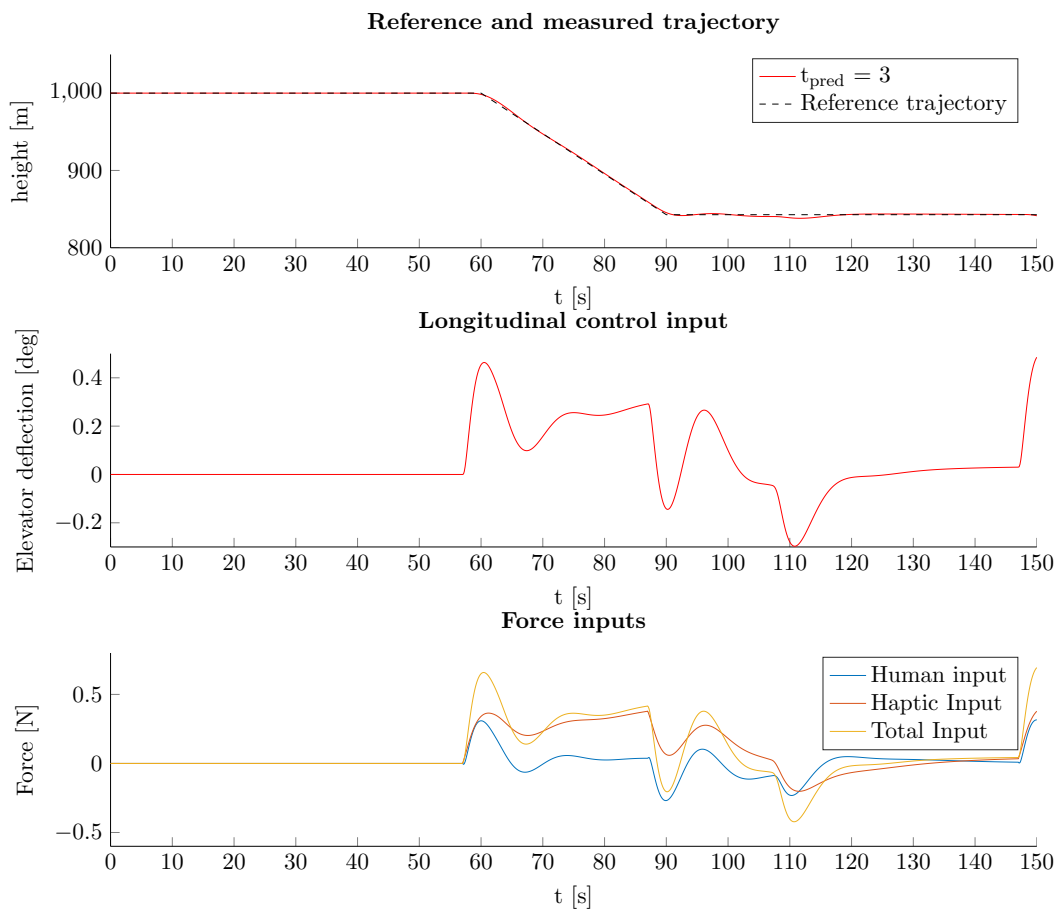


Figure 3-10: Haptic and human control inputs according to the Simulink model ($HA = 0.5$)

Part III

Appendices

Appendix A

Simulink Architecture

Before the actual experiment was implemented and flown, offline simulations were performed to design the controller on which the haptic controller was based. This was done in Simulink, the complete architecture can be found in Figure A-1, the architecture of the predictors and controllers are shown in Figures A-2, A-3 and A-4.

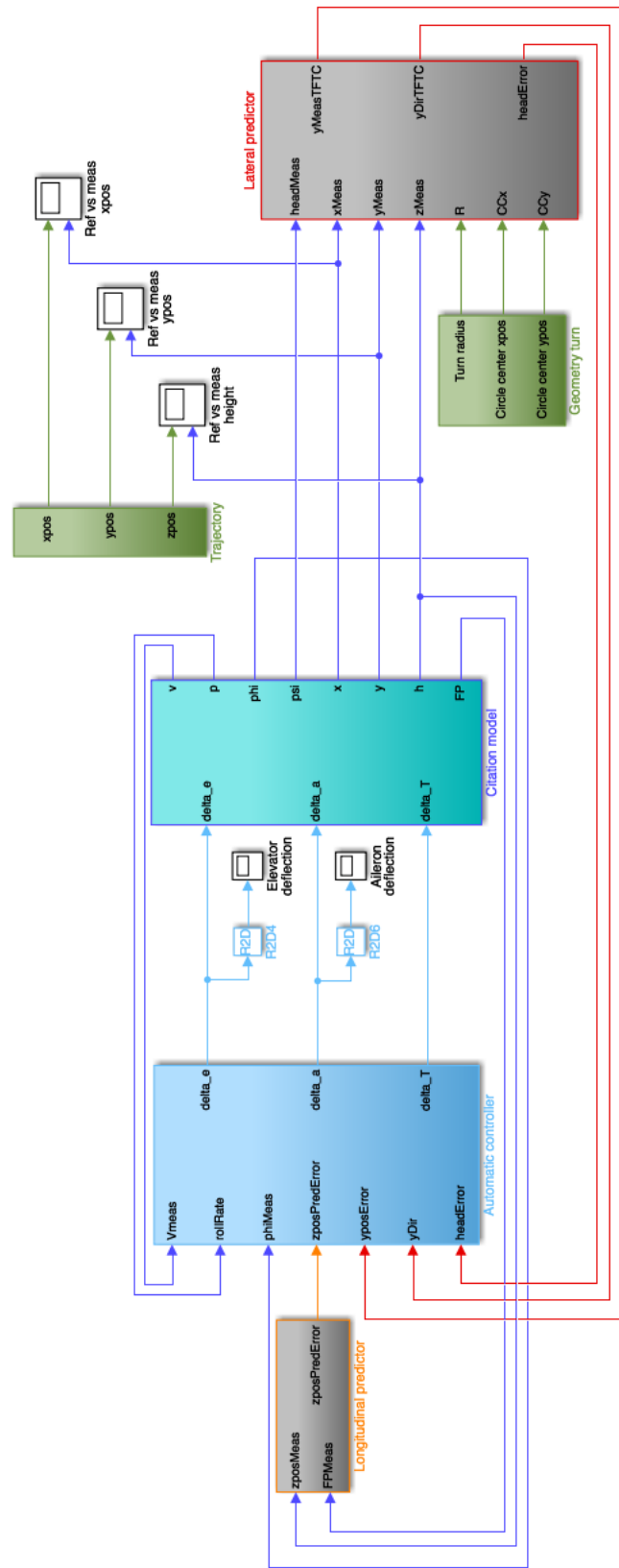


Figure A-1: Complete architecture of the controller in used for offline simulations in Simulink

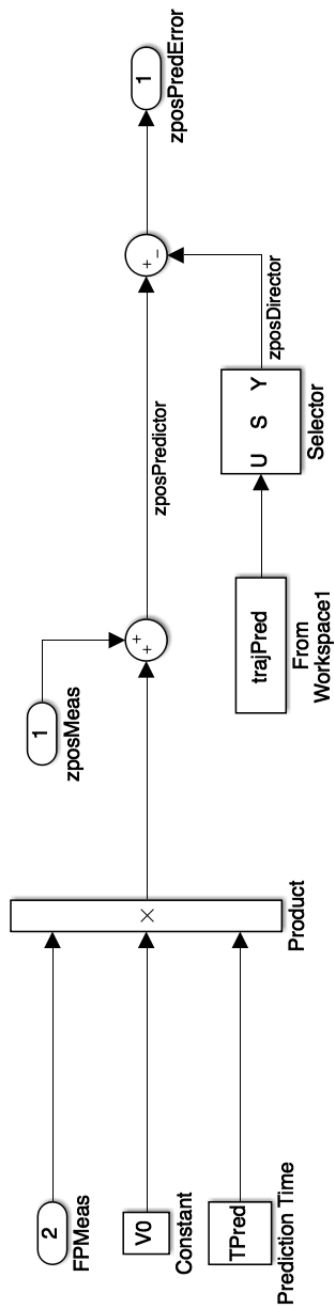


Figure A-2: Architecture of the longitudinal predictor in Simulink

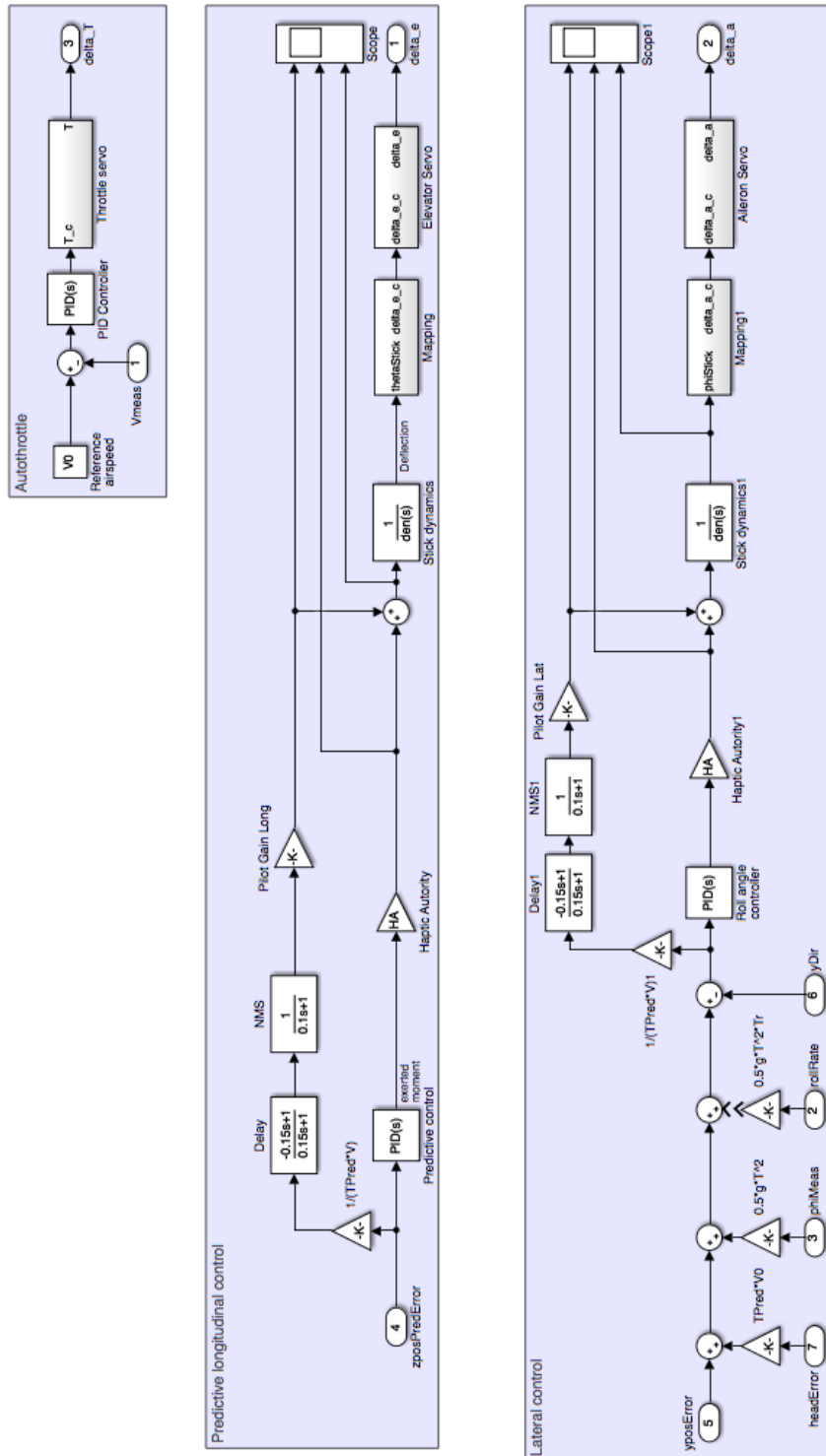


Figure A-4: Architecture of the longitudinal, lateral and throttle controller in Simulink

Appendix B

Experiment Briefing

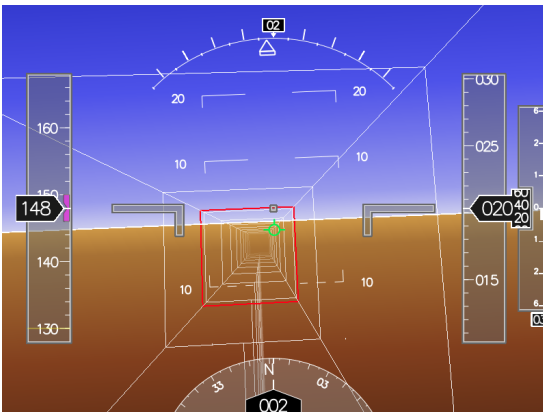
This document serves to provide information regarding the human-in-the loop experiment called Haptic Tunnel-in-the-Sky for Increasing Task-Sharing Performance. The experiment will be conducted in the SIMONA Research Simulator operated by the Control and Simulation division of the faculty of Aerospace Engineering of Delft University of Technology. After reading this document, the participant should have a better understanding of the goal of the human-in-the-loop experiment, the task that will be performed, as well as the general setup of the experiment.

B-1 Goal of the experiment

The goal of the experiment is to analyze the effects of feedback on a primary flight task through a virtual tunnel-in-the-sky and the task-sharing performance of the participants. Next to this, the effects of haptic feedback on tasks of different difficulty will be investigated.

B-2 Experiment Task

During the experiment the participants will control a simulated Cessna Citation I trimmed for straight, level flight at 148 kts. There will be two tasks for the participants to perform. The primary task will be to fly as close as possible to the center of the tunnel. These tunnels will have different trajectories and sizes for different runs. What the head-down display will look like is shown in Figure B-1a. A flight path predictor is provided to the pilots, this symbol shows where the aircraft will be after the prediction time, this symbol is indicated in green on the tunnel-in-the-sky display. During some of the runs the pilots will be assisted by haptic feedback applied as forces on the side stick. These haptic forces will be of such force that they can always easily be overruled by the participant.



(a) Head-down display showing a tunnel indicating the trajectory to be flown



(b) Representation of the outside visual with superimposed secondary task as will be used in the experiment

The secondary task will be displayed on the outside visuals superimposed on the terrain and the sky. The pilot will have to indicate the open side of the odd symbol. The secondary task will be reset every few seconds, answering can be done through the trim button on the side-stick. Figure B-1b shows the secondary task superimposed on the outside visuals.

To summarize, the tasks given to the pilots will be:

1. The pilot has to fly in the middle of the tunnel.

2. The pilot has to indicate the correct answer to the secondary task

A correct answer only counts when it is given while the pilot is flying inside of the tunnel. At the end of each run the average error between the middle of the tunnel and the aircraft and number of correct answers will be communicated with the pilot.

B-3 Apparatus

The experiment will be conducted in the SIMONA Research Simulator (SRS) with the motion disabled, the inside and outside view of the SIMONA are shown in Figure B-2. You will be seated in the right seat of the cockpit and use a right-handed side-stick. The aircraft model that will be used in the simulation is a Cessna Citation I. You will have control over the roll and pitch axis of the aircraft. The throttle will be controlled by the autopilot. A tunnel-in-the-sky will be shown on a head down display, this display will also show speed, roll angle, pitch angle and heading.



(a) Outside view



(b) Flightdeck

Figure B-2: The SIMONA (Simulation, MOtion and NAVigation) Research Simulator (SRS) at Delft University of Technology

In the cockpit there will be an eye-tracker installed, this eye-tracker will trace eye movements of the pilots. In order to use this a head model will be made in the beginning of the experiment. To obtain accurate results, the pilot cannot wear glasses during the experiment. The eye-tracker itself uses mounted cameras, so no devices will be attached to the pilots in any way.

B-4 Experiment Procedures

First the pilot will be briefed by reading this document and receiving a verbal briefing from the experimenter. The participant will sign a consent form, the conditions of which are discussed in Section B-5. Secondly the experiment environment will be set-up, the pilot will take a comfortable position in the pilot seat and the head-model of the pilot will be made, this is a procedure completely taken care of by cameras and software, there will be no physical involvement required from the pilot other than sitting in the chair.

Note: the pilot cannot wear glasses in order for the eye-tracker to work properly, contact lenses are allowed.

After setting up, the participant will receive a training, during which all features of the experiment will be added one-by-one. This familiarization and training phase will take approximately an hour but can be shortened or elongated if this is required. After the training phase the evaluation phase will start, where the pilot has to perform the primary and secondary task in 3 blocks. Each block in the experimentation phase will consist of 4 runs of 6 minutes each. Between these blocks and between the training and evaluation phase there will be coffee brakes. The total duration of the experiment will be approximately 3 hours.

During each run different combinations of haptic feedback and tunnel sizes will be provided. After each run the pilot will be asked to rate his mental effort required to perform the task.

Throughout the whole experiment feedback on the performance of the pilot for both tasks will be provided. By giving the average error compared to the middle of the tunnel and indicating the number of correct answers given by the pilot while flying within the limits of the tunnel.

B-5 Your Rights

Participation in the experiment is voluntary. This means that you can terminate your cooperation at any time, even during the experiment.

The data collected during the experiment will remain confidential and anonymous. Your data will be treated such that only the experimenter can link the results to a particular participant. By participating you do agree that your data may be published. If so, this is also done anonymously, such that the published results cannot be traced back to you. Lastly we ask you to not discuss any details of the experiment with anyone, until the complete experiment has finished, to prevent that other participants are biased.

To make sure that you understood the above, you will be asked to sign an informed consent form before the start of the experiment.

Appendix C

Experiment Conditions

C-1 Conditions

During the evaluation phase all participants flew a total of twelve conditions, these conditions can be found in Table C-1. These twelve conditions were later combined into six, as track 1 and 2 are just mirror images of each other. In Table C-2 the training conditions can be found, these conditions were flown in the indicated order, such that participants had to deal with one novelty at the time. First only the tunnel, then the haptics and lastly the secondary task. In Table C-3 the tuning conditions are shown, these conditions have either a completely lateral (no elevation) or completely longitudinal (no heading change) trajectory. This was done so that both haptic controllers could be tuned and tested separately.

Table C-1: Evaluation conditions

Condition#	Track#	VTS	HTS	SecTask
1	1	20	0	On
2	2	20	0	On
3	1	60	0	On
4	2	60	0	On
5	1	20	20	On
6	2	20	20	On
7	1	60	20	On
8	2	60	20	On
9	1	20	60	On
10	2	20	60	On
11	1	60	60	On
12	2	60	60	On

Table C-2: Training conditions

Condition#	Track#	VTS	HTS	SecTask
801	3	60	0	Off
802	4	20	0	Off
803	4	60	60	Off
804	3	20	20	Off
805	3	60	60	On
806	4	20	20	On
807	4	60	20	On
808	3	20	60	On

Table C-3: Tuning conditions

Condition#	Track#	VTS	HTS	SecTask
901	5	20	20	On
902	6	20	20	On

C-2 Latin square design

The order of conditions was randomised and each participant started at the next conditions, creating a Latin square experiment design. This was done to mitigate the measured effects of learning during the evaluation phase.

Table C-4: Latin square design of the experiment

Participant #	P1	P2	P3	P4	P5	P6	P7	P8	P9	P10	P11	P12
Run 1	C9	C7	C10	C3	C1	C12	C2	C6	C11	C5	C8	C4
Run 2	C7	C10	C3	C1	C12	C2	C6	C11	C5	C8	C4	C9
Run 3	C10	C3	C1	C12	C2	C6	C11	C5	C8	C4	C9	C7
Run 4	C3	C1	C12	C2	C6	C11	C5	C8	C4	C9	C7	C10
Run 5	C1	C12	C2	C6	C11	C5	C8	C4	C9	C7	C10	C3
Run 6	C12	C2	C6	C11	C5	C8	C4	C9	C7	C10	C3	C1
Run 7	C2	C6	C11	C5	C8	C4	C9	C7	C10	C3	C1	C12
Run 8	C6	C11	C5	C8	C4	C9	C7	C10	C3	C1	C12	C2
Run 9	C11	C5	C8	C4	C9	C7	C10	C3	C1	C12	C2	C6
Run 10	C5	C8	C4	C9	C7	C10	C3	C1	C12	C2	C6	C11
Run 11	C8	C4	C9	C7	C10	C3	C1	C12	C2	C6	C11	C5
Run 12	C4	C9	C7	C10	C3	C1	C12	C2	C6	C11	C5	C8

Appendix D

Rating Scale Mental Effort

D-1 Rating Scale Mental Effort

The Rating Scale Mental Effort was used to determine the subjective mental effort rating of each pilot after each run. The scale can be found in Figure D-1 (Zijlstra, 1993). The actual scores of each participant are shown in Table D-1, these are the combined scores of each mirrored run.

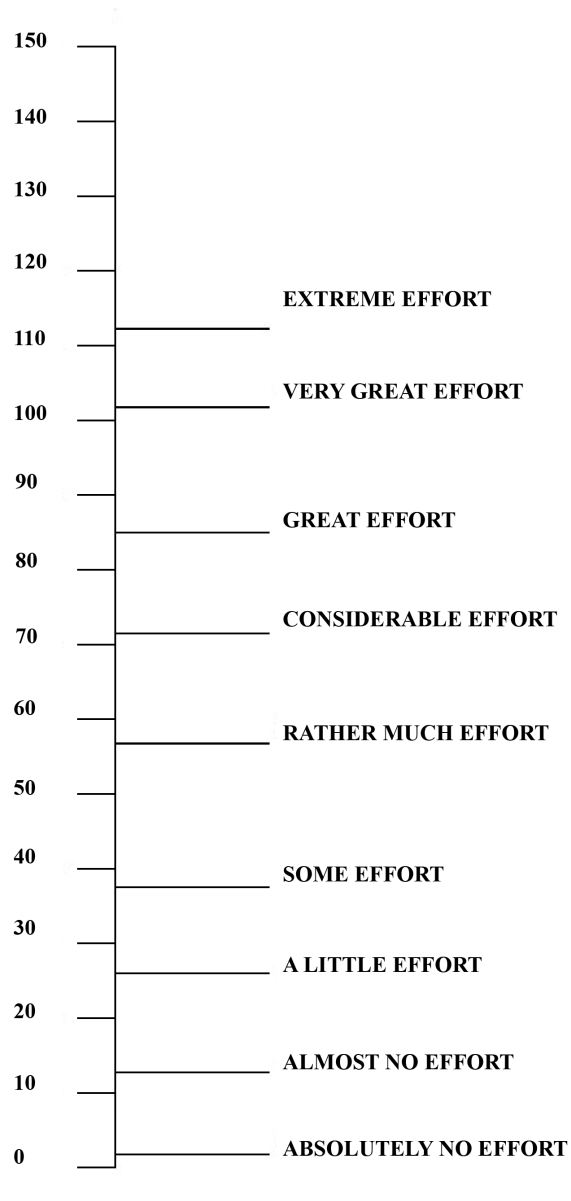


Figure D-1: Rating Scale Mental Effort

D-2 Mental effort ratings

Table D-1: Mental effort rating of each participant for each run

RMSE	CN1	CN2	CN3	CN4	CN5	CN6
P1	70	27.5	32.5	25	32.5	35
P2	65	45	45	40	42.5	45
P3	92.5	77.5	77.5	70	87.5	75
P4	90	77.5	70	65	85	70
P5	87.5	65	70	62.5	72.5	60
P6	40	40	32.5	25	47.5	30
P7	82.5	47.5	72.5	47.5	62.5	60
P8	100	82.5	80	80	95	82.5
P9	70	60	60	60	85	45
P10	62.5	47.5	40	35	65	37.5
P11	87.5	77.5	60	72.5	75	62.5
P12	65	65	37.5	50	60	55

Appendix E

Approval of Ethics Committee

Date 02-02-2017

Contact person Ir. J.B.J. Groot Kormelink, secretary HREC

Telephone +31 152783260

E-mail j.b.j.grootkormelink@tudelft.nl



Human Research Ethics Committee
TU Delft

(<http://hrec.tudelft.nl/>)

Visiting address

Jaffalaan 5 (building 31)

2628 BX Delft

Postal address

P.O. Box 5015 2600 GA Delft

The Netherlands

Ethics Approval Application: Haptic Tunnel-in-the-Sky for Increasing Task-Sharing Performance

Applicant: Beeftink, Derek

Dear Derek Beeftink,

It is a pleasure to inform you that your application mentioned above has been approved.

Good luck with your research!

Sincerely,

Prof. Dr. Sabine Roeser

Chair Human Research Ethics Committee TU Delft

Prof.dr. Sabine Roeser

TU Delft

Head of the Ethics and Philosophy of Technology Section

Department of Values, Technology, and Innovation

Faculty of Technology, Policy and Management

Jaffalaan 5

2628 BX Delft

The Netherlands

+31 (0) 15 2788779

S.Roeser@tudelft.nl

www.tbm.tudelft.nl/sroeser

Appendix F

Rejection of Participants

The data of two participants have been rejected after they performed the experiment. The first one was rejected because the eye-tracker data was corrupted and could therefore not be used. The second participant was not able to stay inside the tunnel for most conditions, as the haptic controller is designed for flying inside or close to the tunnel, the effect of the haptics could not be measured for this participant. To illustrate, the score of all the accepted participants combined and the rejected data are plotted in Figure F-1, it can be seen that most of the RMS scores of the rejected participant can be considered outliers.

Two other pilots have flown to compensate for the rejected data, so that the full Latin square design could be filled.

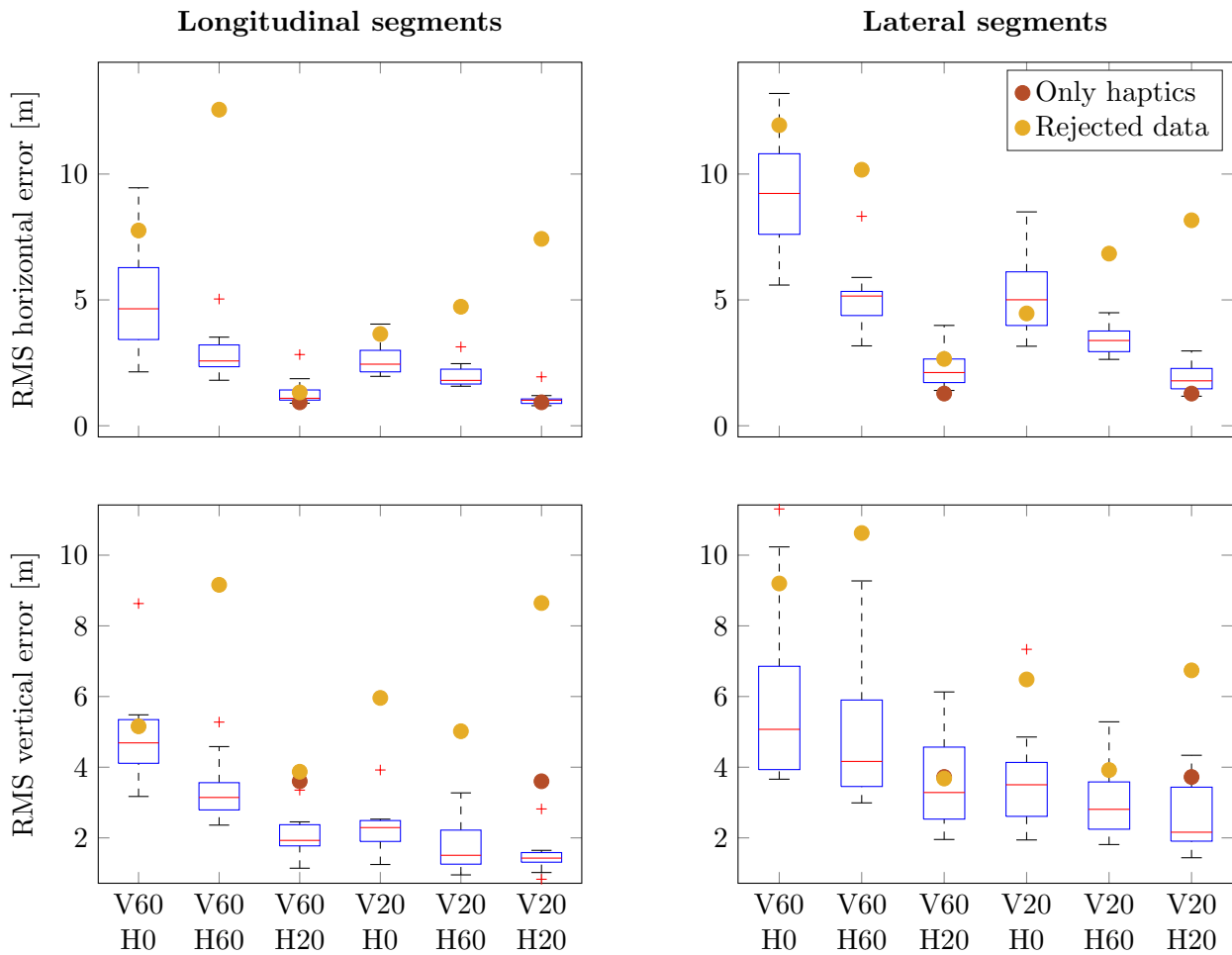


Figure F-1: Boxplot of all the participants and the rejected data

Appendix G

Additional Data

G-1 Time series

To provide a better feeling of where the averaged values in the boxplots come from, in this appendix time series data of the measured variables can be found. Some show clear trends, where others only show the limits of a certain variable. Figures G-1 to G-8 show the effects of haptic feedback on errors, rates, human forces and haptic forces for a visual tunnel size of 60 *m*, Figures G-9 to G-16 do this for a visual tunnel size of 20 *m*. In all error plots in Figures G-1, G-2, G-9 and G-10 it can be seen that the lines with the largest error are those of the non-haptic setting. For the pitch and roll rates, it can be seen in Figures G-3, G-4, G-11 and G-12 that there is a decrease in spread for increasing feedback. The same can be concluded for human forces on the stick, shown in Figures G-5, G-6, G-13 and G-14. For the plots of the haptic forces in Figure G-7, G-8, G-15 and G-16, it can be seen that the haptic forces reach their limit more often for the most strict haptic setting. Moreover, in each plot it can be seen that the data shows different trends for longitudinal and lateral segments.

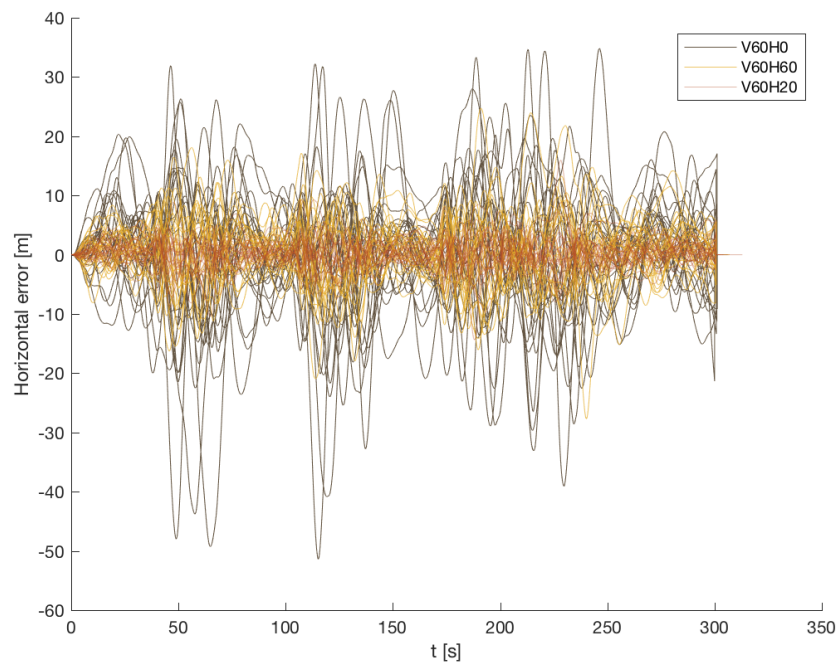


Figure G-1: Time series of the horizontal error of all the runs with a visual tunnel size of 60 *m*

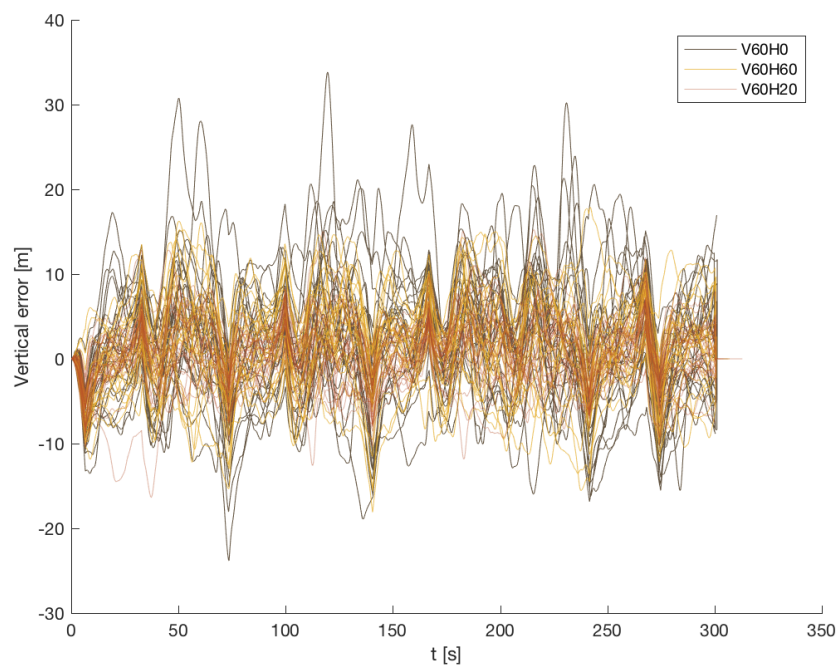


Figure G-2: Time series of the vertical error of all the runs with a visual tunnel size of 60 *m*

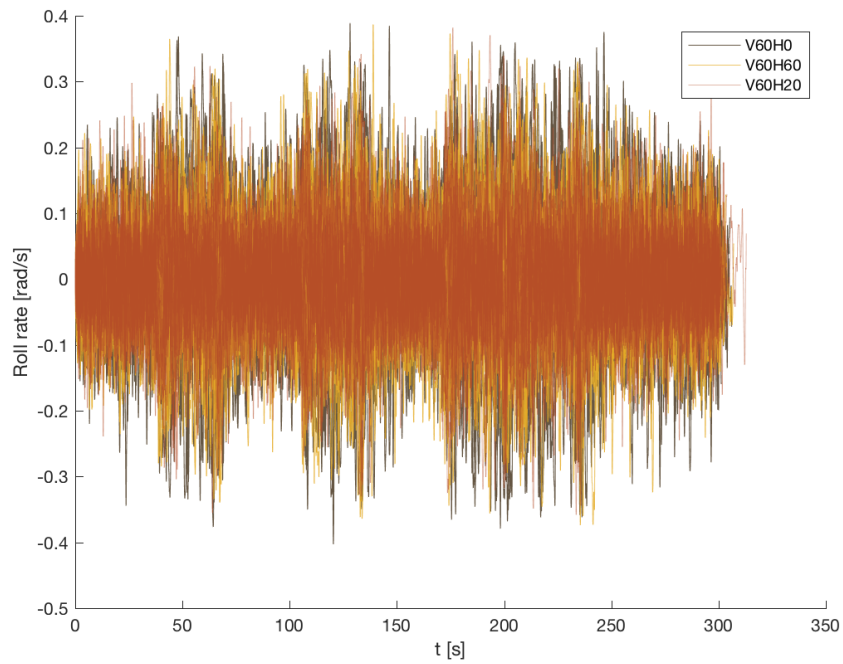


Figure G-3: Time series of the roll rates of all the runs with a visual tunnel size of 60 *m*

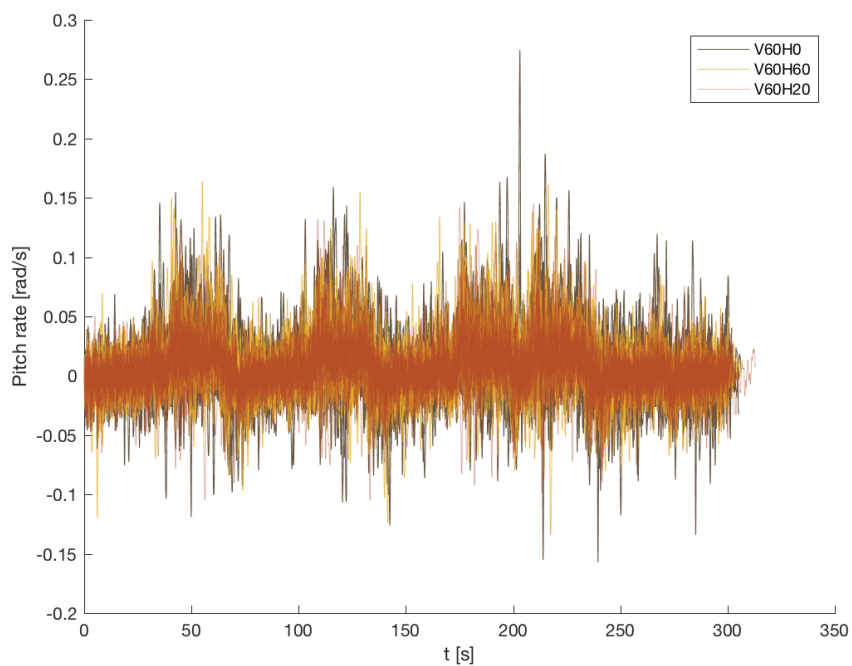


Figure G-4: Time series of the pitch rates of all the runs with a visual tunnel size of 60 *m*

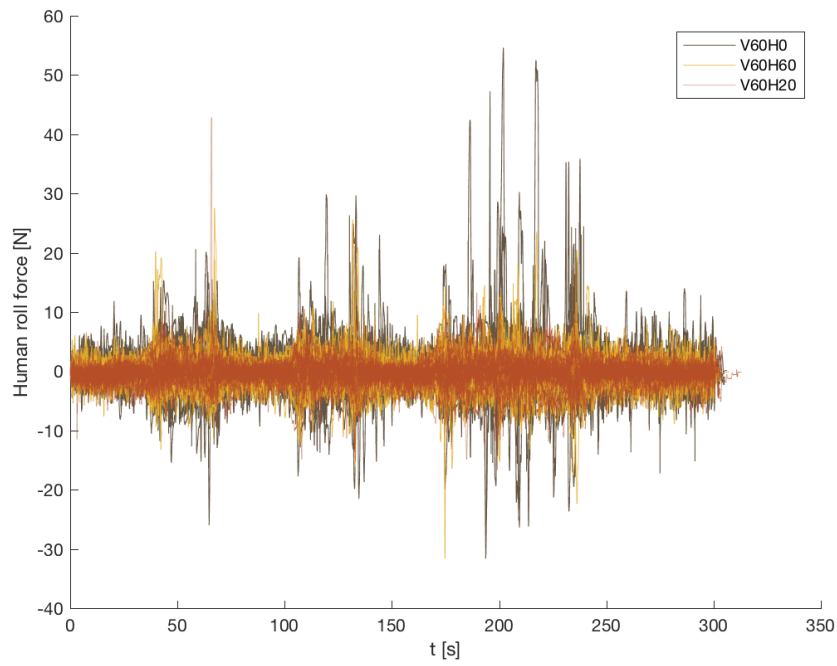


Figure G-5: Time series of the human roll forces of all the runs with a visual tunnel size of 60 m

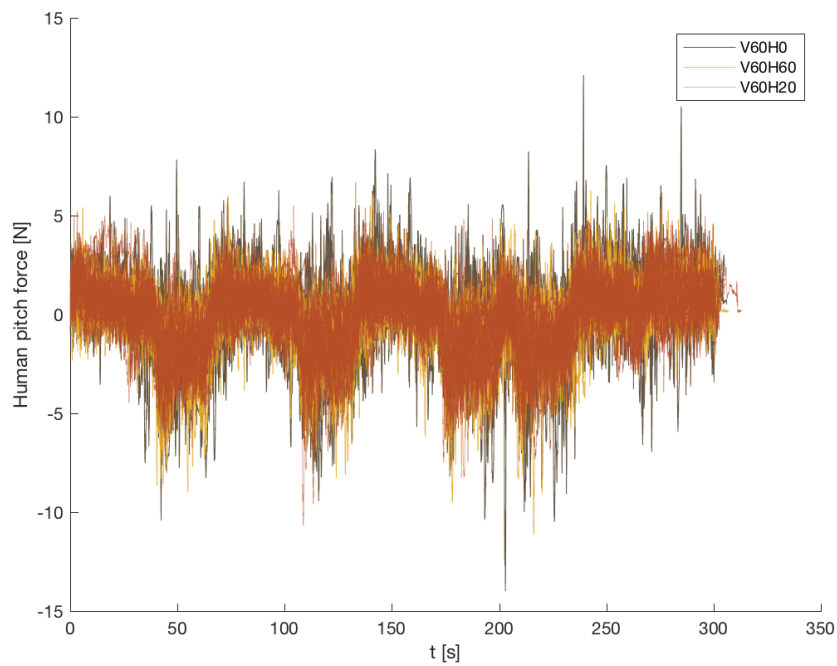


Figure G-6: Time series of the human pitch forces of all the runs with a visual tunnel size of 60 m

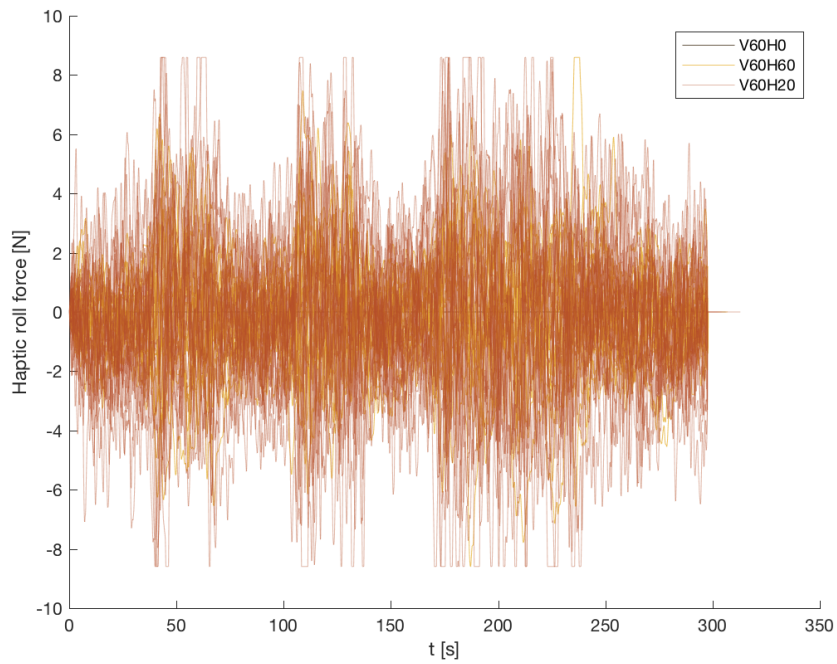


Figure G-7: Time series of the haptic roll forces of all the runs with a visual tunnel size of 60 *m*

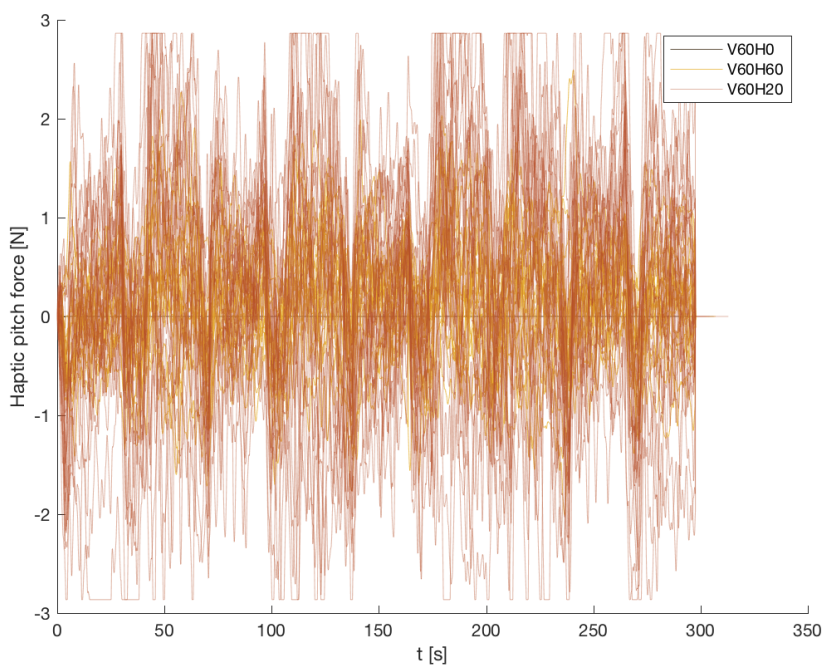


Figure G-8: Time series of the haptic pitch forces of all the runs with a visual tunnel size of 60 *m*

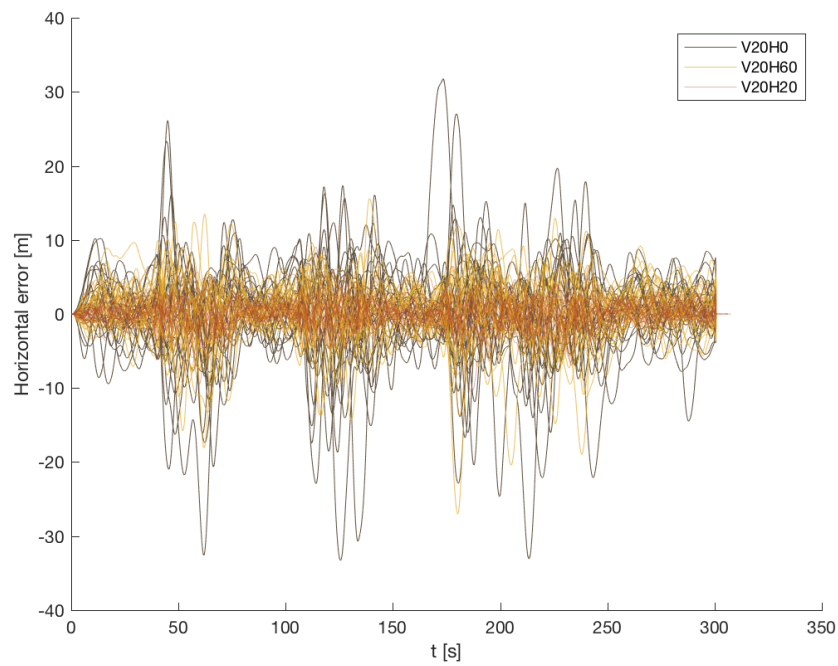


Figure G-9: Time series of the horizontal error of all the runs with a visual tunnel size of 20 *m*

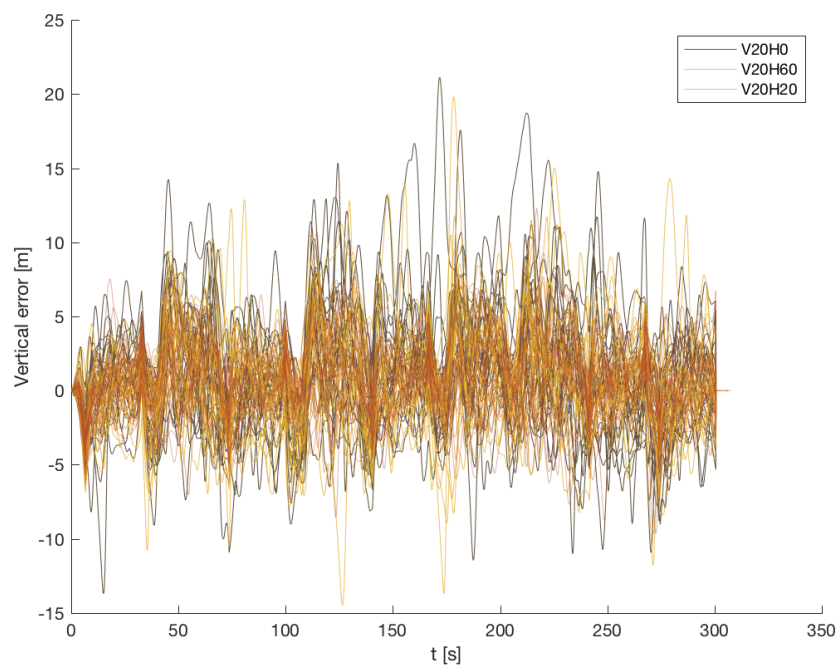


Figure G-10: Time series of the vertical error of all the runs with a visual tunnel size of 20 *m*

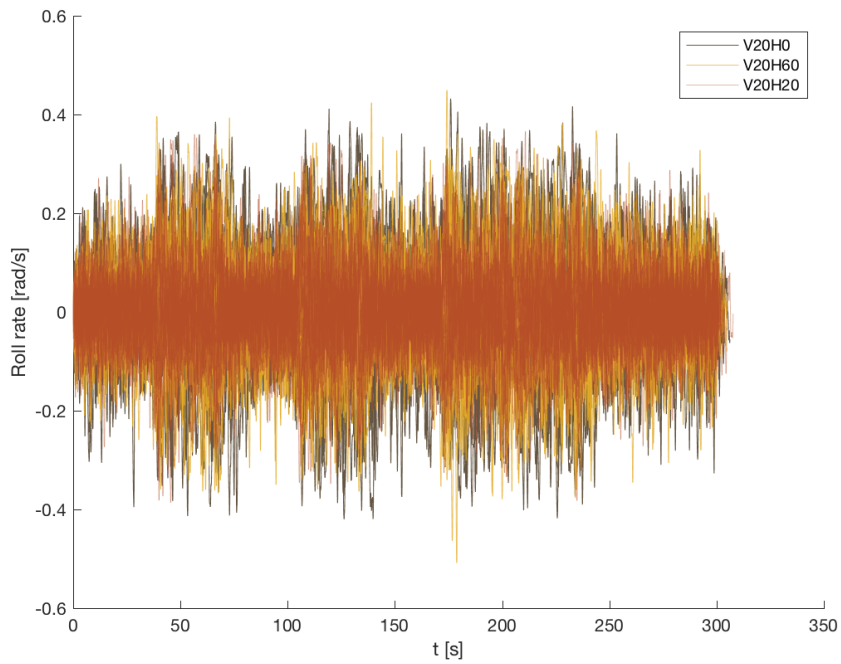


Figure G-11: Time series of the roll rates of all the runs with a visual tunnel size of 20 *m*

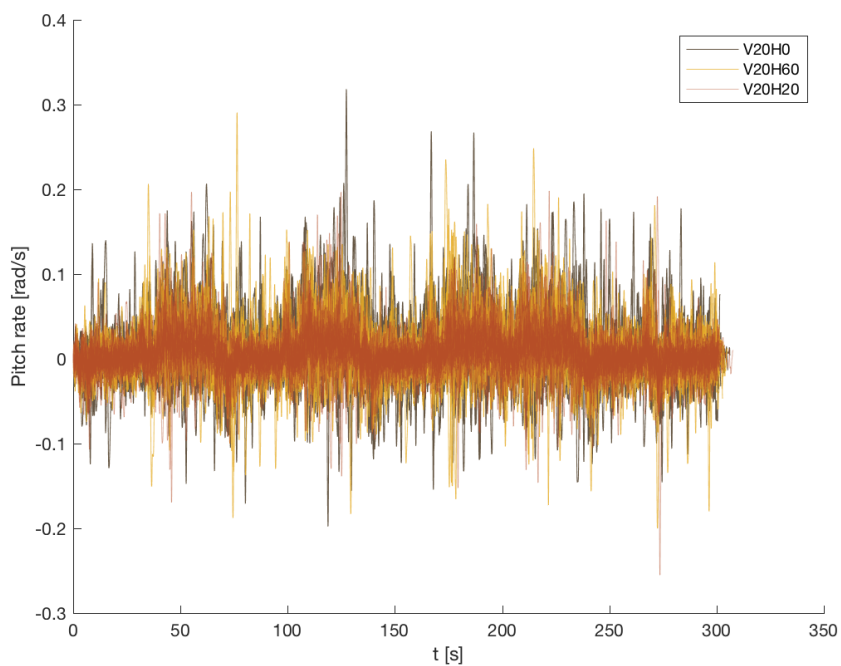


Figure G-12: Time series of the pitch rates of all the runs with a visual tunnel size of 20 *m*

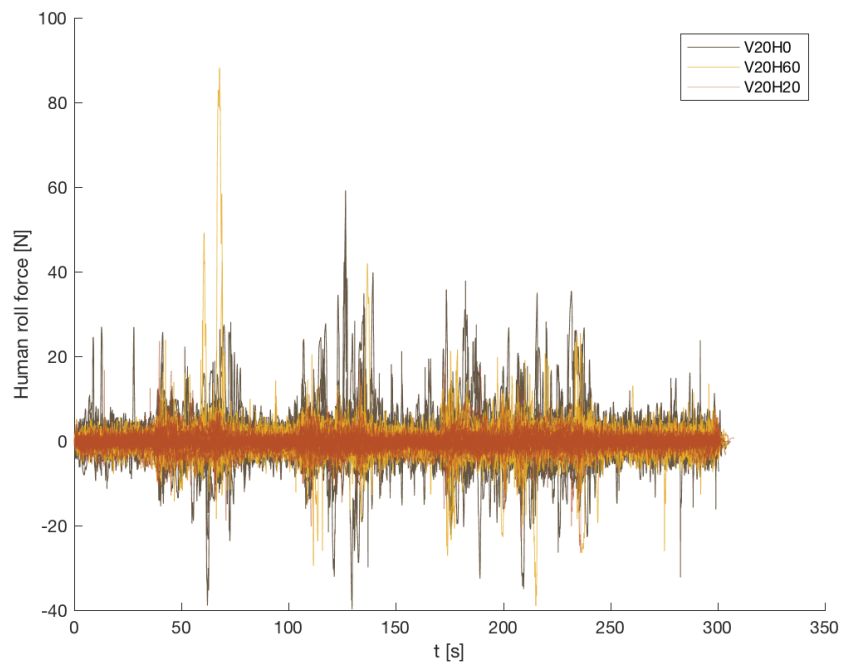


Figure G-13: Time series of the human roll forces of all the runs with a visual tunnel size of 20 *m*.

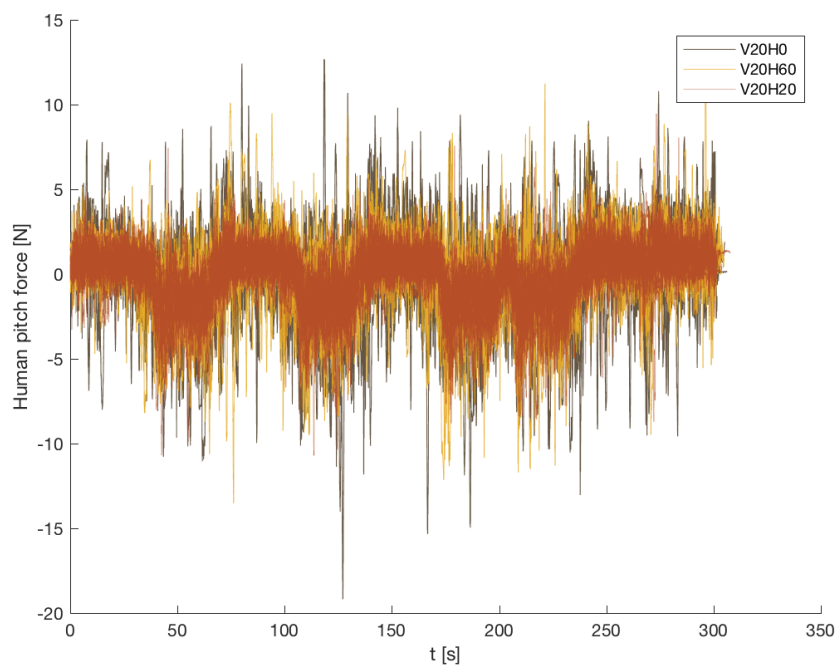


Figure G-14: Time series of the human pitch forces of all the runs with a visual tunnel size of 20 *m*.

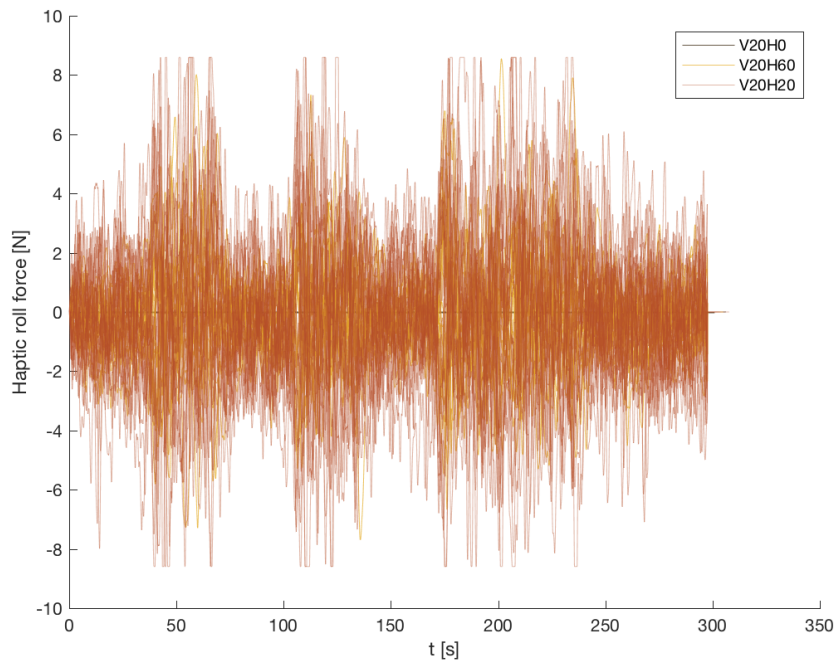


Figure G-15: Time series of the haptic roll forces of all the runs with a visual tunnel size of 20 *m*

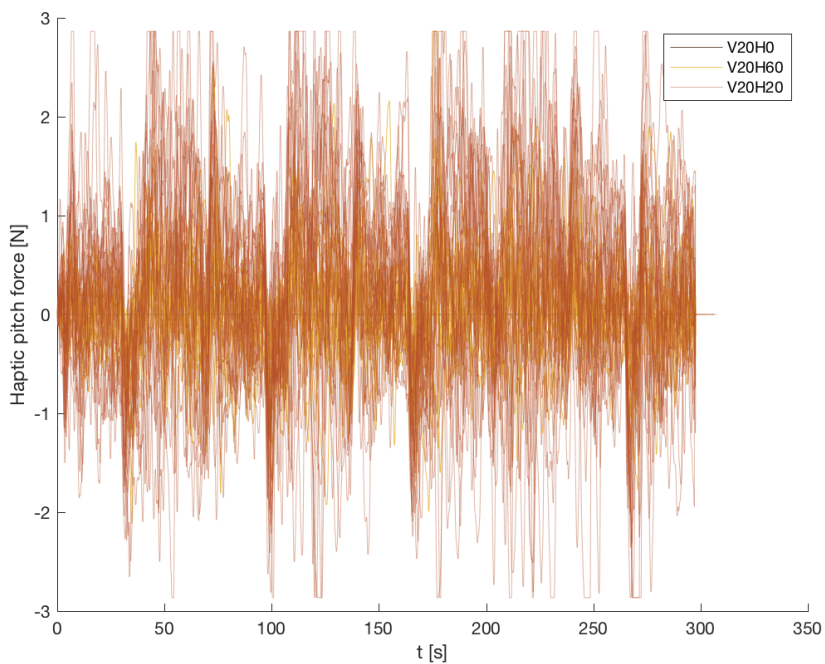


Figure G-16: Time series of the haptic pitch forces of all the runs with a visual tunnel size of 20 *m*

Appendix H

Processing of Eye-Tracker Data

H-1 Filtering raw data

The eye-tracker uses biometric features of the participants' faces, like corners of eyes and mouth, nostrils or birthmarks, to determine the orientation of the head. Next to this, the position of the pupils was used by the software to determine the direction of the gaze. The raw eye-tracker data which was recorded contained noisy elements, as every blink or movement of the face muscles can generate an outlier. Therefore post-processing of the eye-tracker data was required to determine whether a candidate was looking outside or to the TIS display.

Figure H-1 and H-2 show the original and filtered data of a complete run and a zoomed in part of that same run, respectively. In Figure H-1 peaks in the original (blue) data can be seen clearly. Moreover, it can be seen that both the median and Hampel filter, filter most of these outliers. The working of both filters is quite similar, but the Hampel filter uses 7 adjacent data points to determine the median where the median filter uses 13. If the point in the middle of the sample taken is more than 3 standard deviation removed from the median, it is allocated the value of the median.

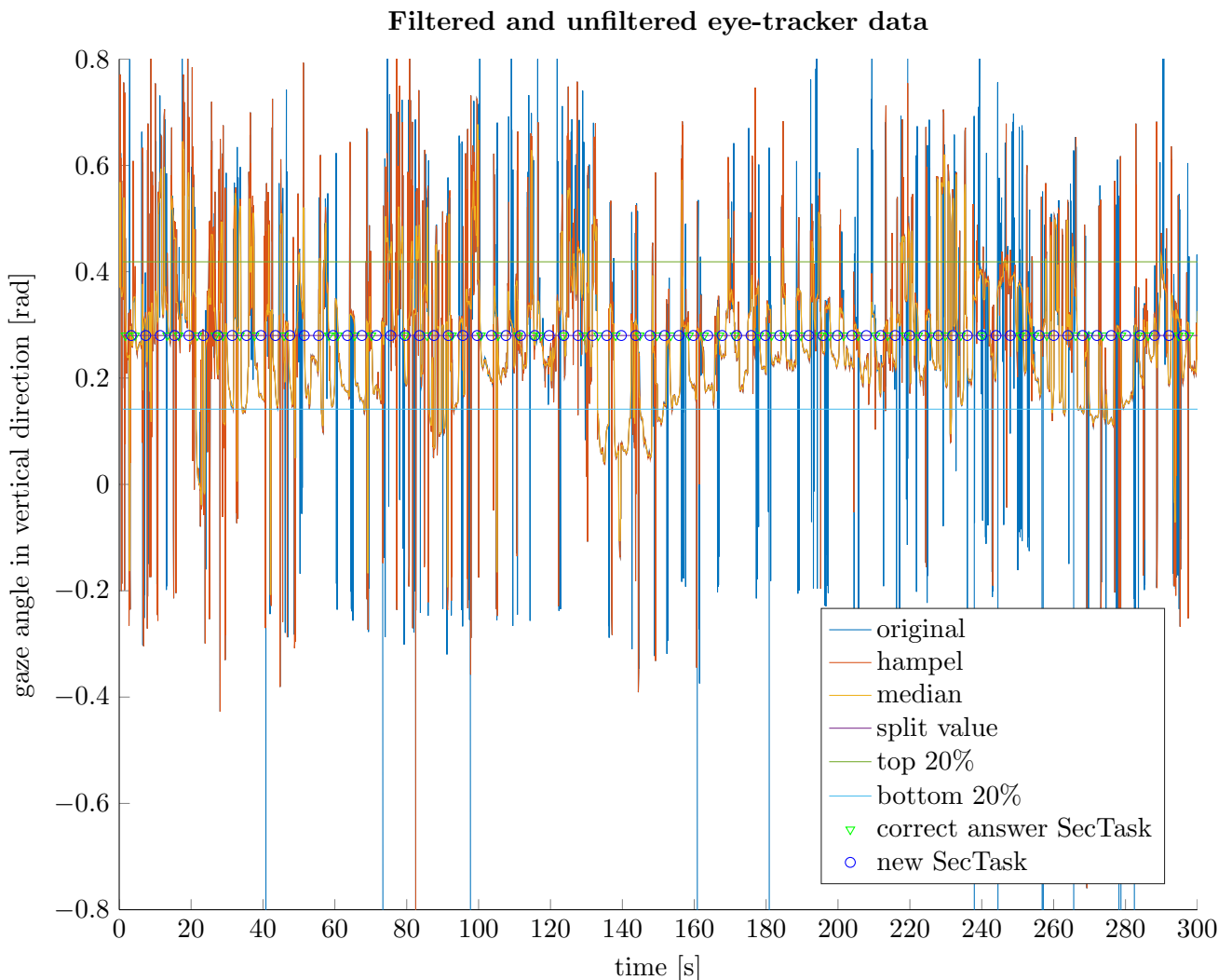


Figure H-1: Filtered eye-tracker data

In Figure H-2 the difference between can be seen. The median filter creates a more plateau-like

(binary) behaviour of the signal, where the Hampel filter follows the original signal closer. The difference is especially apparent just after 50 s.

Data analysis shows that only peaks shorter than 100 ms are removed by the Median filter, which is lower than the minimum time a human needs to switch and adjust his gaze according to different studies $t_{gaze,min} = 180\text{ ms}$ (Majaranta, Ahola, & Špakov, 2009) and $t_{gaze,min} = 124\text{ ms}$ (Mollenbach, Hansen, Lillholm, & Gale, 2009). Suggesting this filtering is retaining all the relevant data.

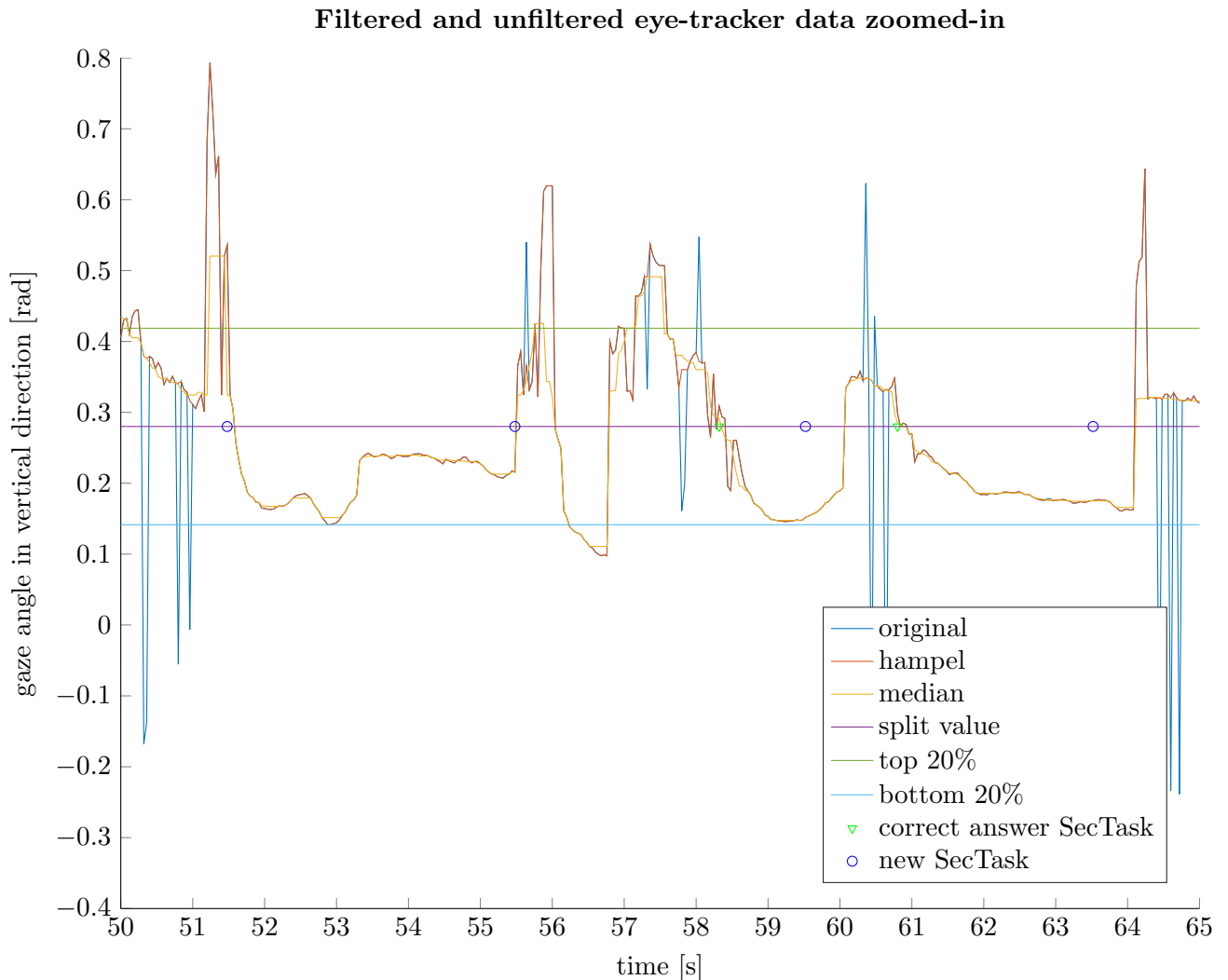


Figure H-2: Filtered eye-tracker data

H-2 Determine the split value

The mean and median of the gaze angle is different for every participant, for every run and even for different segments, as a candidate shifting his body or tilting his head can already cause a shift. Therefore the *split value*, above which a gaze is considered head-up and below which a gaze is considered head-down, was determined separately for every measurement window of 20 s. The split value is determined by taking average of the median of the top and bottom 20%.

Visual inspection of multiple datasets shows that this method gives indeed can separate head-up and head-down orientations correctly.

Appendix I

Statistical Analysis

I-1 Syntax SPSS

IBM's SPSS Statistics was used to run a statistical analysis on the collected data. Figure I-1 shows the syntax used to perform a test of normality, a test of sphericity, a repeated measures ANOVA and a post-hoc Bonferroni corrected analysis for all variables except the subjective effort rating. In this case the syntax for the analysis of the *percentage of correct answers* of the secondary task is given, to perform the analysis for a different variable, only the .sav file needs to be changed. As the subjective effort rating was obtained for full runs, they can not be analyzed for different segment types, the syntax used for the statistical analysis of this data is shown in Figure I-2.

```

1  * Encoding: UTF-8.
2  GET
3  FILE='Users\derekbeefink\Desktop\Statistical Analysis\Secondary task performance\SecCorrect.sav'.
4  DATASET NAME SecCorrect WINDOW=FRONT.
5  GLM LonV60H0 LonV60H60 LonV60H20 LonV20H0 LonV20H60 LonV20H20 LatV60H0 LatV60H60 LatV60H20 LatV20H0
6  LatV20H60 LatV20H20
7  /WSFACTOR=ST 2 Polynomial VTS 2 Polynomial HTS 3 Polynomial
8  /METHOD=SSTYPE(3)
9  /EMMEANS=TABLES(ST) COMPARE ADJ(BONFERRONI)
10 /EMMEANS=TABLES(VTS) COMPARE ADJ(BONFERRONI)
11 /EMMEANS=TABLES(HTS) COMPARE ADJ(BONFERRONI)
12 /EMMEANS=TABLES(ST*VTS)
13 /EMMEANS=TABLES(ST*HTS)
14 /EMMEANS=TABLES(VTS*HTS)
15 /EMMEANS=TABLES(ST*VTS*HTS)
16 /CRITERIA=ALPHA(.05)
17 /WSDESIGN=ST VTS HTS ST*VTS ST*HTS VTS*HTS ST*VTS*HTS.
18
19 EXAMINE VARIABLES=LonV60H0 LonV60H60 LonV60H20 LonV20H0 LonV20H60 LonV20H20 LatV60H0 LatV60H60
20 LatV60H20 LatV20H0 LatV20H60 LatV20H20
21 /PLOT NPLOT
22 /STATISTICS NONE
23 /CINTERVAL 95
24 /MISSING LISTWISE
25 /NOTOTAL.
26

```

Figure I-1: SPSS syntax for all variables except the subjective rating data

```

1  * Encoding: UTF-8.
2  GET
3  FILE='Users\derekbeefink\Desktop\Statistical Analysis\Secondary task performance\RSME.sav'.
4  DATASET NAME RSME WINDOW=FRONT.
5  GLM LonV60H0 LonV60H60 LonV60H20 LonV20H0 LonV20H60 LonV20H20
6  /WSFACTOR=VTS 2 Polynomial HTS 3 Polynomial
7  /METHOD=SSTYPE(3)
8  /EMMEANS=TABLES(VTS) COMPARE ADJ(BONFERRONI)
9  /EMMEANS=TABLES(HTS) COMPARE ADJ(BONFERRONI)
10 /EMMEANS=TABLES(VTS*HTS)
11 /CRITERIA=ALPHA(.05)
12 /WSDESIGN=VTS HTS VTS*HTS.
13
14 EXAMINE VARIABLES=LonV60H0 LonV60H60 LonV60H20 LonV20H0 LonV20H60 LonV20H20
15 /PLOT NPLOT
16 /STATISTICS NONE
17 /CINTERVAL 95
18 /MISSING LISTWISE
19 /NOTOTAL.
20

```

Figure I-2: SPSS syntax for the subjective rating data

I-2 Results

The results of the statistical analysis of the *percentage of correct answers* of the secondary task are shown in Figures I-3, I-4, I-5 and I-6. It can be seen that 5 out of 12 conditions fail the test of normality ($p < 0.05$), meaning that the validity of the results should be checked carefully, using boxplots for example, to see if they make sense. ANOVAs are relatively robust against violations of the normality test, so it was still decided to use a repeated measures ANOVA. For most variables there were no violations of normality.

An ANOVA is more sensitive to violations of sphericity, therefore, if the significance in Figure I-4 drops below 0.05, sphericity cannot be assumed and corrections by means of Greenhouse-Geisser were used. In case of the *secondary task success* sphericity can be assumed for all main effects and interactions between any two variables.

This means that for the within-subjects effects results in Figure I-5, the rows indicating *Sphericity Assumed* can be used. For this particular variable it can be seen that the main effects of changing ST, VTS and HTS are significant ($p \leq 0.05$), as are the interactions $ST \times HTS$ and $VTS \times HTS$.

To get insight beyond the main effects of independent variables with more than two settings a pairwise comparison can be done in an post-hoc analysis. For this analysis a Bonferroni correction was used to adjust for multiple comparisons, the results obtained this way are conservative. In Figure I-6 the results of this analysis are shown, it can be seen that there is a significant effect on *secondary success rate* between all haptic settings, except for change between a haptic tunnel size of 60 and 20 meters.

	Kolmogorov-Smirnov ^a			Shapiro-Wilk		
	Statistic	df	Sig.	Statistic	df	Sig.
LonV60H0	.179	12	.200 [*]	.856	12	.043
LonV60H60	.274	12	.013	.806	12	.011
LonV60H20	.214	12	.135	.809	12	.012
LonV20H0	.168	12	.200 [*]	.969	12	.897
LonV20H60	.286	12	.007	.816	12	.014
LonV20H20	.219	12	.115	.907	12	.195
LatV60H0	.153	12	.200 [*]	.957	12	.742
LatV60H60	.172	12	.200 [*]	.914	12	.241
LatV60H20	.245	12	.046	.887	12	.107
LatV20H0	.129	12	.200 [*]	.962	12	.814
LatV20H60	.188	12	.200 [*]	.854	12	.041
LatV20H20	.174	12	.200 [*]	.874	12	.074

*. This is a lower bound of the true significance.

a. Lilliefors Significance Correction

Figure I-3: Test of normality of the secondary task success statistical analysis

Mauchly's Test of Sphericity^a

Measure: MEASURE_1

Within Subjects Effect	Mauchly's W	Approx. Chi-Square	df	Sig.	Greenhouse-Geisser	Epsilon ^b	
						Huynh-Feldt	Lower-bound
ST	1.000	.000	0	.	1.000	1.000	1.000
VTS	1.000	.000	0	.	1.000	1.000	1.000
HTS	.947	.541	2	.763	.950	1.000	.500
ST * VTS	1.000	.000	0	.	1.000	1.000	1.000
ST * HTS	.977	.231	2	.891	.978	1.000	.500
VTS * HTS	.822	1.955	2	.376	.849	.988	.500
ST * VTS * HTS	.357	10.296	2	.006	.609	.644	.500

Tests the null hypothesis that the error covariance matrix of the orthonormalized transformed dependent variables is proportional to an identity matrix.

a. Design: Intercept

Within Subjects Design: ST + VTS + HTS + ST * VTS + ST * HTS + VTS * HTS + ST * VTS * HTS

b. May be used to adjust the degrees of freedom for the averaged tests of significance. Corrected tests are displayed in the Tests of Within-Subjects Effects table.

Figure I-4: Results of Mauchly's test of sphericity

Tests of Within-Subjects Effects						
Measure: MEASURE_1						
Source		Type III Sum of Squares	df	Mean Square	F	Sig.
ST	Sphericity Assumed	1277.910	1	1277.910	4.823	.050
	Greenhouse-Geisser	1277.910	1.000	1277.910	4.823	.050
	Huynh-Feldt	1277.910	1.000	1277.910	4.823	.050
	Lower-bound	1277.910	1.000	1277.910	4.823	.050
Error(ST)	Sphericity Assumed	2914.842	11	264.986		
	Greenhouse-Geisser	2914.842	11.000	264.986		
	Huynh-Feldt	2914.842	11.000	264.986		
	Lower-bound	2914.842	11.000	264.986		
VTS	Sphericity Assumed	1399.847	1	1399.847	13.220	.004
	Greenhouse-Geisser	1399.847	1.000	1399.847	13.220	.004
	Huynh-Feldt	1399.847	1.000	1399.847	13.220	.004
	Lower-bound	1399.847	1.000	1399.847	13.220	.004
Error(VTS)	Sphericity Assumed	1164.753	11	105.887		
	Greenhouse-Geisser	1164.753	11.000	105.887		
	Huynh-Feldt	1164.753	11.000	105.887		
	Lower-bound	1164.753	11.000	105.887		
HTS	Sphericity Assumed	1883.240	2	941.620	12.083	.000
	Greenhouse-Geisser	1883.240	1.900	991.252	12.083	.000
	Huynh-Feldt	1883.240	2.000	941.620	12.083	.000
	Lower-bound	1883.240	1.000	1883.240	12.083	.005
Error(HTS)	Sphericity Assumed	1714.417	22	77.928		
	Greenhouse-Geisser	1714.417	20.898	82.036		
	Huynh-Feldt	1714.417	22.000	77.928		
	Lower-bound	1714.417	11.000	155.856		
ST * VTS	Sphericity Assumed	55.293	1	55.293	.799	.391
	Greenhouse-Geisser	55.293	1.000	55.293	.799	.391
	Huynh-Feldt	55.293	1.000	55.293	.799	.391
	Lower-bound	55.293	1.000	55.293	.799	.391
Error(ST*VTS)	Sphericity Assumed	761.124	11	69.193		
	Greenhouse-Geisser	761.124	11.000	69.193		
	Huynh-Feldt	761.124	11.000	69.193		
	Lower-bound	761.124	11.000	69.193		
ST * HTS	Sphericity Assumed	569.886	2	284.943	7.349	.004
	Greenhouse-Geisser	569.886	1.955	291.449	7.349	.004
	Huynh-Feldt	569.886	2.000	284.943	7.349	.004
	Lower-bound	569.886	1.000	569.886	7.349	.020
Error(ST*HTS)	Sphericity Assumed	853.038	22	38.774		
	Greenhouse-Geisser	853.038	21.509	39.660		
	Huynh-Feldt	853.038	22.000	38.774		
	Lower-bound	853.038	11.000	77.549		
VTS * HTS	Sphericity Assumed	367.821	2	183.910	3.538	.047
	Greenhouse-Geisser	367.821	1.698	216.567	3.538	.056
	Huynh-Feldt	367.821	1.976	186.133	3.538	.047
	Lower-bound	367.821	1.000	367.821	3.538	.087
Error(VTS*HTS)	Sphericity Assumed	1143.672	22	51.985		
	Greenhouse-Geisser	1143.672	18.683	61.216		
	Huynh-Feldt	1143.672	21.737	52.613		
	Lower-bound	1143.672	11.000	103.970		
ST * VTS * HTS	Sphericity Assumed	92.481	2	46.241	1.137	.339
	Greenhouse-Geisser	92.481	1.217	75.966	1.137	.319
	Huynh-Feldt	92.481	1.289	71.752	1.137	.322
	Lower-bound	92.481	1.000	92.481	1.137	.309
Error(ST*VTS*HTS)	Sphericity Assumed	894.919	22	40.678		
	Greenhouse-Geisser	894.919	13.391	66.828		
	Huynh-Feldt	894.919	14.178	63.121		
	Lower-bound	894.919	11.000	81.356		

Figure I-5: Within-subjects effects effects as obtained by the repeated measures ANOVA

Pairwise Comparisons

Measure: MEASURE_1

(I) HTS	(J) HTS	Mean Difference (I-J)	Std. Error	Sig. ^b	95% Confidence Interval for Difference ^a	
					Lower Bound	Upper Bound
1	2	-5.988 [*]	1.822	.022	-11.127	-.850
	3	-8.647 [*]	1.963	.003	-14.183	-3.112
2	1	5.988 [*]	1.822	.022	.850	11.127
	3	-2.659	1.603	.376	-7.178	1.860
3	1	8.647 [*]	1.963	.003	3.112	14.183
	2	2.659	1.603	.376	-1.860	7.178

Based on estimated marginal means

*. The mean difference is significant at the .05 level.

b. Adjustment for multiple comparisons: Bonferroni.

Figure I-6: Rating Scale Mental Effort

References

- Abbink, D. (2006). *Neuromuscular analysis of haptic gas pedal feedback during car following* (Unpublished doctoral dissertation). Delft University of Technology.
- Abbink, D., Mulder, M., & Boer, E. (2012). Haptic shared control: Smoothly shifting control authority? *Cognition, Technology and Work*, *14*(1), 19–28. doi: 10.1007/s10111-011-0192-5
- Alaimo, S. M. C., Pollini, L., Innocenti, M., & Bresciani, J. P. (2012). Experimental Comparison of Direct and Indirect Haptic Aids in Support of Obstacle Avoidance for Remotely Piloted Vehicles. , *2*, 628–637.
- Anderson, M. W. (1996). Flight Test Certification of Multipurpose Head-Up Display for General Aviation Aircraft. *Journal of Aircraft*, *33*(3), 532–538.
- De Vlugt, E. (2004). *Identification of Spinal Reflexes*. Delft University of Technology. doi: DOI:oclc/150297636
- de Stigter, S., Mulder, M., & van Paassen, M. M. (2005). On the Equivalence Between Flight Directors and Flight Path Predictors in Aircraft Guidance. *Proc. of the AIAA Modeling and Simulation Technologies Conference, San Francisco (CA)*(AIAA-2005-5962), 1–20.
- de Stigter, S., Mulder, M., & van Paassen, M. M. (2007). Design and Evaluation of a Haptic Flight Director. *Journal of Guidance, Control, and Dynamics*, *30*(1), 35–46. Retrieved from <http://arc.aiaa.org/doi/abs/10.2514/1.20593> doi: 10.2514/1.20593
- Flemisch, F. O., Kelsch, J., Loper, C., Schieben, A., Schindler, J., & Matthias, H. (2008). Cooperative Control and Active Interfaces for Vehicle Assistance and Automation. *FISITA World Automotive Congress*(2), 301–310.
- Gast, M. (1998). *Autopilot/Flight Director Stall Protection System*. Google Patents. Retrieved from <https://www.google.com/patents/US5803408>
- Gibson, J. (1950). *The Perception of the Visual World*. Oxford: Houghton Mifflin.
- Gibson, J. (1979). *The Ecological Approach to Visual Perception*. Boston: Houghton Mifflin.
- Gibson, J., Olum, P., & Rosenblatt, F. (1955). Parallax and Perspective during Aircraft Landings. *The American Journal of Psychology*, *68*(3), 372–385.
- Grunwald, A. (1984). Tunnel display for four-dimensional fixed-wing approaches. *Journal of Guidance, Control, and Dynamics*, *7*(3), 369–377.
- Grunwald, A., Robertson, J., & Hatfield, J. (1980). Evaluation of a computer-generated perspective tunnel display for flight-path following. *NASA Technical Documents*(March).

- Grunwald, A., Robertson, J., & Hatfield, J. (1981). Experimental Evaluation of a Perspective Tunnel Display for Three-Dimensional Helicopter Approaches. *Journal of Guidance, Control, and Dynamics*, 4(5), 623–631.
- Gursky, B. I., Olsman, W. F. J., & Peinecke, N. (2014). Development of a tunnel-in-the-sky display for helicopter noise abatement procedures. *CEAS Aeronautical Journal*, 5(2), 199–208. doi: 10.1007/s13272-014-0100-9
- Lee, K. (2010). *Effects of flight factors on pilot performance, workload, and stress at final approach to landing phase of flight* (Unpublished doctoral dissertation). University of Central Florida.
- Lintern, G., Waite, T., & Talleur, P. (1999). Functional Interface Design for the Modern Aircraft Cockpit. *International Journal of Aviation Psychology*, 9(3), 203–223. doi: 10.1207/s15327108ijap0903
- Lombaerts, T., Looye, G., Ellerbroek, J., & Rodriguez, M. (2016). Design and Piloted Simulator Evaluation of Adaptive Safe Flight Envelope Protection Algorithm. (January), 1–25. doi: 10.2514/6.2016-0093
- Majaranta, P., Ahola, U.-K., & Špakov, O. (2009). Fast gaze typing with an adjustable dwell time. *Proceedings of the 27th international conference on Human factors in computing systems - CHI 09*, 357. Retrieved from <http://dl.acm.org/citation.cfm?id=1518701.1518758> doi: 10.1145/1518701.1518758
- McRuer, D. T., & Jex, H. R. (1967). A Review of Quasi-Linear Pilot Models. *Human Factors in Electronics, IEEE Transactions on, HFE-8*(3), 231–249. doi: 10.1109/THFE.1967.234304
- Mollenbach, E., Hansen, J. P., Lillholm, M., & Gale, A. G. (2009). Single stroke gaze gestures. *Proceedings of the 27th international conference extended abstracts on Human factors in computing systems - CHI EA '09*, 4555. Retrieved from <http://portal.acm.org/citation.cfm?doid=1520340.1520699> doi: 10.1145/1520340.1520699
- Mulder, M. (1999). *Cybernetics of tunnel-in-the-sky displays*. Delft: Delft University Press. doi: 10.4233/uuid:627f30e0-0a70-43f5-b4c8-043c36dda641
- Mulder, M. (2003a). An Information-Centered Analysis of the Tunnel- in-the-Sky Display, Part One: Straight Tunnel Trajectories. *International Journal of Aviation Psychology*, 13(1), 1–22. Retrieved from <http://dx.doi.org/10.1207/S15327108IJAP1301{-}1> doi: 10.1207/S15327108IJAP1301
- Mulder, M. (2003b). An Information-Centered Analysis of the Tunnel- in-the-Sky Display, Part Two: Curved Tunnel Trajectories. *The International Journal of Aviation Psychology*, 8414(July 2011), 37–41. doi: 10.1207/S15327108IJAP1302
- Mulder, M., & Mulder, J. A. (2005). Cybernetic Analysis of Perspective Flight-Path Display Dimensions. *Journal of Guidance, Control, and Dynamics*, 28(3), 398–411. doi: 10.2514/1.6646
- Mulder, M., & van der Vaart, H. (2006). An Information-Centered Analysis of the Tunnel-in-the-Sky Display, Part 3: The Interception of Curved Trajectories. *International Journal of Aviation Psychology*, 16(1), 51–76. doi: 10.1207/s15327108ijap1601
- Newman, R., & Mulder, M. (2003). Pathway displays: a literature review. *Digital Avionics Systems Conference, 2003. DASC '03. The 22nd, 2*, 1–10. doi: 10.1109/DASC.2003.1245921
- Parasuraman, R., & Riley, V. (1997). Humans and Automation: Use, Misuse, Disuse, Abuse. *Human Factors: The Journal of the Human Factors and Ergonomics Society*, 39(2), 230–253. doi: 10.1518/001872097778543886
- Petermeijer, S., Abbink, D., Mulder, M., & de Winter, J. (2013). The Effect of Haptic Support Systems on Driver Performance and Behavior : A Literature Review. *IEEE Transaction on Haptics*, 8(April 2013), 1–13. doi: 10.1109/TOH.2015.2437871
- Regal, D., & Whittington, D. (1995). Guidance symbology for curved flight paths. *Proceedings*

- of the Eight Symposium on Aviation Psychology*, 74 – 79.
- Smisek, J., Van Paassen, M. M., Mulder, M., & Abbink, D. A. (2013). Neuromuscular analysis based tuning of haptic shared control assistance for UAV collision avoidance. *2013 World Haptics Conference, WHC 2013*, 389–394. doi: 10.1109/WHC.2013.6548440
- Sunil, E., Smisek, J., Van Paassen, M. M., & Mulder, M. (2014). Validation of a tuning method for haptic shared control using neuromuscular system analysis. *Conference Proceedings - IEEE International Conference on Systems, Man and Cybernetics, 2014-Janua*(January), 1499–1504. doi: 10.1109/smc.2014.6974128
- Wallace, L. (1994). *Two Decades With NASA Langley's 737 Flying Laboratory* (First ed.; Tech. Rep.). Washington D.C..
- Way, T. (1987). *Multi-Crew Pictorial Format Display Evaluation*. Boeing Military Airplane Company.
- Wickens, C. D. (2002). Multiple resources and performance prediction. *Theoretical Issues in Ergonomics Science*, 3(2), 159–177. doi: 10.1080/14639220210123806
- Wilckens, V. (1973). Improvements in Pilot/Aircraft-Integration by Advanced Contact Analog Displays. *NASA Technical Documents*.
- Zijlstra, F. (1993). Efficiency in work behaviour: A design approach for modern tools. *Delft University press*(January 1993), 1–186. Retrieved from <http://www.csa.com/partners/viewrecord.php?requester=gs{&}collection=TRD{&}recid=N9516953AH> doi: 90-6275-918-1